

**Fire Performance of High-Strength Concrete:
A Report of the State-of-the-Art**

L.T. Phan

Building and Fire Research Laboratory
National Institute of Standards and Technology
Gaithersburg, Maryland 20899

December, 1996



U.S. Department of Commerce
Michael Kantor, Secretary
Technology Administration
Mary L. Good, Under Secretary for Technology
National Institute of Standards and Technology
Arati A. Prabhakar, Director

ABSTRACT

A review is presented of experimental and analytical studies on the performance of concrete when exposed to short-term, rapid heating as in a fire. Emphasis is placed on concretes with high original compressive strengths, that is, high-strength concretes (HSC). The compiled test data revealed distinct difference in mechanical properties of HSC and normal strength concrete (NSC) in the range between room temperature and about 450 °C. The differences decreased at temperature above 450 °C. What is more important is that many test programs, but not all, reported that HSC experienced explosive spalling during the fire tests. The spalling is theorized to be caused by the buildup of pore pressure during heating. HSC is believed to be more susceptible to this pressure build up because of its low permeability compared with NSC. However, no explanations were found for why spalling did not occur in all HSC specimens. Analytical models for predicting the buildup of internal pressure during heating are also reviewed. The report also includes a comparison of test results with existing code provisions on the effects of fire on concrete strength. It is shown that the Eurocode provisions and the CEB design curves are more applicable to NSC than to HSC. In fact, these provisions are unsafe when compared with HSC test results. The review showed a lack of experimental data for lightweight HSC and HSC heated under a constant preload to simulate the stress conditions in HSC columns. The report concludes with an outline of a research plan to gain an understanding of the failure mechanisms in fire exposed HSC. The ultimate goal of the research is to develop tools for predicting the performance of HSC when exposed to fire.

Keywords: building technology; compressive strength; concrete; elastic modulus; explosive spalling; fire tests; high-strength concrete; standard test methods; temperature.

ACKNOWLEDGEMENTS

The author gratefully acknowledges the guidance, careful review, and constructive comments provided by his group leader, Dr. Nicholas J. Carino, of the Structures Division at NIST. The author expresses his gratitude to Mr. James P. Hurst, who is the current chairman of ACI Committee 216, and Dr. G.N. Ahmed, both of the Portland Cement Association, and to Dr. Dat Duthinh of the Structures Division at NIST, for providing thoughtful and expert review of this report. Finally, gratitude is extended to Ms. Cynthia Kuo whose valuable help in digitizing and plotting many of the figures in this report made its completion possible.

TABLE OF CONTENTS

ABSTRACT	iii
ACKNOWLEDGEMENTS	iv
LIST OF TABLES	vii
LIST OF FIGURES	viii
1. INTRODUCTION	1
1.1 General	1
1.2 Research Objectives and Scope	3
1.3 Scope of Report	3
2. EXPERIMENTAL STUDIES ON FIRE PERFORMANCE OF HSC	5
2.1 Introduction	5
2.2 Test Methods used for Determination of Mechanical Properties of HSC	6
2.2.1 Idealized Test Methods	6
2.2.2 Common Test Methods	7
2.3 Experimental Studies	8
2.3.1 Materials Tests	8
2.3.1.1 <i>Castillo and Durani (1990)</i>	8
2.3.1.2 <i>Hertz (1984, 1991)</i>	12
2.3.1.3 <i>Diederichs, Jumppanen, and Penttala (1988)</i>	15
2.3.1.4 <i>Hammer (1995)</i>	18
2.3.1.5 <i>Abrams (1971)</i>	22
2.3.1.6 <i>Sullivan and Shanshar (1992)</i>	25
2.3.1.7 <i>Morita, Saito, and Kumagai (1992)</i>	28
2.3.1.8 <i>Furumura, Abe, and Shinohara (1995)</i>	29
2.3.1.9 <i>Felicetti, Gambarova, Rosati, Corsi, and Giannuzzi (1996)</i> ...	31
2.3.1.10 <i>Noumowe, Clastres, Debicki, and Costaz (1996)</i>	34
2.3.2 Element Tests	36
2.3.2.1 <i>Beam Tests by Hansen and Jensen, 1995 (Also Opheim, 1995; and Jensen et al., 1996)</i>	36
2.3.2.2 <i>Beam Tests by Sanjayan and Stocks, 1991</i>	39
2.3.2.3 <i>Beam Tests by Saito, Kumagai, and Morita, 1992 (in Japanese)</i>	42
2.3.2.4 <i>Report of Column Tests by Diederichs, Jumppanen, and Schneider, 1995</i>	43
2.3.2.5 <i>Slab Tests by Shirley, Burg, and Fiorato, 1987</i>	44
2.3.3 Other Studies	46
2.3.3.1 <i>Nassif, Burley, and Rigden, 1995</i>	46
2.3.3.2 <i>Lin, Lin, and Powers-Couche, 1996</i>	48

2.4 Summary	49
2.4.1 Effect of Temperature on Compressive Strength of HSC	49
2.4.2 Effect of Temperature on Modulus of Elasticity of HSC	57
2.4.3 Effect of Temperature on Stress-Strain Relationship of HSC	58
2.4.4 Effect of Temperature on HSC Tensile Strength	59
2.4.5 Spalling of HSC at High Temperature	59
3. MODELING TECHNIQUES FOR THERMAL BEHAVIOR OF CONCRETE	61
3.1 Introduction	61
3.2 Modeling of Concrete Thermal Behavior	61
3.2.1 Bazant and Thonuthai (1979)	61
3.2.2 Ahmed and Hurst (1995)	63
3.2.3 England and Khoylou (1995)	66
3.2.4 Noumowe, Clastres, Debicki, Costaz (1996)	68
3.3 Summary	70
4. FIRE TEST METHODS AND PROPERTIES OF HEATED CONCRETE ACCORDING TO CODES AND COMMITTEE REPORTS	71
4.1 Introduction	71
4.2 Fire Test Methods	71
4.2.1 International Standard ISO 834 (1975)	71
4.2.2 ASTM E 119 (1988)	73
4.2.3 Japanese Industrial Standard JIS A 1304 (1994)	75
4.3 Properties of Heated Concrete	76
4.3.1 CEN - Comité Europeen de Normalisation	76
4.3.2 ACI Committee Report 216R-89	80
4.3.3 CEB Bulletin D'Information N° 208 (RILEM - Committee 44-PHT)	81
4.3.4 CRSI - Reinforced Concrete Fire Resistance	85
4.4 Applicability of Code Design Recommendations to HSC	85
4.5 Summary	91
5. SUMMARY, DISCUSSION, AND RECOMMENDATIONS	93
5.1 Summary	93
5.2 Discussion and Recommendations	95
6. REFERENCES	97

LIST OF TABLES

Table 2.1	Compressive Strengths at High Temperature (Hammer, 1995)	19
Table 2.2	Modulus of Elasticity at High Temperature (Hammer, 1995)	19
Table 2.3	Concrete Material Properties (Hansen and Jensen, 1995)	37
Table 2.4	Summary of Observations of Hansen and Jensen's Tests	38
Table 2.5	Summary of Concrete Strengths (Shirley et al., 1987)	44
Table 2.6	Summary of Fire Endurance of 102 mm Thick Slabs (Shirley et al., 1987)	45
Table 2.7	Summary of Materials Test Programs Reviewed	51
Table 2.8	Summary of Structural Element Test Programs Reviewed	53
Table 4.1	Time-Temperature Data on ISO 834 Standard Fire Curve	72
Table 4.2	Time-Temperature Data of Points for ASTM E 119 Standard Fire Curve	74
Table 4.3	Time-Temperature Values of Points on Standard Fire Curve of JIS A 1304	75
Table 4.4	Values for the two parameters to describe the ascending branch of the stress-strain relationships of concrete at elevated temperature according to CEN ENV 1994-1-2	78

LIST OF FIGURES

Figure 2.1 Compressive Strength vs. Temperature Relationships (Castillo and Durani, 1990)	10
Figure 2.2 Modulus of Elasticity vs. Temperature Relationships (Castillo and Durani, 1990)	10
Figure 2.3 Load-Deformation Behavior of HSC at High Temperatures (Castillo and Durani, 1990)	11
Figure 2.4 Load-Deformation Behavior of NSC at High Temperatures (Castillo and Durani, 1990)	11
Figure 2.5 Variation of Compressive Strengths with Temperature (Hertz, 1984)	13
Figure 2.6 Variation of Elastic Modulus with Temperature (Hertz, 1984)	13
Figure 2.7 Variation of Residual Strength with Temperature for Different Specimen Sizes (Hertz, 1991)	14
Figure 2.8 Variation of Residual Modulus of Elasticity with Temperature for Different Specimen Sizes (Hertz, 1991).	15
Figure 2.9 Variation of Compressive Strength with Temperature for Different Concretes (Diederichs et al., 1988)	16
Figure 2.10 Variation of Elastic Moduli with Temperature for Different Concretes (Diederichs et al., 1988)	16
Figure 2.11 Stress-Strain Relationships of HSC Made with Fly Ash (Diederichs et al., 1988)	17
Figure 2.12 Stress-Strain Relationships of NSC Made with Ordinary Portland Cement (Diederichs et al., 1988)	17
Figure 2.13 Compressive Strengths of 90-day Concretes vs. Temperature (Hammer, 1995) ..	20
Figure 2.14 Elastic Moduli of 90-day Concretes vs. Temperature (Hammer, 1995)	20
Figure 2.15 Compressive Strength of 150-day Concretes vs. Temperature (Hammer, 1995) ..	20
Figure 2.16 Elastic Moduli of 150-day Concretes vs. Temperature (Hammer, 1995)	20
Figure 2.17 Mass Loss vs. Strength Loss for 90-day Concretes (Hammer, 1995)	21
Figure 2.18 Mass Loss vs. Strength Loss for 150-day Concretes (Hammer, 1995)	21
Figure 2.19 Strength of Carbonate Aggregate Concrete versus Temperature (Abrams, 1971) ..	23
Figure 2.20 Strength of Siliceous Aggregate Concrete versus Temperature (Abrams, 1971) ..	23
Figure 2.21 Strength of Lightweight Aggregate Concrete versus Temperature (Abrams, 1971)	24
Figure 2.22 Strength versus Temperature for Stressed Tests (Abrams, 1971)	24
Figure 2.23 Strength versus Temperature for Unstressed Tests (Abrams, 1971)	24
Figure 2.24 Strength versus Temperature for Unstressed Residual Strength Test (Abrams, 1971)	24
Figure 2.25 Compressive Strength versus Temperature from Unstressed Tests (Sullivan and Shansar, 1992)	26

Figure 2.26 Compressive Strength versus Temperature from Unstressed Residual Strength Tests (Sullivan and Shanshar, 1992).	26
Figure 2.27 Strength of Firebrick/Silica Fume Concrete versus Temperature (Sullivan and Shansar, 1992)	27
Figure 2.28 Strength for Firebrick/Slag Concrete versus Temperature (Sullivan and Shansar, 1992)	27
Figure 2.29 Strength for Firebrick/OPC Concrete versus Temperature (Sullivan and Shansar, 1992)	27
Figure 2.30 Strength for Lytag OPC Concrete versus Temperature (Sullivan and Shansar, 1992)	27
Figure 2.31 Residual Compressive Strength versus Temperature (Morita et al., 1992)	28
Figure 2.32 Residual Normalized Strength versus Temperature (Morita et al., 1992)	28
Figure 2.33 Residual Elastic Modulus versus Temperature (Morita et al., 1992)	29
Figure 2.34 Residual Normalized Elastic Modulus vs. Temperature (Morita et al., 1992)	29
Figure 2.35 Compressive Strength versus Temperature (Furumura et al., 1995)	30
Figure 2.36 Elastic Modulus versus Temperature (Furumura et al., 1995)	30
Figure 2.37 Typical Stress-Strain Relationships for 42 MPa-concrete (Furumura et al., 1995)	30
Figure 2.38 Comparison of Stress-Strain Relationships for Concretes at 300 °C (Furumura et al., 1995)	30
Figure 2.39 Residual Concrete Strength versus Temperature (Felicetti et al., 1996)	31
Figure 2.40 Residual Elastic Modulus versus Temperature (Felicetti et al., 1996)	31
Figure 2.41 Stress-Strain Curves for 95 MPa Concrete after Heating to Exposure Temperature (Felicetti et al., 1996)	32
Figure 2.42 Stress-Strain Curves for 72 MPa Concrete after Heating to Exposure Temperature (Felicetti et al., 1996)	32
Figure 2.43 Tensile Stress-Strain Curves for 95 MPa Concrete after Heating to Exposure Temperature (Felicetti et al., 1996)	32
Figure 2.44 Tensile Stress-Strain Curves for 72 MPa Concrete after Heating to Exposure Temperature (Felicetti et al., 1996)	32
Figure 2.45 Load-Deflection Response of Reinforced Beams versus Temperature (Felicetti et al., 1996)	33
Figure 2.46 Load-Deflection Response of Unreinforced Beams versus Temperature (Felicetti et al., 1996)	33
Figure 2.47 Residual Tensile Strengths of HSC and NSC versus Temperature (Noumowe et al., 1996)	34
Figure 2.48 Elastic Moduli of HSC and NSC versus Temperature (Noumowe et al., 1996)	34
Figure 2.49 Porosity of HSC and NSC versus Temperature (Noumowe et al., 1996)	35
Figure 2.50 Mass Loss of HSC and NSC versus Temperature (Noumowe et al., 1996)	35
Figure 2.51 ISO Hydrocarbon Fire Curve, Furnace Temperature, and Time Period When Spalling was Observed (Hansen and Jensen, 1995)	38

Figure 2.52	Temperature vs. Time At Different Locations in the Specimens (Sanjayan and Stocks, 1991)	41
Figure 2.53	Specimen Loss vs. Time for HSC and NSC Specimens (Sanjayan and Stocks, 1991)	41
Figure 2.54	Standard Fire Curve and Temperature at Different Points in Beam Specimen (Saito et al., 1992)	42
Figure 2.55	ASTM E 119 Heating Regime and Average Temperatures on the Unexposed Surfaces of the Slabs (Shirley et al., 1987)	45
Figure 2.56	Chord Loading Modulus Ratio versus Temperature (Ecc is the value of the control specimen at 20 °C, Nassif et al., 1995)	47
Figure 2.57	Unloading Modulus Ratio versus Temperature (Euc is the value of the control specimen at 20 °C, Nassif et al., 1995)	47
Figure 2.58	Damage Index versus Temperature (Nassif et al., 1995)	47
Figure 2.59	Non-linearity Index versus Temperature (Nassif et al., 1995)	47
Figure 2.60	Plastic Strain versus Temperature (Nassif et al., 1995)	48
Figure 2.61	Ultrasonic Pulse Velocity Ratio (fire tested/unfire tested) versus Temperature (Nassif et al., 1995)	48
Figure 2.62	Summary of Compressive strength-temperature relationships for normal weight concrete, obtained by unstressed tests	54
Figure 2.63	Summary of Compressive strength-temperature relationships for lightweight concrete, obtained by unstressed tests	54
Figure 2.64	Summary of Compressive strength-temperature relationships for normal weight concrete, obtained by unstressed residual strength tests	55
Figure 2.65	Summary of Compressive strength-temperature relationships for lightweight concrete, obtained by unstressed residual strength tests	55
Figure 2.66	Summary of Compressive strength-temperature relationships for normal weight concrete, obtained by stressed tests	56
Figure 2.67	Summary of Compressive strength-temperature relationship for lightweight concrete, obtained by stressed tests	56
Figure 2.68	Summary of Modulus of elasticity-temperature relationships obtained from unstressed tests for normal and lightweight concrete	57
Figure 2.69	Summary of Modulus of elasticity-temperature relationships obtained from unstressed residual strength tests for normal and lightweight concrete.	58
Figure 2.70	Typical load-deformation relationship at different temperature for (a) HSC and (b) NSC (Castillo and Durani, 1990)	59
Figure 3.1	Comparison of measured Unexposed Surface Temperatures with Predictions for Different Slabs (Ahmed and Hurst, 1995)	65
Figure 3.2	Comparison of Predicted Temperature in 152-mm Concrete Slab with Experimental Results (Ahmed and Hurst, 1995)	65
Figure 3.3	Predicted Pore Pressure History at Different Depths in 152-mm Thick Slab (Ahmed and Hurst, 1995)	65

Figure 3.4 Predicted Pore Pressure Distribution at Various Times in 152-mm Thick Slab (Ahmed and Hurst, 1995)	65
Figure 3.5 Idealization of concrete as porous cubical forms with elastic cement paste skeleton (England and Khoylou, 1995)	67
Figure 4.1 Standard Fire Curve for ISO 834	72
Figure 4.2 ASTM E 119 Standard Fire Curve	74
Figure 4.3 JIS A 1304 Standard Time-Temperature Curve	76
Figure 4.4 Mathematical model for stress-strain relationships of concrete under compression at elevated temperatures (ENV 1994-1-2).	77
Figure 4.5 Strength Reduction Factor for Concrete with Respect to Temperature (CEN ENV 1994-1-2)	79
Figure 4.6 Variation of Strain at Ultimate Strength with Respect to Temperature (CEN ENV 1994-1-2)	79
Figure 4.7 Variation of E/E_0 with Temperature (ACI 216R-89)	80
Figure 4.8 Variation of G/G_0 with Temperature (ACI 216R-89)	80
Figure 4.9 Compressive Strength of Siliceous Normal Weight Concrete at High Temperature	81
Figure 4.10 Compressive Strength of Lightweight Concrete at High Temperature	82
Figure 4.11 Effect of Temperature on Modulus of Elasticity	82
Figure 4.12 Effect of Temperature on Tensile Strength	83
Figure 4.13 Threshold for Spalling of Concrete Elements with Different Thicknesses [Meyer-Ottens (1975)]	84
Figure 4.14 Comparison of Design Curves for Compressive Strength and Results of <i>Unstressed</i> Tests of Normal Weight Aggregate Concrete	87
Figure 4.15 Comparison of Design Curves for Compressive Strength and Results of <i>Unstressed</i> Tests of Lightweight Aggregate Concrete	87
Figure 4.16 Comparison of Design Curves for Compressive Strength and Results of <i>Unstressed Residual Strength</i> Tests of Normal Weight Aggregate Concrete ...	88
Figure 4.17 Comparison of Design Curves for Compressive Strength and Results of <i>Unstressed Residual Strength</i> Tests of Lightweight Aggregate Concrete	88
Figure 4.18 Comparison of Design Curves for Compressive Strength and Results of <i>Stressed</i> Tests of Normal Weight Aggregate Concrete	89
Figure 4.19 Comparison of Design Curves for Compressive Strength and Results of <i>Stressed</i> Tests of Lightweight Aggregate Concrete	89
Figure 4.20 Comparison of Design Curves for Modulus of Elasticity and Results of <i>Unstressed</i> Tests	90
Figure 4.21 Comparison of Design Curves for Modulus of Elasticity with Results of <i>Unstressed Residual Strength</i> Tests	90
Figure 4.22 Standard Temperature Time Curves	91

1. INTRODUCTION

1.1 General

High strength concrete (HSC) is a state-of-the-art material that can now be manufactured by most concrete plants due to the availability of a variety of additives such as silica fume and water reducing admixtures. HSC offers significant advantages over lower or normal strength concrete (NSC). In terms of economic advantage, cost studies have shown that HSC can carry the same compression load at less cost than NSC (*PCA Concrete Technology*, 1980), and thus the higher material costs for HSC are more than compensated for. In terms of architectural advantage, HSC allows smaller size columns to be used in high-rise construction. This results in more usable space in the building. These advantages, coupled with today's ease of manufacturing, have resulted in HSC being used more widely in structural applications. The American Concrete Institute Committee 363 report, (ACI 363R-92) *State-of-the-Art Report on High-Strength Concrete*, documents successful applications of HSC for buildings, bridges, and special structures. In buildings, HSC is used most often for columns. A list of HSC buildings, which were built in the 1980s, with specified compressive strength ranging from 50 to 97 MPa, is provided by the ACI 363R-92 report. In bridges, HSC is used to construct precast prestressed girders. The reported specified concrete strength in bridge applications ranges from 42 to 76 MPa. Applications of HSC in special structures to take advantage of its durability and low permeability, such as in arch dams, prestressed concrete poles, and offshore structures are also reported.

A question may be raised as to what compressive strength level does a concrete mixture have to attain to be regarded as HSC. In reality, there is no specific strength level which causes drastic change in material properties of concrete that can be used to clearly separate HSC and NSC. The definition of HSC evolves with its gradual development and usage over the years. ACI 393R-92 provides some historical background concerning the definition of HSC. According to this committee report, concrete with a compressive strength of 34 MPa used to be considered as HSC in the 1950s. This was because higher strength concrete was not widely available at many of the concrete manufacturing plants at that time, and thus most designers had little choice but to specify concrete with strength that would be available. Progressively since then, however, concrete of higher strengths, from 40 MPa in the 1960s to approaching 138 MPa more recently, have become commercially available, and the definition of HSC has thus changed accordingly. Currently, ACI 393R-92 adopts the following definition for HSC:

“The immediate concern of Committee 363 shall be concretes having specified compressive strengths for design of 6000 psi (41 MPa) or greater, but for the present time, considerations shall not include concrete made using exotic materials or techniques.”

The word “exotic” was included in the above definition to exclude from consideration such concretes as polymer-impregnated concrete, epoxy concrete, or concrete made with artificial normal and heavy-weight aggregates.

This definition of HSC will be used in this report. Concretes with compressive strengths in excess of 40 MPa will be referred to as HSC, and concretes with lower compressive strengths will be referred to as NSC in this report.

It is well established that the structural properties of concrete are modified by thermal exposure. Concrete, in general, is believed to lose approximately 25% of its original compressive strength when heated to 300 °C, and approximately 75% when exposed to 600 °C. The elastic modulus is believed to be reduced in similar fashion. Concrete stress-strain relationships are also unfavorably modified by high temperature exposure. The variations in properties of heated concrete have been reported extensively in professional committee reports such as ACI 216R-89, CEB Bulletin D'Information N° 208, RILEM Committee 44-PHT, the CEN Eurocodes, and the Concrete Reinforcing Steel Institute's *Reinforced Concrete Fire Resistance*. However, the conclusions and recommendations offered by these reports are based primarily on data from tests of NSC specimens.

Neville (1973) provided a good summary of knowledge related to the fire performance of NSC. He noted that exposure to fire subjects a concrete member to high thermal gradients and there is a tendency for the hot surface layers to separate and spall from the cooler interior. He also reported that a definite loss in strength is observed at temperatures above 300 °C, and that the strength loss is greater in saturated concrete than in dry concrete. In addition, high moisture content contributes to the tendency for spalling during fire tests of concrete members, and spalling is absent when the moisture content of the concrete is in equilibrium with air. The loss in strength is greater for mixtures with high cement contents. The type of aggregate has a significant influence on the fire behavior, with a lower strength reduction occurring in concrete made with aggregates that do not contain silica, such as limestone, basic igneous rocks, crushed brick, and blast-furnace slag. Dolomitic limestone is particularly beneficial in improving fire performance because the calcination process absorbs heat, and the lower density calcined material provides a greater insulating effect.

Recent results of fire tests have shown that there are well-defined differences between the properties of HSC and NSC at high temperatures. However, what is more important about HSC is the occurrence of explosive spalling when HSC is subjected to rapid heating, as in the case of a fire. This failure mechanism was mentioned but not dealt with sufficiently in the aforementioned committee reports. Thus it remains to be examined to what extent the recommendations in these reports are applicable to HSC. Experimental studies have shown that explosive spalling of HSC is affected by the following factors: (1) rate of temperature rise, (2) mineralogical composition of the aggregates, (3) thermal induced mechanical stresses, (4) reinforcement arrangement, (5) moisture content, and (6) density of the concrete matrix.

HSC is achieved mainly by using a low water-cement (w/c) ratio and silica fume. Thus HSC has lower permeability and water content compared with NSC. It has been theorized, and somewhat qualitatively validated by experiments, that the higher susceptibility of HSC to explosive spalling when subjected to high temperature is due, in part, to the lower permeability of HSC which limits the ability of moisture to escape from the pores. This results in a build-up of pore pressure within

the cement paste. As heating increases, the pore pressure also increases. This increase in vapor pressure continues until the internal stresses becomes so large as to cause explosive spalling of the heated concrete. This failure mechanism has been observed on an inconsistent basis by researchers. Often, explosive spalling has occurred to only a few of HSC specimens from a larger group of specimens that were subjected to identical testing conditions. This erratic behavior makes it difficult to predict with certainty when HSC will fail by explosive spalling.

1.2 Research Objectives and Scope

The long-term objective of this project is to ensure that premature structural collapse of HSC structures will not occur during a fire. Understanding the performance of HSC when exposed to high temperature is an important first step in meeting this objective. To achieve the long term goal, the following three specific objectives have been established for this research project:

1. To develop an understanding of the performance of HSC when exposed to high temperatures, especially understanding the explosive spalling failure mechanism that has been often observed.
2. To develop analytical tools for assessing fire performance and for predicting the failure mechanism of HSC.
3. To develop a practical model for fire design of HSC structures and to develop draft provisions to implement this model into code provisions.

To achieve objectives 1 and 2, research results will be reviewed, and additional experiments will be planned to develop sufficient experimental data for accurate characterization of the behavior of HSC when subjected to fire. The data will also be used for the development, calibration and validation of models to predict spalling failure of HSC when subjected to fire.

To achieve objective 3, the results of experimental and parametric studies will be synthesized to produce practical constitutive relationships for HSC at various temperatures. These constitutive relationships will be presented to code writing organizations for possible implementation to aid in the fire design of HSC structures.

1.3 Scope of Report

The report consists of 5 chapters.

Chapter 2 reviews experimental studies of HSC at high temperature. The experimental studies reviewed consist of both materials test programs and structural element test programs. Also reviewed are studies which used the stiffness damage test and the scanning electron microscopy to assess the behavior of HSC at high temperature. A summary of important behavioral trends revealed

by these studies concludes this chapter.

Chapter 3 reviews modeling techniques developed to study the thermal behavior of concrete by characterizing the moisture transport and the internal stress developed during high temperature exposure.

Chapter 4 reviews the fire test methods prescribed by major standard organizations such as the International Standard Organization (ISO), the American Society for Testing and Materials (ASTM), and Japanese Industrial Standards (JIS). Code provisions on the structural properties of concrete exposed to high temperature are also reviewed in this chapter.

Chapter 5 summarizes key information obtained from this review and provides recommendations for future action.

2. EXPERIMENTAL STUDIES ON FIRE PERFORMANCE OF HSC

2.1 Introduction

The effects of high temperature on the mechanical properties of concrete have been investigated since the 1940s (Menzel, 1943; Binner, 1949; Malhotra, 1956; Saemann, 1957; Gustafsson, 1967). These studies may be divided into two categories: *materials testing* and *element testing*. *Materials testing* involves mainly tests of plain concrete specimens. The results of *materials testing* provide information on the effects of temperature on mechanical properties, such as compressive strength, modulus of elasticity, and ultimate strain. *Element testing* involves tests of reinforced concrete structural elements such as beams, columns, and slabs. Results of *element testing* can be used to assess the fire endurance of particular concrete structural elements and to provide data for development of rules for fire design of concrete structures (CEB Bulletin D'Information No. 208, 1991).

Since these early studies were conducted prior to the advent of HSC for use in construction, the test specimens were usually made of concretes with either low or normal strength. Since the focus of this report is on the fire performance of HSC, these early studies, and more recent studies which did not use HSC (Mohamedbhai, 1983), are not reviewed in this chapter. Also absent are studies which investigated the performance of HSC under long-term, sustained high temperature (Carette et al., 1983; Kasami et al., 1975) since sustained high temperature exposure differs from performance during a fire (short-term exposure). Thus only reviews of more recent experimental studies which considered HSC are included in this chapter. The studies reviewed, include 10 *materials testing* programs (Castillo, 1990; Hertz, 1984; Diederichs, 1988; Hammer, 1995; Sullivan, 1982; Abrams, 1971; Morita, 1992; Furumura, 1995; Felicetti, 1996; and Noumowe, 1996) and 6 *element testing* programs (Hansen, 1995; Ophem, 1995; Sanjayan, 1991; Saito, 1992; Kumagai, 1992; Shirley, 1987).

A number of different test methods were used in the reviewed experimental programs to determine the mechanical properties of HSC at elevated temperatures. The test methods can be generally grouped into two categories: *Steady State Temperature Tests* and *Transient Temperature Tests* (Schneider, 1982; Schneider, 1985; Comité Euro-International du Béton, 1991). The test method selected for a particular study depended on the desired test data, e.g., stress-strain relationships, stress vs. time relationships at different temperatures, strain vs. time relationships at different temperatures, etc. Different test methods were also selected to simulate the internal stress conditions related to specific concrete structural elements, such as beams and columns. The interpretation and applicability of the test results depend on the specific test method employed. Thus, to better understand the results of the experiments reviewed in this chapter, brief descriptions of test methods commonly used in fire testing of HSC are given in the following section.

2.2 Test Methods used for Determination of Mechanical Properties of HSC

2.2.1 Idealized Test Methods

There are six idealized test methods for testing concrete at high temperature. Four of which belong to the category of the *steady state temperature tests*, and two belong to the category of the *transient temperature tests*. These test methods are widely described in the literatures (Schneider, 1982; Schneider, 1985; Comite Euro-International du Beton, 1991). Each test method is designed to yield the particular data required by the test program. Typically, *steady state temperature tests* are characterized by a period during which the specimen is heated to target temperature, followed by a period during which the target temperature is maintained until a steady state condition is developed (stability of temperature at various sections or points in the specimens). Load is applied after the steady-state condition has been attained. *Transient temperature tests* are characterized either by one of the following: simultaneous application of heating and loading, the load may be applied before heating, the load may develop during heating, such as by restraint against thermal expansion. These six *test methods* are summarized below to aid in better understanding the procedure for fire testing of HSC and in interpreting results from the reviewed experimental programs.

Steady state tests include:

1. *Stress Rate Controlled test*: The test specimen is heated to the specified temperature with a constant heating rate. When the test temperature is reached, it is maintained until a homogeneous temperature distribution is achieved. The specimen is then subjected to a constant rate of loading until the ultimate load is achieved. Data from this type of test can be used to determine compressive strength, modulus of elasticity, and strain at ultimate strength as a function of temperature. Also, stress-strain relationship (up to the ultimate strength) at different temperature can be developed.
2. *Strain Rate Controlled test*: The test specimen is heated to the specified temperature with a constant heating rate. When the specimen has reached a steady state condition, it is loaded at a constant strain rate. This kind of test allows the complete stress-strain curve to be developed, from which it is possible to determine the mechanical energy dissipated by the specimen up to complete failure. The measured data are influenced by the strain rate. The data can be used to establish the same properties mentioned in the *stress rate controlled* test, but also the dissipated mechanical energy.
3. *Steady State Creep Test*: The test specimen is slowly heated to the target temperature and a steady state condition is allowed to develop. After the steady state condition is reached, the load is applied. Both the target temperature and the load are kept constant during the test period, which is typically longer than the test period of other types of tests. The measured results are creep deformation (strain) due to sustained constant load at different temperature. The elastic deformation which occurs immediately following the application of load is separated from the creep deformation which results from long term, sustained loading. This type of test is not applicable to a concrete structure in a fire since the test duration is

normally far longer than the duration of building fires.

4. *Relaxation Test*: The test specimen is heated to target temperature, and a steady state condition is allowed to develop prior to application of load (similar to the *steady state creep test*). The initial, elastic strain resulting immediately from the application of load (not creep strain) is recorded. The specimen is maintained at this initial strain during the duration of the test, and measurements of stress as a function of time are recorded. Similar to the *steady state creep test*, the duration of this test exceeds the practical duration of building fires. Thus this test has little relevance to performance under a fire situation.

Transient Tests include:

5. *Transient Creep Test*: The specimen is subjected to a constant applied load, usually a percentage of the specimen's ultimate strength measured at room temperature, prior to heating. The specimen is then heated at a constant rate until failure occurs. The measurements result in a family of strain versus time curves corresponding to different applied loads.

6. *Transient Relaxation Test*: Load is applied to the specimen prior to heating, and an initial strain is recorded. This initial strain is maintained for the duration of the test by adjusting the applied load while the specimen is heated at a specified rate. The test is terminated when the applied stress level falls to zero. The measurements can be expressed as stress versus time relationships for different initial strain levels.

Unlike the *steady state creep* and *relaxation tests*, where the test durations far exceed practical durations of building fires, the *transient creep* and *relaxation tests* simulate the transient conditions which concrete members might experience in real fire situations. Thus data obtained from the *transient tests* have relevance to performance of concrete structure during fires.

2.2.2 Common Test Methods

Most of the test programs reviewed in this report did not follow strictly the idealized test methods outlined above. Rather, the test methods that were used may be described as being derived from the above idealized test methods. Three test methods, commonly referred to as *stressed*, *unstressed*, and *unstressed residual strength tests*, have been used in most experimental programs on the fire performance of HSC. General descriptions of these test methods are given below:

1. *Stressed Test*: A preload, often in the range of 20 to 40 percent of the ultimate compressive strength at room temperature (usually 20 °C), is applied to the concrete specimen prior to heating, and the load is sustained during the heating period. Heat is applied at a constant rate until a target temperature is reached, and the temperature is maintained until a thermal steady state is achieved (reportedly 5 to 10 minutes). Load or

strain is then increased at a prescribed rate until the specimen fails. The results are usually compressive strengths and moduli of elasticity at different temperatures. As can be seen from the previous descriptions of the six idealized test methods, the *stressed test* is a modified version of the *steady state temperature, stress or strain rate controlled test*. The results of this test are most suitable for representing fire performance of concrete in a column or in the compression zone of beam.

2. *Unstressed Test*: The specimen is heated, without preload, at a constant rate to the target temperature, which is maintained until a thermal steady state is reached within the specimen. Load or strain is then applied at a prescribed rate until failure occurs. This test method is identical to the *steady state temperature, stress or strain rate controlled test*. The results of this test are most suitable for representing fire performance of concrete in the tension zone of beam, or concrete in an element which has a small preload.

3. *Unstressed Residual Strength Test*: The specimen is heated without preload at a prescribed rate to the target temperature, which is maintained until a thermal steady state is reached within the specimen. The specimen is then allowed to cool, also following a prescribed rate, to room temperature. Load or strain is applied at room temperature until the specimen fails. The *unstressed residual strength test* differs from all the test methods described above, and its results are most suitable for assessing the post-fire (or residual) properties of concrete.

2.3 Experimental Studies

Two main groups of experimental studies are reviewed in this report: (1) the *materials test* group, and (2) the *element test* group. *Materials tests* involve testing of plain HSC cylinders and/or cubes, often using the common test methods outlined in section 2.2.2. The results of *materials tests* show the effects of high temperature on engineering material properties and can be used to develop material constitutive models for analytical purposes. *Element tests* involve testing of reinforced HSC structural members, such as beams, columns, and slabs. The results of *element tests* show the effects of high temperature on structural elements and can be used for validating analytical model developed using data obtained from *materials tests*.

2.3.1 Materials Tests

2.3.1.1 Castillo and Durani (1990)

The effects of transient high temperature on the strength and load-deformation behavior of HSC were investigated by Castillo and Durani (1990). Two types of concrete mixtures were used, a normal strength mixture (Mix I) with a water/cement ratio of 0.68 and a specified concrete strength of 27.6 MPa, and a high-strength mixture (Mix II) with a water/cement ratio of 0.327 and a specified concrete strength of 62.1 MPa. Both mixtures were made from Type I portland cement with natural

river sand and crushed limestone. Superplasticizer was used in Mix II to obtain a workable mixture. The specimens were 51 x 102 mm high cylinders. Maximum aggregate size was 9.5 mm.

For each type of concrete, two types of test were performed: *stressed* and *unstressed*. Tests were performed in a closed-loop servo-controlled 985-kN hydraulic testing machine equipped with an electric furnace. The load was applied under strain rate control. The measured compressive strengths at testing were 31 MPa (Mix I, at 65 days), 63 MPa (first batch of Mix II, at 67 days), and 89 MPa (second batch of Mix II, at 90 days).

For each set of cylinders tested at a given temperature, three specimens from the same batch were also tested at room temperature to provide reference values. The temperatures were varied from 100 to 800 °C in 100 °C increments. The heating rate for all specimens averaged between 7 and 8 °C/min.

Molds were removed from the specimens 24 hrs after casting, and the specimens were stored in a moist room at 23 °C and 100 percent relative humidity for a period of 60 to 90 days. Two weeks prior to testing, the specimens were removed from the moist room and kept at room temperature with 55 to 65 percent relative humidity until the time of test. During the heating period, moisture in the specimens was allowed to escape freely. The moisture content of the specimens at the time of testing was not measured.

In the *unstressed tests*, the specimens were heated to the desired temperature, which was maintained for 5 to 10 minutes to attain a steady state condition at the center of the specimen. The specimens were then loaded until failure.

In the *stressed tests*, 40 percent of the ultimate compressive strength at room temperature was applied to the specimens and sustained during the heating period. After the temperature reached the steady state, the load was increased at the prescribed rate until the specimen failed. The control specimens were tested at room temperature on the day of the high-temperature tests. The results of both test methods are plotted in the form of normalized compressive strengths and moduli of elasticity versus temperature, and load-deformation curves at different temperatures, as shown in Figures 2.1 to 2.4.

Each data point in Figures 2.1 and 2.2 represents an average of the maximum compressive strength of at least three specimens normalized with respect to the maximum compressive strength at room temperature (25 °C). The trend observed in these Figures is common to both mixtures. The load-deformation plots showed that the normal strength concrete (NSC) specimens had a ductile type of failure up to 100 °C. At 200 °C, the NSC specimens failed in a brittle manner soon after reaching their peak strengths. Between 300 to 800 °C, the NSC specimens were able to undergo large post-peak strains and the decrease in load was more gradual. The HSC specimens showed a brittle type of failure up to 200 °C. At 300 °C, about one-third of the HSC specimens were reported to have failed explosively during loading. With further increases in temperature, the HSC specimens began to

exhibit a more gradual failure. Between 600 to 800 °C, the HSC specimens were able to undergo large post-peak strains and decrease in load was more controlled and gradual. Under the preloaded condition (*stressed tests*), the HSC specimens (89 MPa concrete) could not sustain the load beyond 700 °C, and about one-third of the specimens failed in an explosive manner between temperatures of 320 to 360 °C while load was being increased.

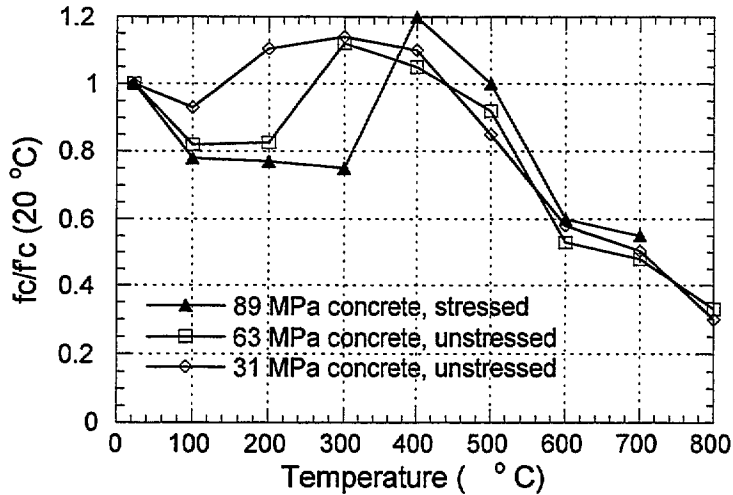


Figure 2.1. Compressive Strength vs. Temperature Relationships (Castillo and Durani, 1990)

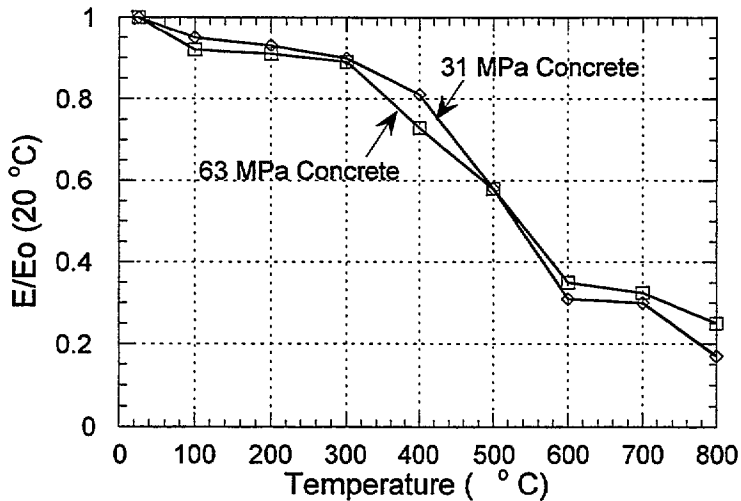


Figure 2.2. Modulus of Elasticity vs. Temperature Relationships (Castillo and Durani, 1990)

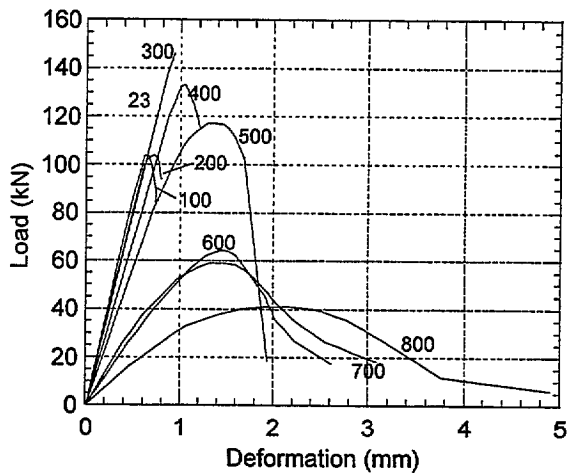


Figure 2.3. Load-Deformation Behavior of HSC at High Temperatures (Castillo and Durani, 1990)

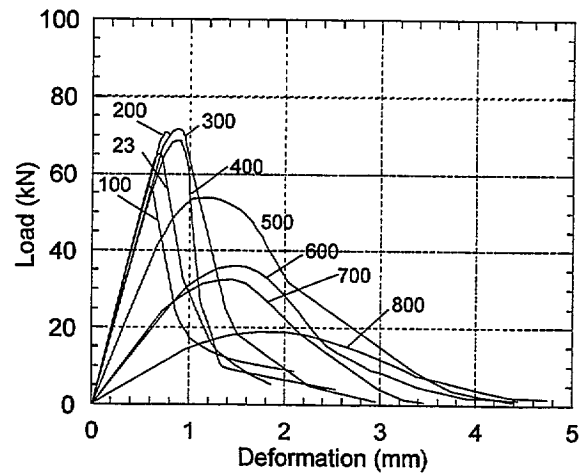


Figure 2.4. Load-Deformation Behavior of NSC at High Temperatures (Castillo and Durani, 1990)

The following conclusions were drawn from this study:

- When exposed to temperatures in the range of 100 to 300 °C, HSC showed a 15 to 20 percent loss of compressive strength. Whereas the NSC showed no such strength loss. As the strength of concrete increased, the loss of strength from exposure to high temperature also increased.
- After an initial loss of strength, HSC recovered its strength between 300 and 400 °C, reaching a maximum value of 8 to 13 percent above the room temperature strength. As the strength of concrete increased, the recovery in strength also occurred at a higher temperature.
- At temperatures above 400 °C, HSC progressively lost its compressive strength which dropped to about 30 percent of the room temperature strength at 800 °C. This decrease was similar to that of the NSC.
- None of the preloaded specimens were able to sustain the load beyond 700 °C. About one-third of these specimens failed in an explosive manner in the temperature range of 320 to 360 °C while being heated under a constant preload.
- The modulus of elasticity of the HSC decreased by 5 to 10 percent when exposed to temperatures in the range of 100 to 300 °C. At 800 °C, the modulus of elasticity was only 20 to 25 percent of the value at room temperature. Similar variations of modulus of elasticity were observed for HSC and NSC. Beyond 300 °C, the elastic modulus decreased at a faster rate with increase in temperatures.

2.3.1.2 Hertz (1984, 1991)

Two test series were conducted by Hertz (Hertz, 1984 and Hertz, 1991). The principal variables in the two test series included: temperature, cylinder size, and percentage of steel fibers added to the concrete mix to reduce the risk of explosion.

In test series 1, fifteen silica-fume concrete cylinders (14 to 20 percent silica fume), of dimensions 100 x 200 mm, were tested according to the *unstressed residual strength test* method. The concrete density was measured as 2,680 kg/m³. The concrete had an average measured compressive strength at room temperature of 150 MPa. The unconventional silica fume concrete in series 1 (called *Densit*) was composed of :

		kg/m ³
Diabase fraction	4-16 mm	1080
Quartz sand -	1-4 mm	404
Quartz sand -	0.25-1 mm	202
Quartz sand -	0-0.25 mm	101
Sand-lime cement		500
Elkem silica		100
Mighty (superplasticizer)		25
Water		80

After casting, the specimens were stored for 20 days under water and for 60 days at 20 °C and 60 percent relative humidity. The specimens were then heated in an electric oven at a rate of 1 °C/min to temperature levels of 20, 150, 350, 450, and 650 °C. Each temperature level was maintained for 2 hours for a thermal steady state to develop, and then the oven was cooled down at a rate of 1 °C/min. Seven days after the heating and cooling cycle, the specimens were loaded at a constant stress rate. Three replicate specimens were tested for each condition. The results of test series 1 are presented in terms of compressive strength and modulus of elasticity versus temperature, as shown in Figures 2.5 and 2.6.

The results of test series 1 indicated that on average the residual compressive strength of HSC (compressive strength after exposure to heat) increased with temperature up to 350 °C, and decreased with higher temperature exposure. However, the behavior was erratic with strength at 150 °C varying from 0.8 to 1.4 of the room temperature values. The study also reported four of the fifteen specimens exploded during heating. One at 350 °C, two at 450 °C, and one at 650 °C. Examination of the exploded specimens showed that fractures crossed the aggregates as well as the cement paste matrix.

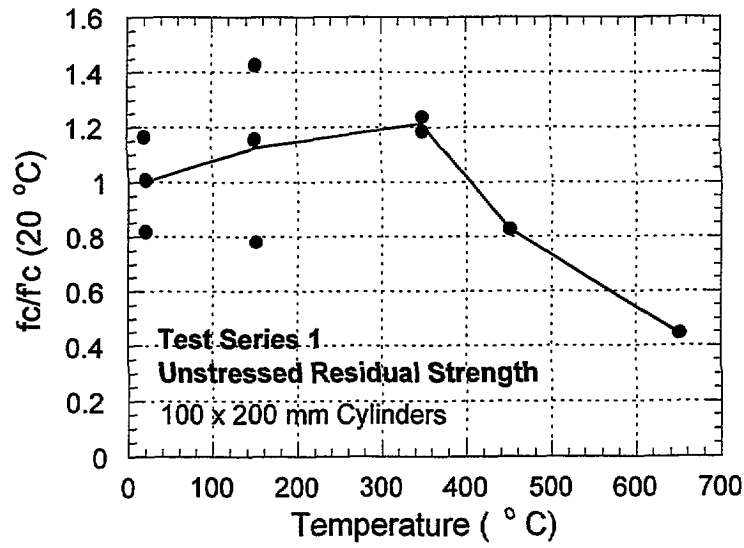


Figure 2.5 Variation of Compressive Strengths with Temperature (Hertz, 1984)

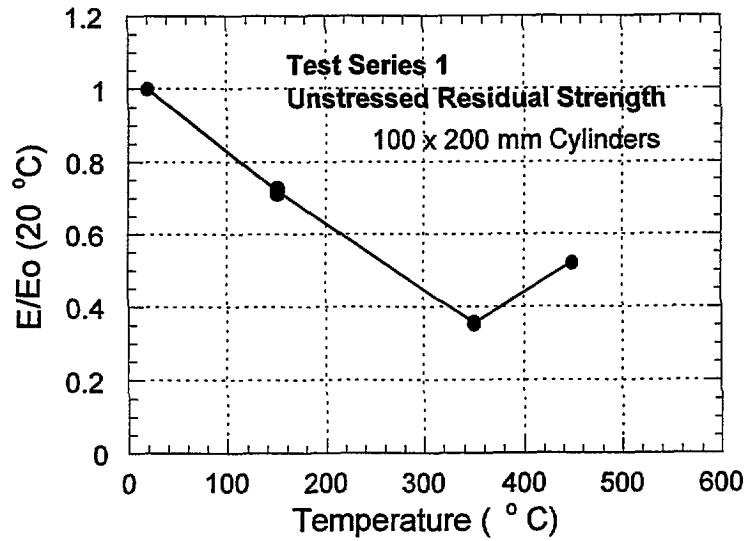


Figure 2.6. Variation of Elastic Modulus with Temperature (Hertz, 1984)

In test series 2, silica fume concrete (called Densit) with a lightweight aggregate of burned bauxite was used. The concrete included steel fiber reinforcement (0.4 x 12 mm steel fibers) at proportions of 0.0, 1.5, and 3.0 percent by volume of concrete to improve the resistance to thermal stresses and, if possible, to diminish the risk of explosion. Three sizes of cylinders were used: 100 x 200 mm (24 cylinders), 57 x 100 mm (24 cylinders), and 28 x 52 mm (24 cylinders). *Unstressed residual tests* were also used, as in test series 1. The cylinders were heated at a constant heating rate of 1 °C/min to temperatures of 200, 400, and 600 °C, which were maintained for 1 hour for the steady state to develop. The specimens were then allowed to cool at rate of 1 °C/min. The results are shown in Figures 2.7 and 2.8.

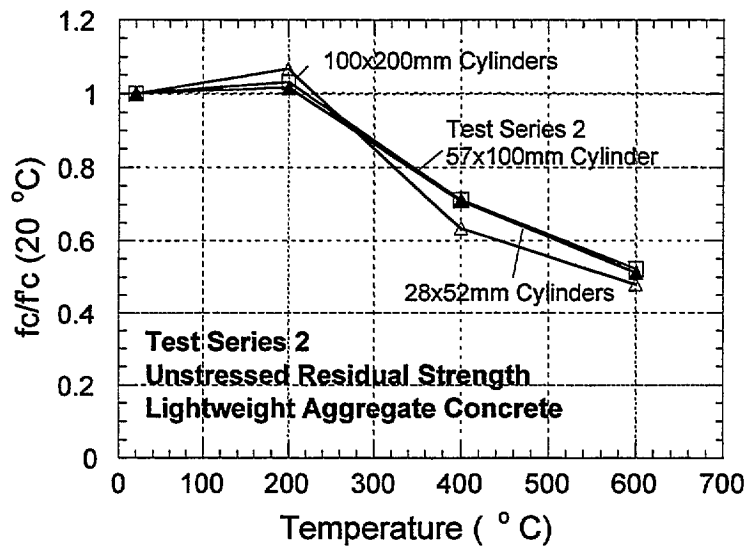


Figure 2.7 Variation of Residual Strength with Temperature for Different Specimen Sizes (Hertz, 1991)

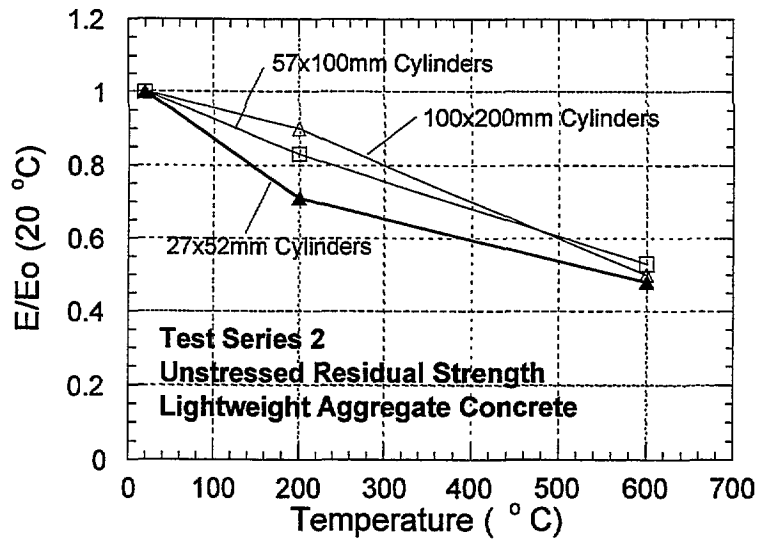


Figure 2.8. Variation of Residual Modulus of Elasticity with Temperature for Different Specimen Sizes (Hertz, 1991).

The trend in behavior is similar to test series 1. A small gain in residual compressive strength was observed for all cylinder sizes between the temperature range of 23 to 200 °C, followed by a decrease in residual strength at higher temperature. Hertz observed that only the largest size of cylinders (100 x 200 mm) with the highest fiber content (3 percent) exploded (three specimens). Two exploded at 400 °C, and one at 600 °C.

The study offered the following general conclusions:

- Concrete densified by means of silica fume may explode during heating;
- The presence of steel fiber does not reduce the risk of explosion;
- Lightweight concrete is not recommended in place of normal weight concrete when spalling is concerned.

2.3.1.3 Diederichs, Jumppanen, and Penttala (1988)

Diederichs et al. (1988) performed *unstressed (strain rate controlled) tests, transient creep tests, and transient relaxation tests* on specimens made of three different HSC concretes. One was a blast furnace slag cement concrete (series Tr), one was a portland cement with silica fume concrete (series Si), and one was a portland cement with class F fly ash concrete (series Lt). In addition, normal strength concrete with ordinary portland cement (series OPC) was also tested for comparison.

Besides compressive strength, specimen shape (cubes and cylinders) and heating rate (2 °C/min and 32 °C/min) were also examined. Concrete cubes (100 x 100 x 100 mm) and concrete cylinders (80 x 300 mm) were exposed to temperatures up to 850 °C. The concretes had the following properties:

Concrete series	Si	Lt	Tr	OPC
Density (kg/m ³)	2,648	2,594	2,654	2,390
Cube strength (MPa)				
- 28 days	114.4	87.3	91.4	48.0
- 90 days	100.8	106.9	111.9	36.0
Cylinder strength (MPa)				
- 90 days	106.6	91.8	84.5	32.9

The published report was not clear on the number of specimens tested. In general, the specimens were heated without external load at a rate of either 2 °C/minute or 32 °C/minute, up to the desired temperatures. The specimens were then kept for 2 hours at the desired temperatures to reach a steady state condition, and tested in compression at a constant strain rate of about 0.05% per minute. The results of the *unstressed tests* are shown in Figures 2.9 to 2.12. Figures 2.9 and 2.10 show the variations of compressive strengths and moduli of elasticity of all concretes with respect to temperatures. Figures 2.11 and 2.12 show typical stress-strain relationships for HSC and NSC, respectively.

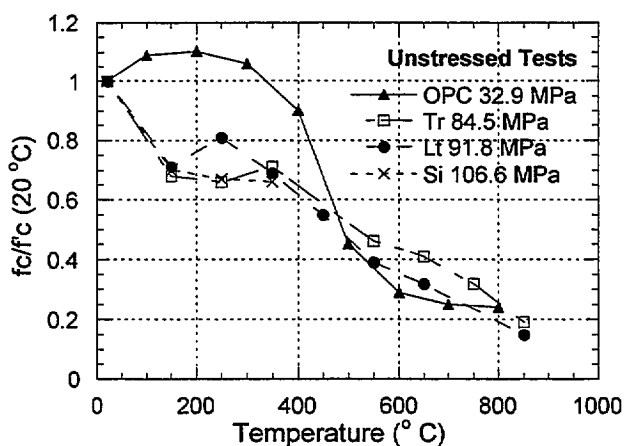


Figure 2.9. Variation of Compressive Strength with Temperature for Different Concretes (Diederich et al., 1988)

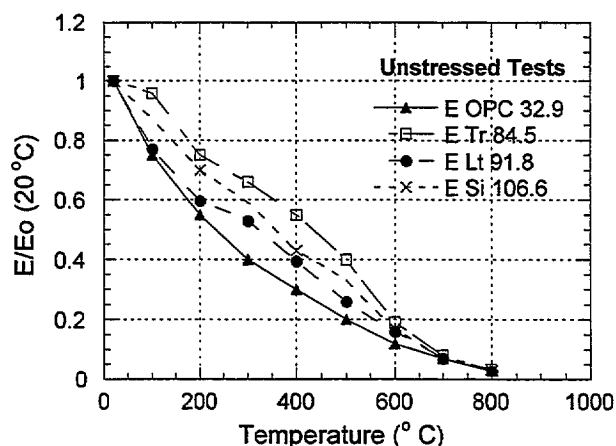


Figure 2.10. Variation of Elastic Moduli with Temperature for Different Concretes (Diederichs et al., 1988)

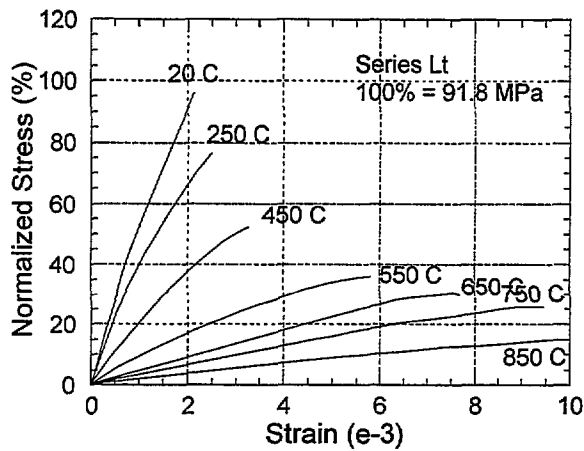


Figure 2.11 Stress-Strain Relationships of HSC Made with Fly Ash (Diederichs et al., 1988)

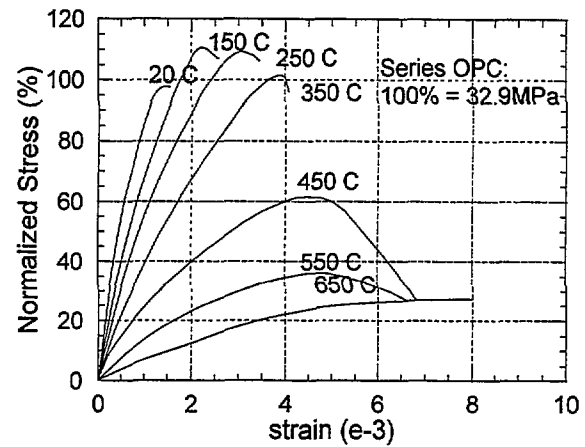


Figure 2.12 Stress-Strain Relationships of NSC Made with Ordinary Portland Cement (Diederichs et al., 1988)

The Figures show that stress-strain, compressive strength-temperature, and modulus of elasticity-temperature relationships of HSC differ from those of normal strength concrete. The following observations were made:

- HSC specimens failed in a more brittle manner than normal strength concrete specimens.
- Destructive spalling did not occur in any of the specimens heated at rate of 2 °C/minute.
- Slight spalling occurred to some cylinders used in the *transient creep* and *transient relaxation tests* (preloaded prior to heating) which were heated at a high rate of 32 °C/minute.
- Spalling occurred in all pre-loaded cubes heated at a rate of 32 °C/min.

The following conclusions were drawn from this study:

- The so-called “dry-hardening” which causes the increase of strength in normal strength concrete between 150 to 350 °C was not observed for HSC, instead the strength of HSC decreased in this temperature range.
- Besides heating rate and paste density, the dimensions and shapes of specimens are also important with respect to explosive spalling.

2.3.1.4 Hammer (1995)

Hammer (1995) conducted *unstressed (stress rate controlled) tests* to study the effects of the following variables on the fire performance of HSC:

1. *Concrete Compressive strength*: which was varied between 69 MPa to 118 MPa. The variation in compressive strength was achieved by changing the water/cement ratio from 0.27 to 0.50. Five different concrete mixtures were used as follow:

Concrete Mixtures	w/c Ratio	Silica Fume
ND65	0.50	5% (by mass of cement)
ND95	0.36	5%
ND95-0	0.36	0%
ND115	0.27	5%
LWA75	0.36	5%

2. *Aggregate Type*: lightweight aggregate vs. normal weight crushed gravels.
3. *Temperature*: varied from 20, 100, 200, 300, 450, and 600 °C.

The specimens were 100 x 310 mm cylinders. Two specimens were tested at each temperature level, one at 90 day of age and one at 150 day of age. The cylinders were stripped, the ends were cut, then cured at room temperature (20 °C) under plastic two days before testing.

Five cylinders, to be tested one each at the targeted temperatures of 100, 200, 300, 450, and 600 °C, were weighed and heated together at a rate of 2 °C/minute. Each cylinder was removed from the oven at the targeted temperature and weighed again for mass loss (moisture evaporation). The cylinder was reheated using a steel tube covered by a heating element and loaded. The time between removal from the oven to the start of testing was typically 8 minutes. The loading plates were also heated to minimize heat loss. The loading rate was 0.80 MPa/s. The measured concrete strengths and moduli of elasticity are summarized in Tables 2.1 and 2.2.

The test results, in terms of variations of compressive strengths and moduli of elasticity with respect to temperatures are shown in Figures 2.13 to 2.16. Also plotted in Figures 2.17 and 2.18 are the relationships between the measured mass loss and the strength loss.

Table 2.1 Compressive Strengths at High Temperature (Hammer, 1995)

Temp. °C	Age (days)	Concrete Strengths (MPa)				
		ND65	ND95	ND95-0	ND115	LWA75
20	90	69.3	96.4	83.1	118.4	89.6
	150	69.3	102.2	81.9	117.4	94.1
100	90	58.2	83.9	62.8	102.8	72.8
	150	61.6	88.7	63.7	93.7	82.8
200	90	47.1	69.4	54.0	85.3	67.7
	150	50.3	68.7	66.2	84.7	70.6
300	90	44.6	60.3	70.6	76.2	55.8
	150	42.5	63.5	64.6	85.2	56.6
450	90	49.6	70.2	68.7	85.6	61.6
	150	52.2	73.3	72.2	87.2	66.2
600	90	26.7	37.8	34.0	47.1	47.7
	150	27.1	37.5	42.2	44.6	39.3

Table 2.2 Modulus of Elasticity at High Temperature (Hammer, 1995)

Temp.	Age (days)	E-Modulus (GPa)				
		ND65	ND95	ND95-0	ND115	LWA75
20	90	27.2	30.5	30.5	35.3	22.5
	150	27.9	29.5	30.4	36.0	24.4
100	90	20.7	25.8	19.7	26.7	21.1
	150	23.8	27.9	20.7	27.2	23.0
200	90	15.7	21.2	18.6	24.0	16.8
	150	17.7	23.1	21.8	25.0	27.2
300	90	15.8	19.3	20.9	23.0	15.7
	150	17.6	22.5	21.2	26.3	16.9
450	90	9.1	14.2	13.0	16.3	12.8
	150	10.3	14.6	15.6	17.0	13.9
600	90	3.6	5.0	6.7	6.5	8.6
	150	3.9	7.3	5.9	6.7	7.5

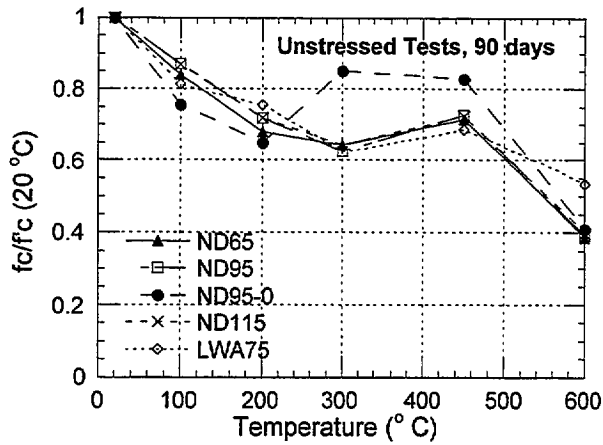


Figure 2.13 Compressive Strengths of 90-day Concretes vs. Temperature (Hammer, 1995)

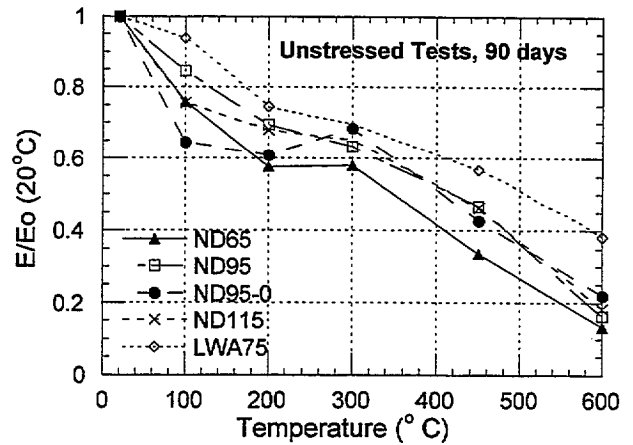


Figure 2.14 Elastic Moduli of 90-day Concretes vs. Temperature (Hammer, 1995)

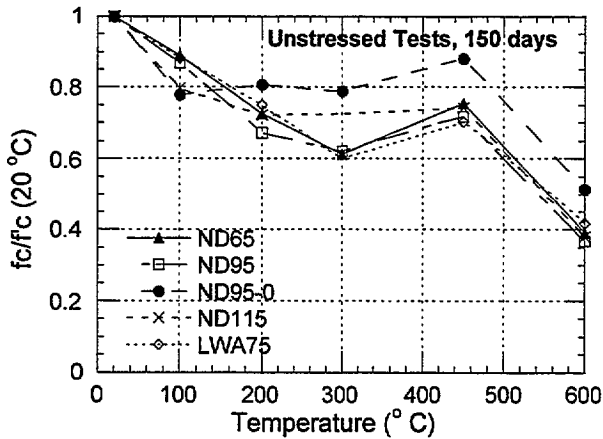


Figure 2.15 Compressive Strength of 150-day Concretes vs. Temperature (Hammer, 1995)

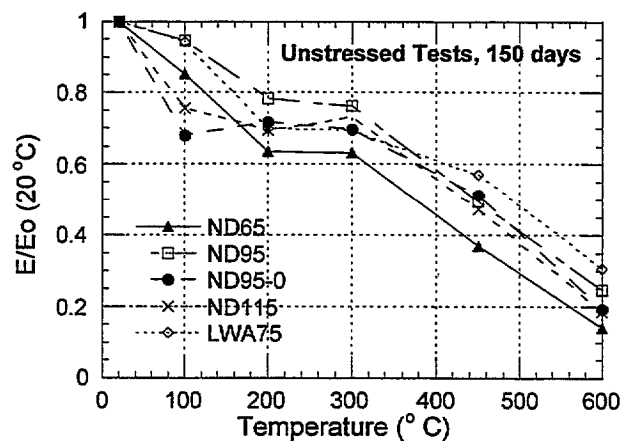


Figure 2.16 Elastic Moduli of 150-day Concretes vs. Temperature (Hammer, 1995)

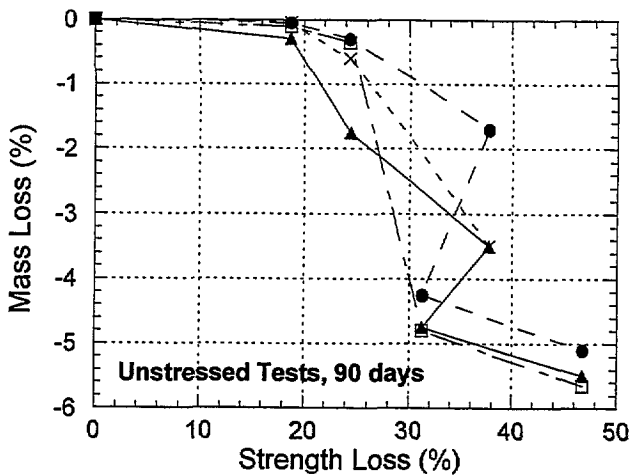


Figure 2.17 Mass Loss vs. Strength Loss for 90-day Concretes (Hammer, 1995)

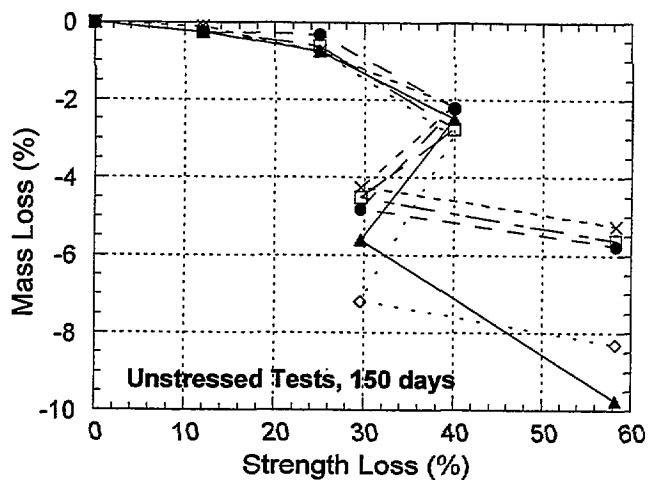


Figure 2.18 Mass Loss vs. Strength Loss for 150-day Concretes (Hammer, 1995)

The following conclusions were presented:

- The difference in terms of strength loss with increasing temperature for the different concretes examined in this study was insignificant, except for ND95-0 (no silica fume concrete) which showed a gain in strength between 200 to 300 °C.
- A typical “*breakpoint*” in the strength-temperature curves was observed at 300 °C. The study reported that at this temperature an explosive failure followed by the release of a lot of steam was observed. No such explosive failure or steam release was observed at the other temperatures. The author speculated that the reason for the reduced strength even at low temperatures (between 100 to 300 °C), is the high internal pressure due to the reduced ability of moisture to escape from HSC.
- An increase in compressive strength was observed for all concretes, except for ND95-0, between 300 to 450 °C. For mix ND95-0, the strength increase occurred earlier, between 200 to 300 °C.
- Moduli of elasticity of all concretes decreased at a faster rate at temperature above 300 °C.
- Concrete without silica fume (ND95-0) show slightly better performance in terms of lower strength loss.
- The replacement of normal weight coarse aggregate with light-weight aggregate does not seem to affect the temperature dependent strength loss.

2.3.1.5 Abrams (1971)

This study is one of the early studies on the effects of short-term exposure of concrete to high temperatures. It is reviewed here, even though NSC was used, because its results were widely used in codes and committee reports as basic information on fire performance of concrete (see chapter 4). The study examined four variables, including:

1. *Aggregate types*: Three types of aggregate were considered: carbonate (dolomitic sand and gravel from Elgin, Illinois), siliceous (sand and gravel from Eau Claire, Wisconsin), and expanded shale lightweight aggregates. All were 19 mm maximum size.
2. *Test Methods*: The three common test methods described in section 2.2.2 were considered: *unstressed test* (heated without load and tested hot), *stressed test* (heated with load and tested hot), and *unstressed residual test* (tested at room temperature after heating).
3. *Concrete Strengths*: Ranging from 22.8 to 44.8 MPa.
4. *Temperature*: Ranging from 93 to 871 °C.

The specimens were cylinders, 75 x 150 mm, and were cast in groups of 11 (4 for high temperature tests, 6 for room temperature tests, and 1 for monitoring humidity). Three different concretes (for the three different aggregates), each with two specified compressive strengths of 22.8 and 44.8 MPa, were used. The two lightweight concrete mixtures contained normal weight sand from Elgin, Illinois. The specimens were stored at 30 to 40% R.H. and 21 to 24 °C until the R.H. at the center of the specimen reached 75%. Specimens not tested immediately after reaching 75% R.H. were placed in a room maintained at 70 to 80% R.H. and 21 to 24 °C until time of test. Some specimens were dried to constant mass at 110 °C.

Thermocouples were placed inside the cylinders at four locations to monitor internal temperatures. In general, it took about 3 to 4 hours to achieve uniform temperature within the specimens. Test were not conducted until the difference in temperature between the four thermocouples was within 11 °C for test temperatures up to 316 °C. For higher test temperatures, the difference was set to 3 percent of the test temperature. Test results, in terms of variations of compressive strengths with respect to temperature, obtained for different test methods and different types of aggregate are shown in Figures 2.19 to 2.24. The following conclusions were reported:

- Up to about 480 °C, all three concretes exhibited similar strength loss characteristics under each test condition (*stressed*, *unstressed*, and *unstressed residual*). Above 480 °C, the siliceous aggregate concrete had greater strength loss and retained less strength for all three test conditions. Specimens made of carbonate aggregates and lightweight coarse aggregates behaved about the same over the entire temperature range and retained more than 75% of their original strength at temperatures up to 649 °C in *unstressed tests*. For the siliceous aggregate, the strength was 75% of the original strength at 430 °C.

- Compressive strengths of specimens with preload (*stressed tests*) were generally 5 to 25% higher than those without preload (*unstressed tests*). Also the preloads of 25, 40, and 55% of the room temperature compressive strength, had insignificant effect on compressive strengths of the *stressed* specimens.
- The *unstressed residual* specimens had the lowest strength compared with *stressed* and *unstressed* specimens tested at high temperatures.
- Within the range of compressive strength tested (up to 44.8 MPa), the original compressive strength had little effect on the strength reduction at the test temperatures.

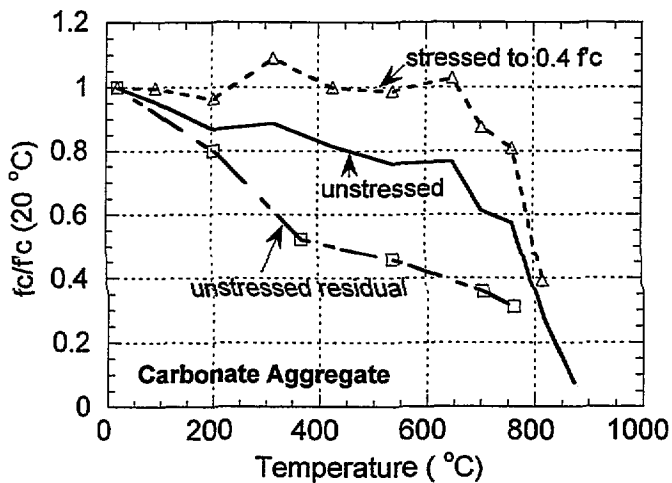


Figure 2.19 Strength of Carbonate Aggregate Concrete versus Temperature (Abrams, 1971)

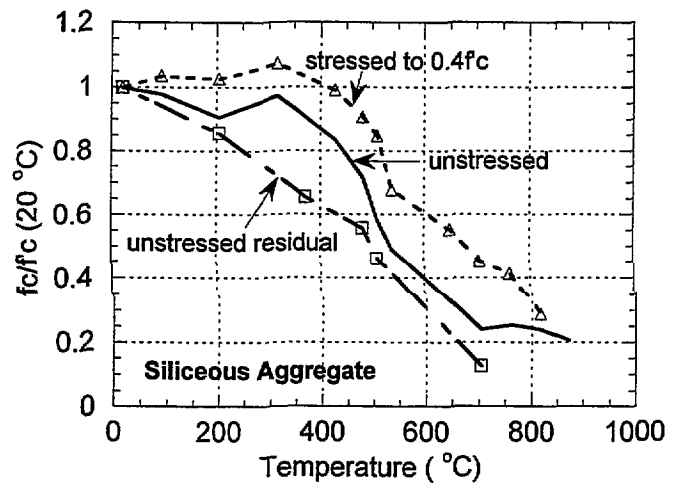


Figure 2.20 Strength of Siliceous Aggregate Concrete versus Temperature (Abrams, 1971)

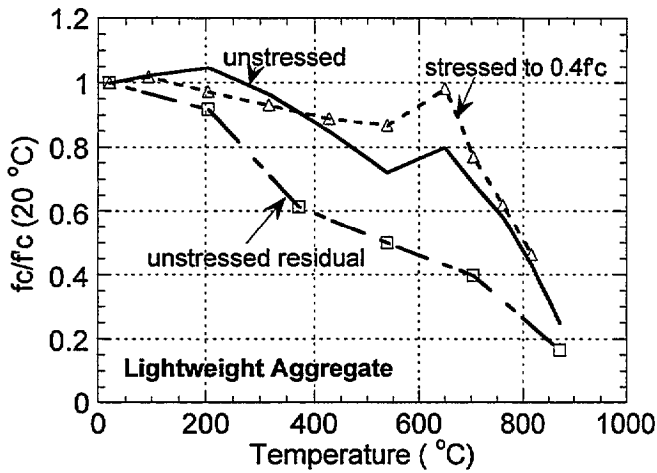


Figure 2.21 Strength of Lightweight Aggregate Concrete versus Temperature (Abrams, 1971)

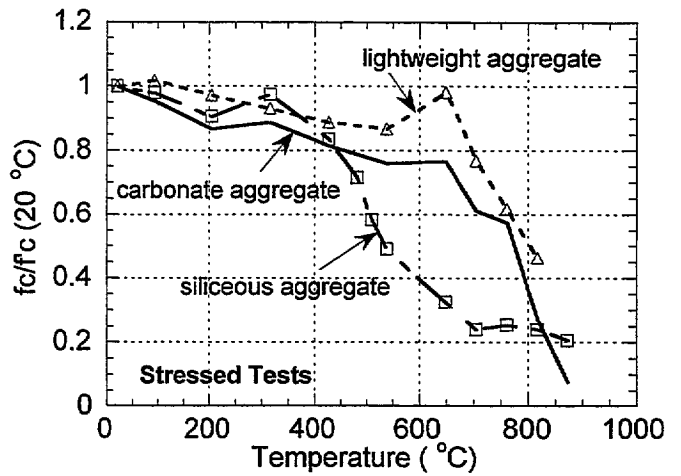


Figure 2.22 Strength versus Temperature for Stressed Tests (Abrams, 1971)

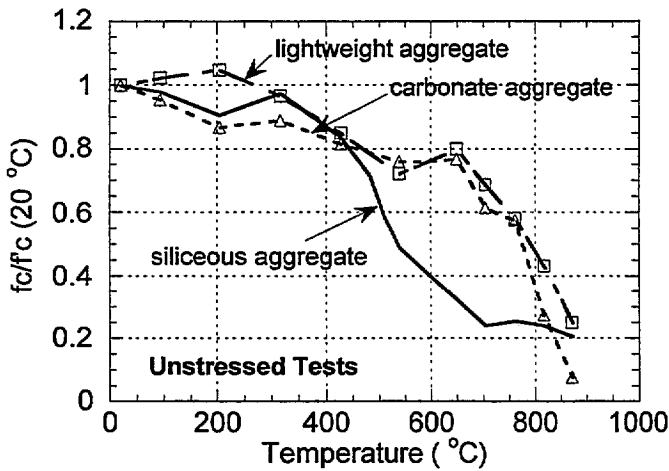


Figure 2.23 Strength versus Temperature for Unstressed Tests (Abrams, 1971)

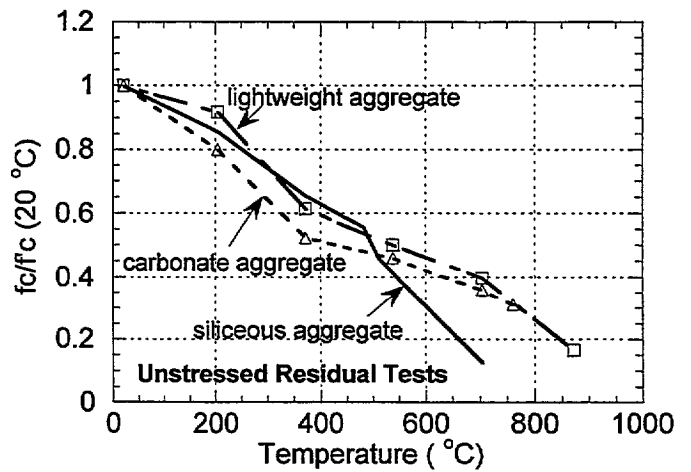


Figure 2.24 Strength versus Temperature for Unstressed Residual Test (Abrams, 1971)

2.3.1.6 Sullivan and Shanshar (1992)

This study was conducted at the Imperial College in London in 1982. The stated objectives were to select a concrete mixture which could perform as well at high temperatures as at ambient temperature and to find a compatible aggregate for optimum performance (high strength retention at high temperature). The maximum temperature used in this test program was 600 °C.

Two test series were carried out, corresponding to two test methods: *Unstressed residual strength test* (series 1) and *unstressed test* (series 2). The specimens were short cylinders (64 x 64 mm), made of concretes with two types of aggregates. One aggregate type was Lytag (LA) which is a proprietary lightweight aggregate (expanded pulverized fuel ash). The other aggregate was crushed firebrick (FB). The aggregates were described as “thermally stable” and had maximum sizes of approximately 13 mm.

Five concrete mixtures were used, with measured standard 28-day compressive strengths ranging from 37.8 to 65 MPa,

- Cement+LA	(44.9 MPa),
- Cement+Silica Fume (10% Cement)+LA	(65 MPa)
- Cement+FB	(57.5 MPa)
- Cement+Silica Fume (10%)+FB	(37.8 MPa)
- Cement+Slag(65% cement)+FB	(50 MPa)

The *unstressed residual strength* tests (series 1) were performed on all mixtures after heating at a rate of 1 °C/min to temperature levels of 50, 80, 100, 120, 200, 300, 450, 520, and 600 °C. The specimens were held at the test temperature for a period of 9 to 22 hours to allow a thermal steady state to develop, and then allowed to cool naturally to room temperature within the furnace.

The *unstressed* tests (series 2) were conducted after heating at approximately 1.5 °C/min and maintained for a period of 2 to 6 hours at temperature levels of 80, 100, 120, 200, 300, 450, 520, and 600 °C.

The results of this study are shown in Figures 2.25 to 2.30. As may be seen from these figures, compressive strengths of the *unstressed residual strength* specimens (Figure 2.25) are characterized by an inconsistent strength gain up to about 120 °C, followed by a loss of strength with increased temperatures. For the *unstressed* specimens (Figure 2.26), the trend is an initial loss of strength at 80 °C, followed by a strength recovery between the range of 80 °C and 300 °C, and a permanent loss of strength at temperature above 300 °C. These trends were observed for all concretes except for the firebrick slag concrete. Comparisons between the *unstressed residual strength tests* and *unstressed tests* also show different trends for different types of concrete, as shown in Figures 2.25 and 2.26. In general, the *unstressed residual strength* tests resulted in lower strengths than the *unstressed* tests. Part of this difference may be due to the different durations of the exposure time

at the elevated temperature for the two types of tests. The study concluded that:

- Concretes with inert lightweight aggregate, such as Lytag, have lower residual strength at temperature above 150 °C than concrete with firebrick aggregate. Thus type of aggregate is an important factor on the residual strength of concrete exposed to high temperature.
- The replacement of cement by 10% silica fume by mass does not have a significant influence on the performance of concrete exposed to high temperature.
- The use of firebrick aggregate along with slag cement resulted in superior performance under high-temperature exposure.

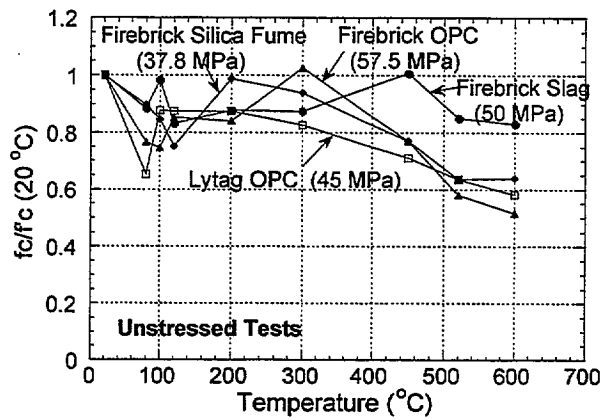


Figure 2.25 Compressive Strength versus Temperature from Unstressed Tests (Sullivan and Shansar, 1992)

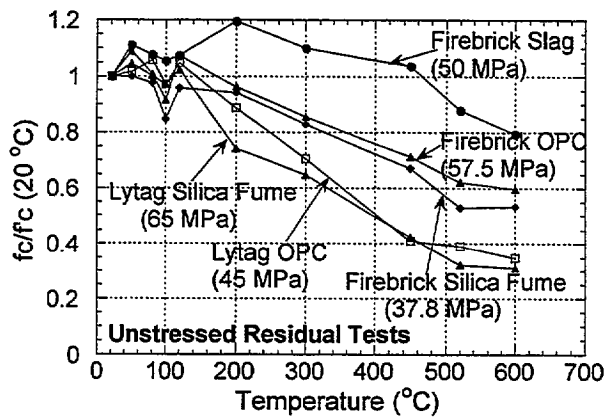


Figure 2.26 Compressive Strength versus Temperature from Unstressed Residual Strength Tests (Sullivan and Shanshar, 1992).

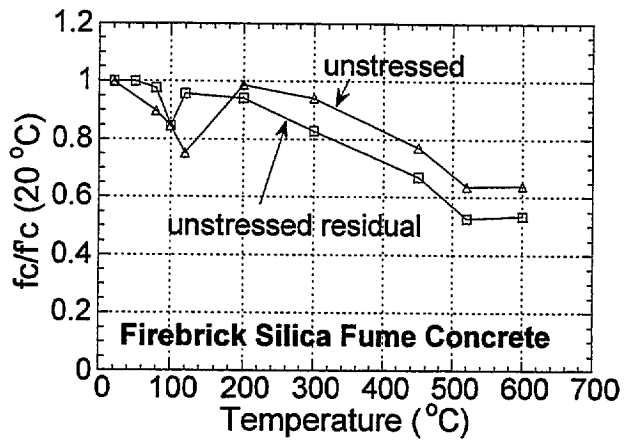


Figure 2.27 Strength of Firebrick/Silica Fume Concrete versus Temperature (Sullivan and Shansar, 1992)

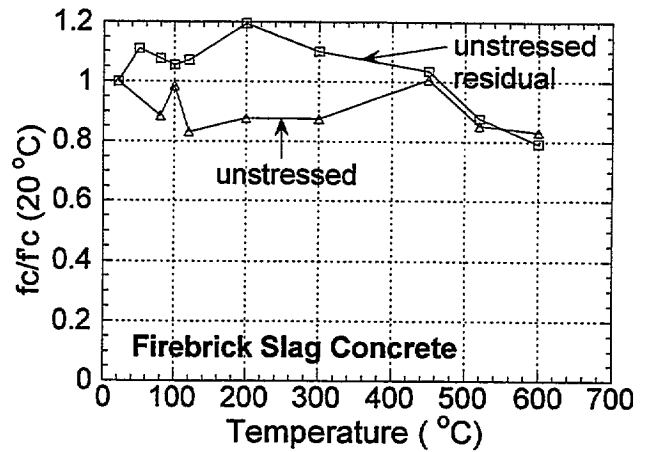


Figure 2.28 Strength for Firebrick/Slag Concrete versus Temperature (Sullivan and Shansar, 1992)

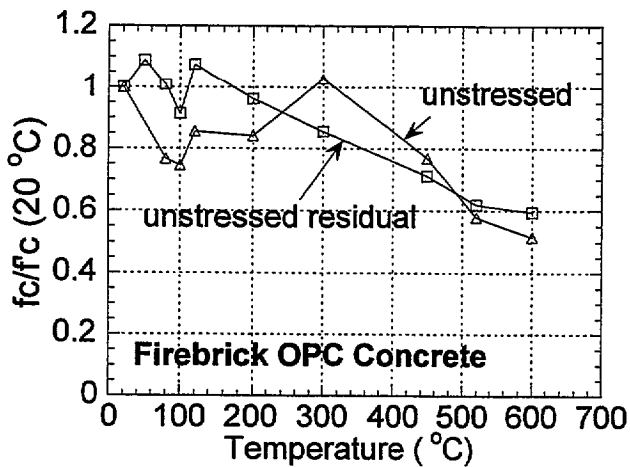


Figure 2.29 Strength for Firebrick/OPC Concrete versus Temperature (Sullivan and Shansar, 1992)

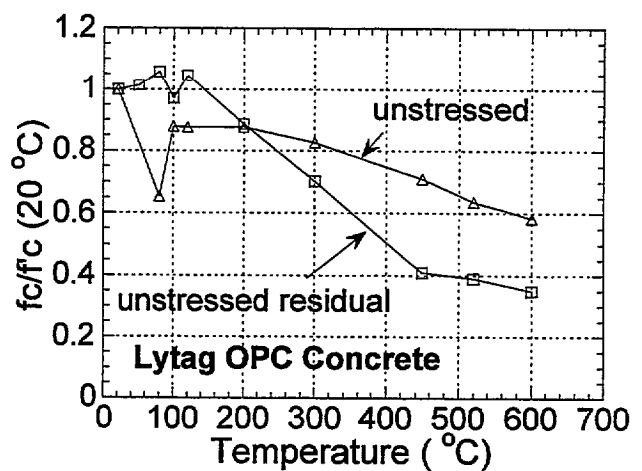


Figure 2.30 Strength for Lytag OPC Concrete versus Temperature (Sullivan and Shansar, 1992)

2.3.1.7 Morita, Saito, and Kumagai (1992)

Morita et al., (1992), conducted *unstressed residual strength* tests on cylinders made from three mixtures with target compressive strengths of 19.6, 39.2, and 58.8 MPa. The cylinders, 100 x 200 mm, were heated at a rate of 1 °C/min to temperatures of 200, 350, and 500 °C. The heat was maintained for 60 minute at these temperatures to allow a steady state to be reached, then the cylinders were allowed to cool to room temperature at a rate of 1 °C/min. For each temperature level, three specimens were tested. Test results, in terms of variation of compressive strength and modulus of elasticity with respect to temperature, are shown in Figures 2.31 to 2.34.

The study concluded that high strength concretes have a higher rate of reduction in residual compressive strength and modulus of elasticity than normal strength concrete after being exposed to temperatures up to 500 °C. The study did not report any spalling problems during heating.

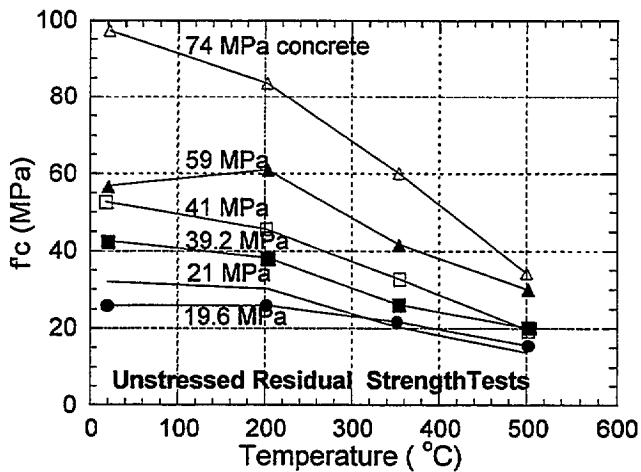


Figure 2.31 Residual Compressive Strength versus Temperature (Morita et al., 1992)

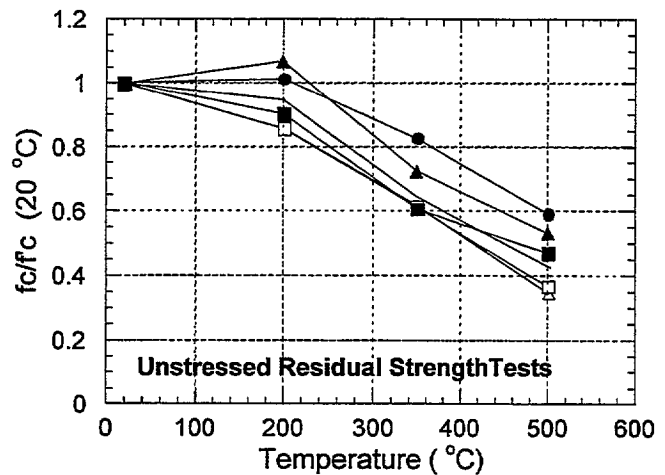


Figure 2.32 Residual Normalized Strength versus Temperature (Morita et al., 1992)

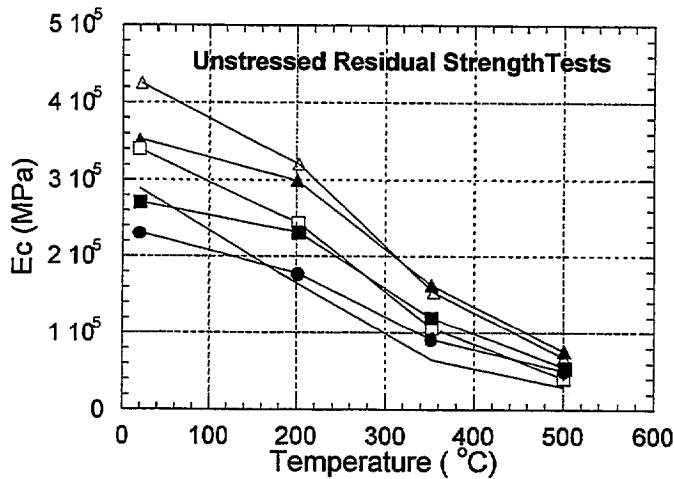


Figure 2.33 Residual Elastic Modulus versus vs. Temperature (Morita et al., 1992)

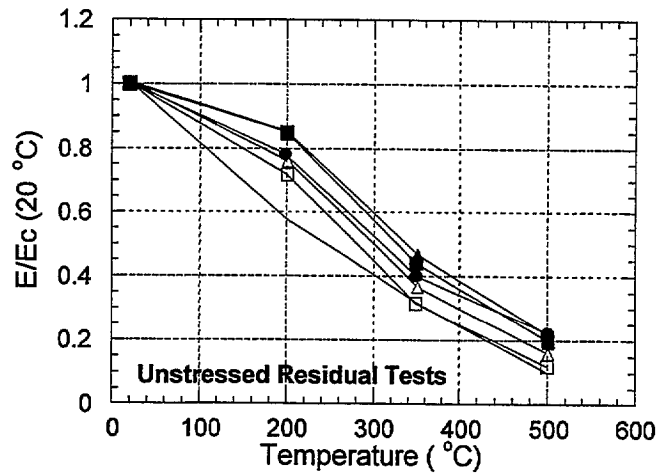


Figure 2.34 Residual Normalized Elastic Modulus vs. Temperature (Morita et al., 1992)

2.3.1.8 Furumura, Abe, and Shinohara (1995)

Furumura et al. (1995) performed *unstressed* tests and *unstressed residual strength* tests on 50 x 100 mm concrete cylinders using three compressive strength levels: 21 MPa (normal strength concrete series FR-21), 42 MPa (high strength concrete series FR-42), and 60 MPa (high strength concrete series FR-60). The concrete was made from ordinary portland cement. The small cylinders were reportedly selected to minimize radial temperature differentials during heating.

Each specimen was subjected to constant temperatures, within the range from 100 to 700 °C with an increment of 100 °C. Three specimens were tested at each temperature level. All specimens were heated at a rate of 1 °C/min and the target temperatures were maintained for two hours to achieve a steady state. The results of the *unstressed* tests, in terms of average compressive strength versus temperature, average modulus of elasticity versus temperature, and typical concrete stress-strain relationships, are shown in Figures 2.35 to 2.38.

Furumura et al. observed that, for the *unstressed* tests, the compressive strength decreased at 100 °C, recovered to the room temperature strength at 200 °C, and then decreased monotonically with increasing temperature beyond 200 °C. For the *unstressed residual strength* tests, the compressive strength decreased gradually with increasing temperature for the entire temperature range without any recovery. The modulus of elasticity, in general, decreased gradually with increasing temperature. The difference between *unstressed* tests and *unstressed residual strength* tests were reduced with increasing temperature.

As expected, the stress-strain curves for HSC are quite different than those of the normal strength

concrete (Figure 2.38). HSC series FR-42 and FR-60 exhibited steeper slopes than the NSC at temperature up to 300 to 400 °C in the *unstressed* test. Spalling failure of the 60 MPa-concrete specimens was observed at temperatures up to 300 °C.

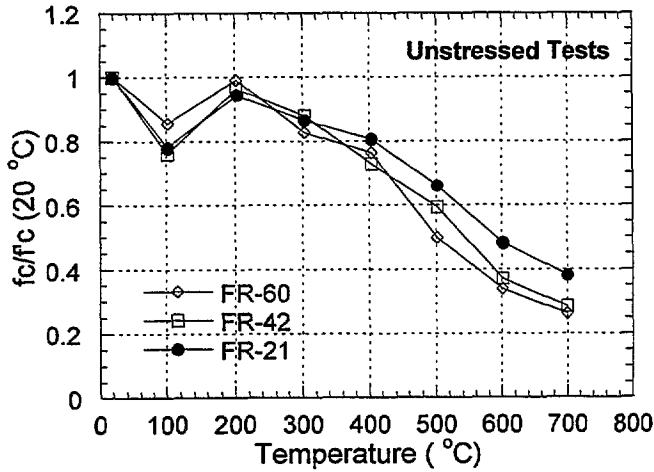


Figure 2.35 Compressive Strength versus Temperature (Furumura et al., 1995)

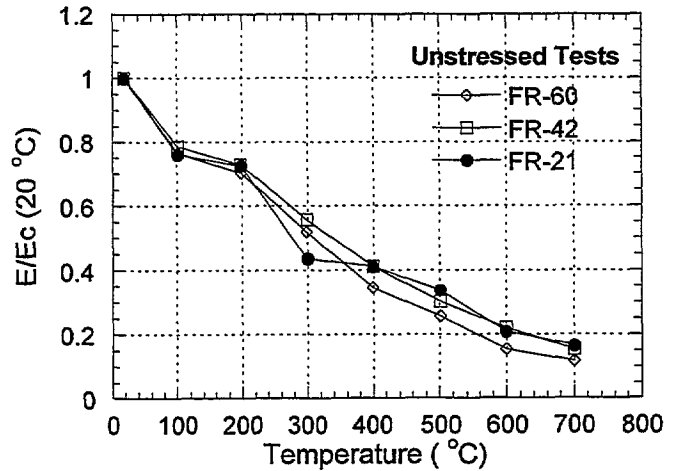


Figure 2.36 Elastic Modulus versus Temperature (Furumura et al., 1995)

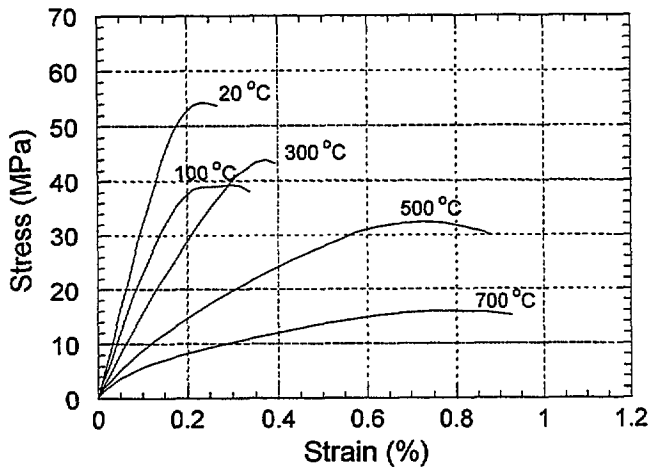


Figure 2.37 Typical Stress-Strain Relationships for 42 MPa-concrete (Furumura et al., 1995)

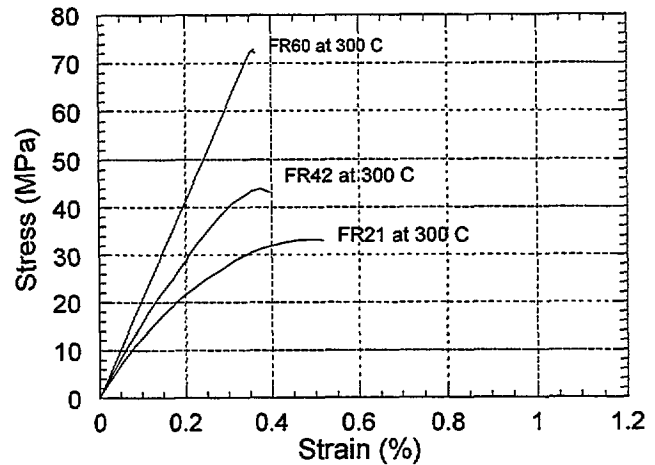


Figure 2.38 Comparison of Stress-Strain Relationships for Concretes at 300 °C (Furumura et al., 1995)

2.3.1.9 Felicetti, Gambarova, Rosati, Corsi, and Giannuzzi (1996)

Felicetti et al. (1996) performed *unstressed residual strength (strain rate controlled)* tests on silica fume based HSC specimens with specified strengths of 72 MPa and 95 MPa. Both concretes used siliceous aggregates, consisting mostly of crushed flint particles, with maximum size of 25 mm. The specimens included cylinders of two different sizes: 100 x 300 mm and 100 x 150 mm; and deep beams with dimensions of 80 x 275 x 500 mm. The 100 x 300 mm cylinders (37 specimens) were tested in uniaxial compression. The 100 x 150 mm cylinders (20 specimens) were notched at midheight and tested in direct tension. The deep beams (3 reinforced and 3 unreinforced) were tested in bending and shear. For uniaxial compression tests, batches of 2 to 4 cylinders were exposed to temperatures of 20, 105, 250, 400, and 500 °C. For direct tension tests, batches of 2 to 3 cylinders were exposed to the same temperatures but only up to 400 °C.

All specimens were cured under water for one week and stored in air for three weeks at 20 °C and 92% R.H. and one month at 20 °C and 65% R.H. Specimens heated to 105 °C were kept at this temperature for 7 days in an oven, and then allowed to cool to room temperature in the closed oven. For specimens exposed to higher temperatures, a heating rate of 12 °C/min was used to heat the specimens to target temperatures, which were maintained for 12 hours. A cooling rate of 12 °C/min was used to cool the specimens to room temperature. Figures 2.39 to 2.42 summarize the results of the uniaxial compression tests, Figures 2.43 to 2.44 summarize the results of the direct tension tests, and Figures 2.45 to 2.46 summarize the results of the beam tests.

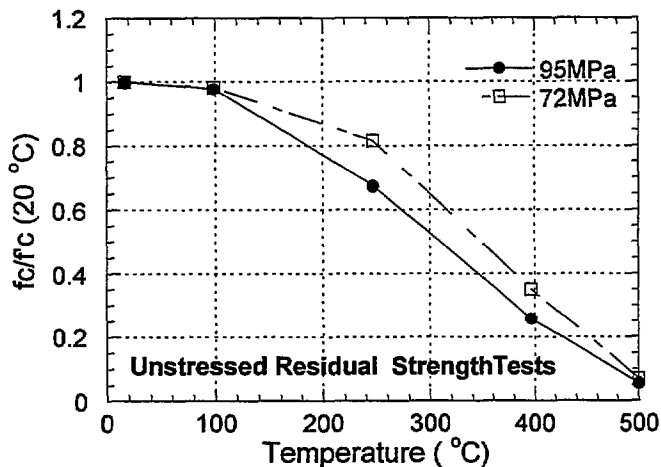


Figure 2.39 Residual Concrete Strength versus Temperature (Felicetti et al., 1996)

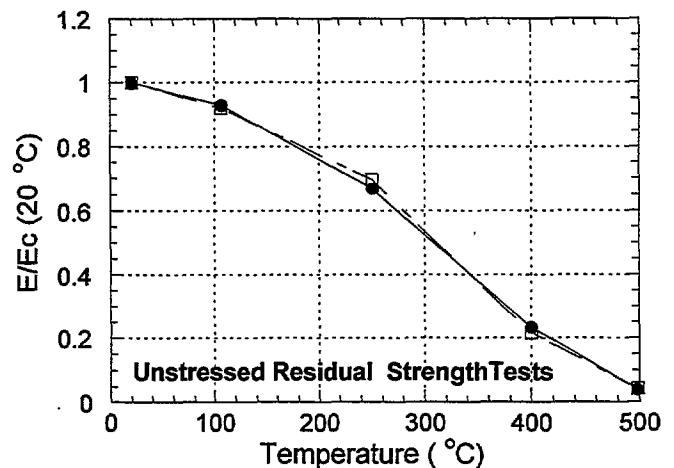


Figure 2.40 Residual Elastic Modulus versus Temperature (Felicetti et al., 1996)

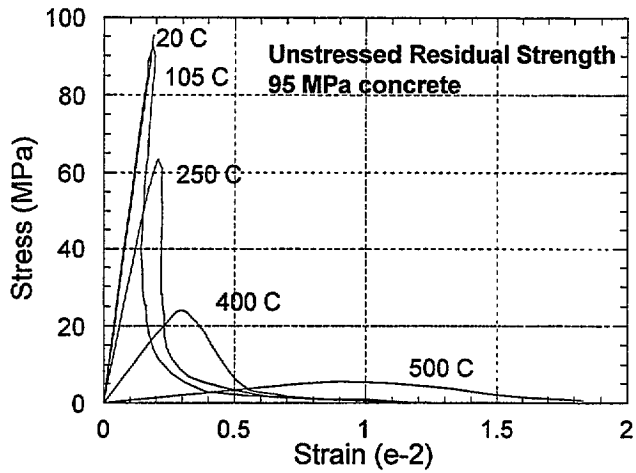


Figure 2.41 Stress-Strain Curves for 95 MPa Concrete after Heating to Exposure Temperature (Felicetti et al., 1996)

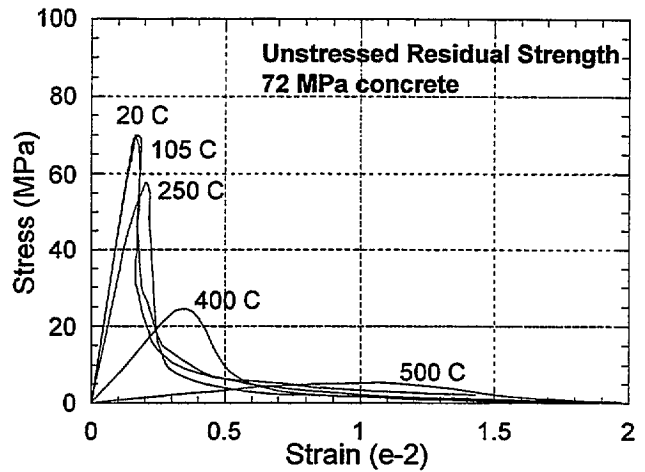


Figure 2.42 Stress-Strain Curves for 72 MPa Concrete after Heating to Exposure Temperature (Felicetti et al., 1996)

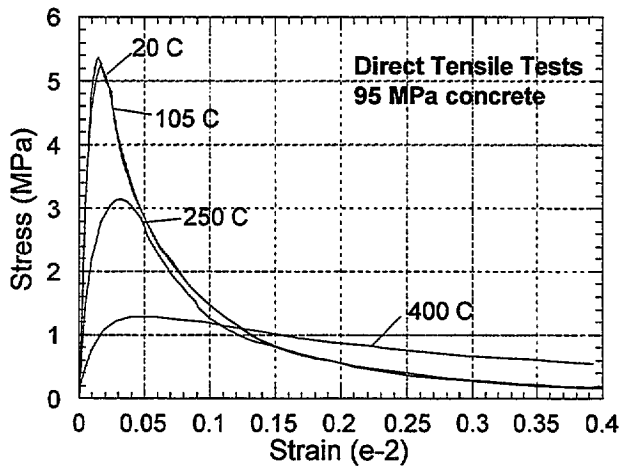


Figure 2.43 Tensile Stress-Strain Curves for 95 MPa Concrete after Heating to Exposure Temperature (Felicetti et al., 1996)

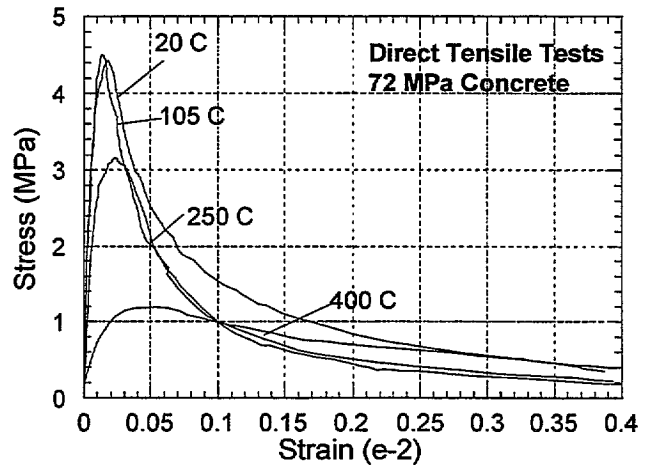


Figure 2.44 Tensile Stress-Strain Curves for 72 MPa Concrete after Heating to Exposure Temperature (Felicetti et al., 1996)

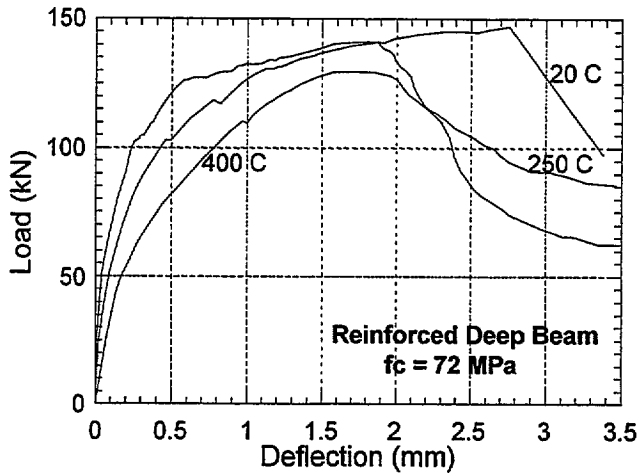


Figure 2.45 Load-Deflection Response of Reinforced Beams versus Temperature (Felicetti et al., 1996)

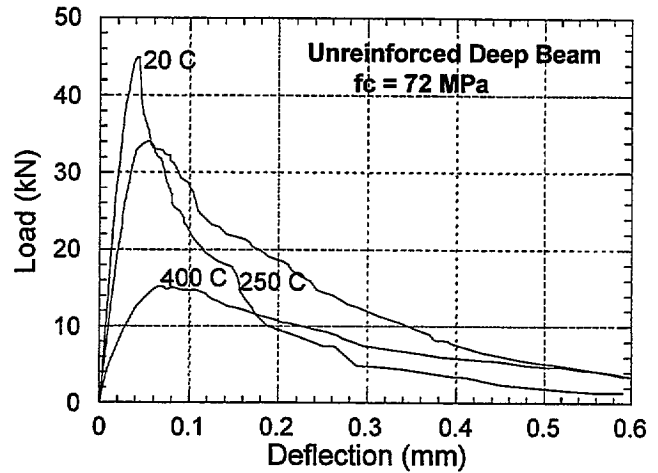


Figure 2.46 Load-Deflection Response of unreinforced beams versus Temperature (Felicetti et al., 1996)

The study revealed similar trends of reductions in compressive strength and modulus of elasticity with increasing temperatures as was observed in other test programs. An exposure temperature of 250 °C appears to be the level which marks the higher rate of strength and modulus reduction. At 400 to 500 °C, most of the flint aggregates appeared cracked or split, with a different color compared with aggregates not exposed to heat. Results of the unreinforced beam tests indicated that the peak load was less sensitive to high temperature than implied by the marked reduction in tensile strength observed in the direct tension tests. For reinforced concrete beams, the peak load was only marginally decreased up to 400 °C. This latter finding reflects the fact that in a RC beam, the flexural capacity is governed primarily by the area of steel and not concrete strength.

2.3.1.10 Noumowe, Clastres, Debicki, and Costaz (1996)

Noumowe et al. (1996) conducted a study on performance of HSC exposed to high temperatures which included experimental and analytical parts. The experimental part is reviewed in this section. The analytical part is reviewed in Chapter 3.

The experimental part consisted of *unstressed residual strength* tests of normal strength and HSC cylinders (160 x 320 mm) and prisms (100 x 100 x 400 mm). A normal strength (38.1 MPa) and a high-strength (61.1 MPa) mixtures were used. The prisms had enlarged ends and were used to measure tensile strength. Both concretes used calcareous aggregates. The specimens were cured at 22 °C and 95% R.H. until the time of testing (at 2 months). The specimens were heated at a rate of 1 °C/min to target temperatures of 150, 300, 450, 500, and 600 °C, which was maintained for 1 hour, and then allowed to cool at 1 °C/min to room temperature. Uniaxial compressive, splitting tensile, and direct tensile tests were performed to obtain residual compressive strength, modulus of elasticity, and residual tensile strength versus temperature relationships. The latter two relationships are shown in Figures 2.47 and 2.48. Measurements of porosity after exposure to different temperatures were performed for both concretes using a mercury porosimeter. The results of the porosity measurements are shown in Figure 2.49. Figure 2.50 shows the percentage loss in mass for the different temperature.

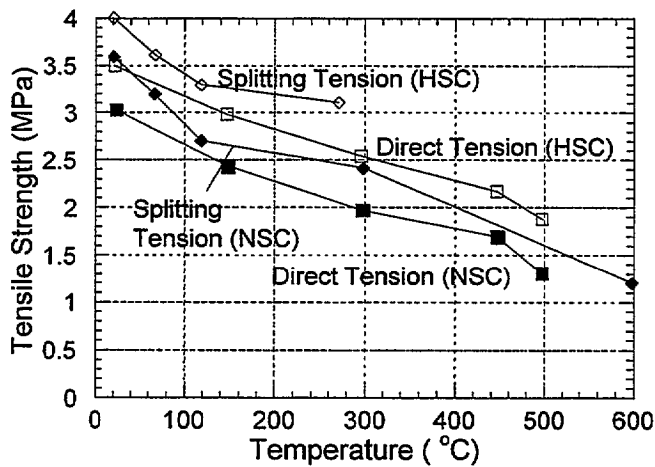


Figure 2.47 Residual Tensile Strengths of HSC and NSC versus Temperature (Noumowe et al., 1996)

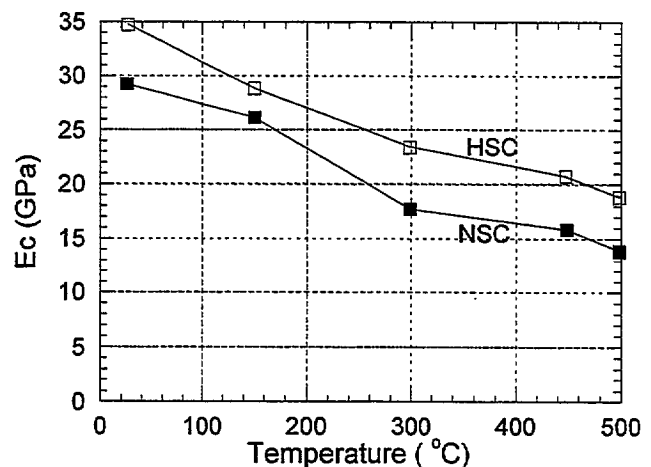


Figure 2.48 Elastic Moduli of HSC and NSC versus Temperature (Noumowe et al., 1996)

The experimental results show that residual tensile strengths for both normal strength and HSC decreased similarly and almost linearly with increasing temperatures. Tensile strengths of HSC at all temperatures were approximately 15% higher than those of normal strength concrete. Also, tensile strengths measured by the splitting tensile tests were consistently higher than by the direct tensile tests. The residual moduli of elasticity of HSC remained approximately 10-25% higher than those of normal strength concrete for the entire temperature range. Porosity measurements indicated that between 25 and 120 °C, the porosity of both concretes were not altered. As temperatures increased, normal strength concrete became increasingly more porous compared with HSC. Mass losses in both concretes were also similar up to 110 °C (less than 1%). Highest rate of mass loss occurred in temperature range of 110 to 350 °C. The rate of weight loss stabilized at temperatures above 350 °C. At any temperature, mass loss in normal strength concrete was higher than that in HSC.

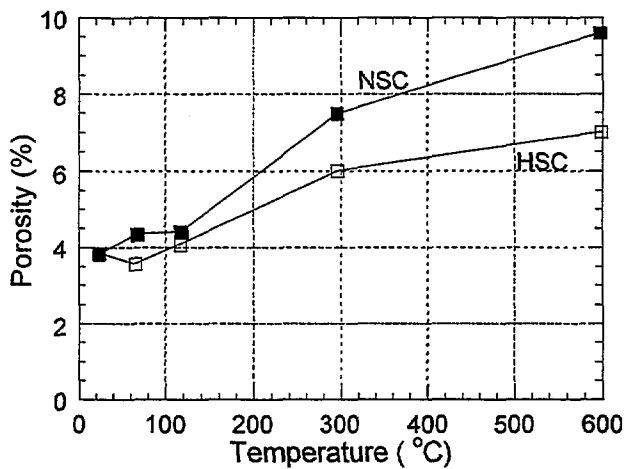


Figure 2.49 Porosity of HSC and NSC versus Temperature (Noumowe et al., 1996)

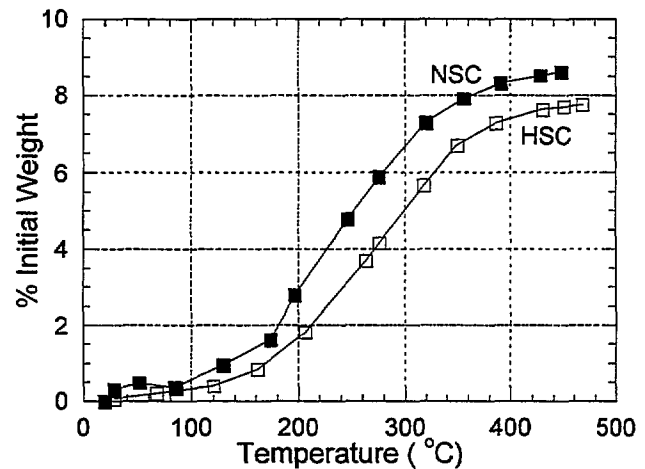


Figure 2.50 Mass Loss of HSC and NSC versus Temperature (Noumowe et al., 1996)

2.3.2 Element Tests

Element tests show the effects of high temperature on structural elements such as beams, columns, walls, or slabs. As in the case of materials tests, a number of studies on fire performance of concrete elements have been conducted. Since this report focuses on fire performance of HSC, only studies which used HSC are reviewed. Element tests generally follow standard test methods, such as International Standard ISO 834, ASTM E-119, or Japanese Industrial Standard JIS A1304. The results of element tests are used to establish fire endurance of concrete elements. These test results provide basic information for the development of design rules for fire resistance of HSC. They also provide experimental data for validation of analytical models.

2.3.2.1 Beam Tests by Hansen and Jensen, 1995 (Also Opheim, 1995; and Jensen et al., 1996)

Three series of beam tests were conducted in this study by the Norwegian Fire Research Laboratory (Hansen and Jensen, 1995). The test specimens were reinforced and prestressed concrete beams having dimensions of 150 x 200 x 2850 mm. Three types of concretes were used: ND (normal density concrete), LWA (lightweight aggregate concrete- Liapor aggregate), and LWAF (lightweight aggregate concrete with fibers - Fibrin fiber type 1823). The concretes were designed to have target 28-day cube strengths (100 x 100 x 100 mm cubes) of 75 MPa and 95 MPa. In addition, some beams were provided with a coating of Lightcem concrete (manufactured by LightCem A/S, Norway) as passive fire protection, and two of the beams in test series 2 were made of lightweight aggregate Lightcem concrete with a target 28-day cube strength of 50 MPa. Standard bars of quality K500TS according to the requirements of Norwegian Standard NS 3570 were used as reinforcement. The longitudinal reinforcing bars were 20 mm and 32 mm, and the stirrups were 8 mm. For prestressing, 26 mm, Dywidag bars, of the type St 835/1030 were used. A prestress force of 300 kN was centrally applied at the ends of the beams, resulting in a mean prestress of approximately 10 MPa.

Test series 1 and 2 consisted of 7 beams each. Series 3 was a reference series for evaluation of residual strength of the fire exposed beams, and consisted of 2 beams.

Series 1 included 7 reinforced LWA concrete beams with a nominal 28-day cube strength of 75 MPa. These are identified as follows:

* Beam No 21	LWA75	LWA aggregate concrete (Liapor aggregate)
* Beam No 31, 32, 35	LWAF75	LWA concrete with fibers (Fibrin fiber type 1823)
* Beam No 41, 42, 43	LWAF75P	LWA concrete with fibers and protected with LightCem LC5 as passive fire protection.

Beams No 32 and 42 were loaded with a concentrated load of 30 kN at mid-span during the fire tests.

Series 2 included 4 reinforced beams (2 of ND concrete and 2 of LWA concrete), 3 prestressed

beams (1 of ND concrete, 1 of LWA concrete, and 1 of LWA concrete with fibers). These are identified as follows:

- * Beams No 61,62 ND95 ND reinforced concrete
- * Beams No 51,52 LWA50 LWA reinforced concrete (Lightcem)
- * Beam No 12 ND95 ND prestressed
- * Beam No 22 LWA75 LWA concrete, prestressed (Liapor aggregate)
- * Beam No 33 LWAF75 LWA concrete with fibers and prestressed.

Series 3 includes 2 reference beams:

- * Beam No 30 LWAF75 LWA concrete with fibers, reinforced.
- * Beam No 34 LWAF75 LWA concrete with fibers, prestressed.

Information on concrete material properties and other test information are summarized in Table 2.3:

Table 2.3 Concrete Material Properties (Hansen and Jensen, 1995)

Type	Beams	f_c (28d) (MPa)	f_{cc} (28d) (MPa)	E_c (28d) (GPa)	Density (kg/m ³)	Age at fire test (days)	Moist. Content (%)
ND95	(11),12	83.4	73.4	32.4	2457	85	3.9
	61,62	89.6	72.5	30.4	2450	64	3.7
LWA75	(20),21,22	75.8	69.2	24.7	1936	48/92	6.9
LWAF75	31,41,42 ¹ ,43	68.9	61.8	23.8	1906	56	6.5
	(30),32 ¹ ,35	78.2	75.3	24.7	1913	54	6.0
	33,(34)	70.1	60.1	23.9	1970	86	8.9
LWAC	51,52 ¹	46.6	42.4	18.2	-	77	-

¹ Loaded at midspan with a concentrated vertical load of 30 kN. The load was applied in 6 steps of 5 kN each, by means of a hydraulic cylinder connected to a steel frame in a self supporting system.

Fire tests were performed in an oil-heated furnace. The furnace has horizontal exposure openings with dimensions of 2500 mm x 5000 mm and a depth of 1500 mm. In test series 1 and 2, the concrete beams were exposed to a hydrocarbon fire on three sides. The heating regime followed the standard time-temperature curve prescribed by ISO 834 for a hydrocarbon fire. The test procedure was also in accordance with ISO 834. Thermocouples were installed on the longitudinal and shear reinforcement at two locations in each beam. The beams were exposed to the ISO 834 hydrocarbon

fire for 2 hours, and the maximum oven temperature reached approximately 1100 °C. The furnace temperature history and the period when spalling was observed are shown in Figure 2.51. Table 2.4 summarizes the results of the tests.

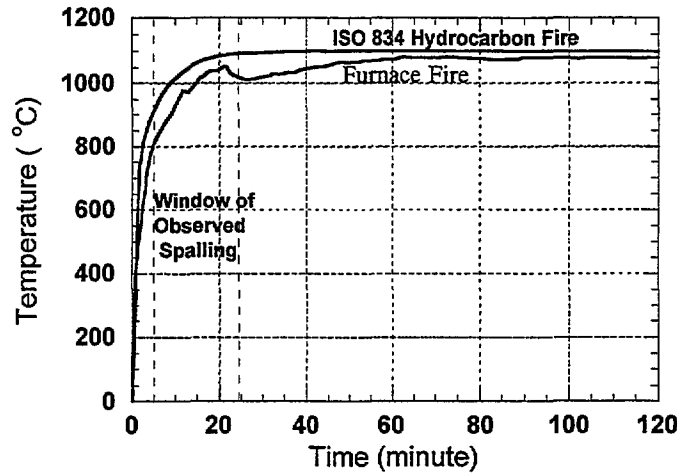


Figure 2.51 ISO Hydrocarbon Fire Curve, Furnace Temperature, and Time Period When Spalling was Observed (Hansen and Jensen, 1995)

Table 2.4. Summary of Observations of Hansen and Jensen's Tests

Concrete Type	No Spalling	Shallow Spalling No Exposed Reinforcement	Severe Spalling Exposed Reinforcement	Collapse
LWAF75	32 ¹ ,33 ²	31	35 ³	
LWAF75P	41, 42 ¹ ,43			
LWA75			21,22 ²	
LightCem	52 ¹	51		
ND95		61,62		12 ²

¹ Beam tested with a vertical load

² Prestressed beam

³ Spalling was limited to the bottom of this beam, and no spalling occurred on the sides. The study reported this spalling as likely being cause by poor concreting.

Sounds of spalling were reported to begin at approximately 5 to 6 minutes into the tests, and they stopped at 25 minute for test series 1 and 20 minute for test series 2. According to the hydrocarbon fire curve, the spalling began at a furnace temperature of 800 °C and ended when the furnace reached its steady state temperature of 1100 °C.

The following conclusions were drawn from this study:

- *Severe spalling* (exposed reinforcement) occurred more in the higher strength lightweight aggregate beams as observed in reinforced and prestressed LWA75 beams, while spalling without exposed reinforcement occurred more in high-strength, normal weight ND beams.
- *Shallow or no spalling* was observed for higher strength lightweight concrete beams with fibers (LWAF).
- *No spalling* was observed for the lightweight beams with fibers and the passive protective coating (LWAFP75).

2.3.2.2 Beam Tests by Sanjayan and Stocks, 1991

Two full-scale T-beams, one made of high-strength concrete with silica fume (105 MPa) and one made of normal strength concrete (27 MPa) were fire tested. The beams were 2.5 m long and the flanges were 1.2 m wide. Different flange thicknesses of 200 mm and 150 mm were cast on each side of the web. The web depth was 450 mm from the top surface, and the web was 250 mm wide. To study the effect of reinforcement cover, the cover to the steel in the 200-mm flange was 75 mm, and for the 150-mm flange the cover was 25 mm. In addition, the main bars in the web were staggered diagonally to obtain reinforcement covers of 25, 50, and 75 mm along the web.

Moisture contents of the test beams were determined by drying concrete sections which had the same cross section as the test specimens and which were cast together with the test specimens. Thermocouples were installed at regular intervals inside the specimens to monitor the temperature distributions during the fire tests. To determine the intensity of spalling, the weight of the specimens were monitored with load cells while the test was in progress. Temperatures measured at 25, 50, and 75 mm from the bottom of the web, and weight loss versus time for both specimens are shown in the Figures 2.52 and 2.53, respectively.

The heating regime followed the standard temperature versus time curve specified by the Australian Standard (AS 1530.4, which is the same as the temperature versus time curve specified by ASTM E-119). The beams were reported to have been stored in the laboratory for 3½ months prior to testing.

About 15 min into the test, with the furnace temperature averaging 691 °C, moisture began to drip from several vertical cracks in both specimens. A larger quantity of moisture dripped from the high-strength concrete specimen. There was no spalling until 18 min into the test, with furnace

temperature averaging 715 °C. Severe explosive spalling of the high-strength concrete beam started when a large piece dislodged from the 200-mm flange. The concrete temperature at a depth of 25 mm, where spalling occurred, averaged 128 °C. Explosive spalling of small pieces of the high-strength concrete specimen from the 200-mm flange continued with increasing intensity until about 40 min into the test. This can be seen in the graph of specimen weight versus time shown in Figure 2.53. Between 20 and 40 min there was a large rate of weight loss corresponding to the spalling.

No spalling was observed in the NSC specimen, even though the temperatures inside the normal strength concrete specimen were only slightly lower than in the HSC specimen (Figure 2.52).

Since this involved only one replicate specimen for each type of concrete, it is difficult to draw definite conclusions. However, the following observations were reported:

- High-strength concrete appears to be more prone to spalling in a fire than normal strength concrete.
- Spalling occurred in the thicker 200-mm flange where the cover of the steel was large (75 mm). In the 150-mm flange, the cover was 25 mm and there was no spalling. No explanation was given for this observation.
- No spalling occurred in the web, possibly because (1) in the web, the concrete was exposed to three sides and therefore the distance for the moisture to escape was much shorter; and (2) the existence of wider flexural cracks in the web.
- The higher moisture content found in the high strength concrete indicates that high strength concrete has slower drying rate than normal strength concrete.

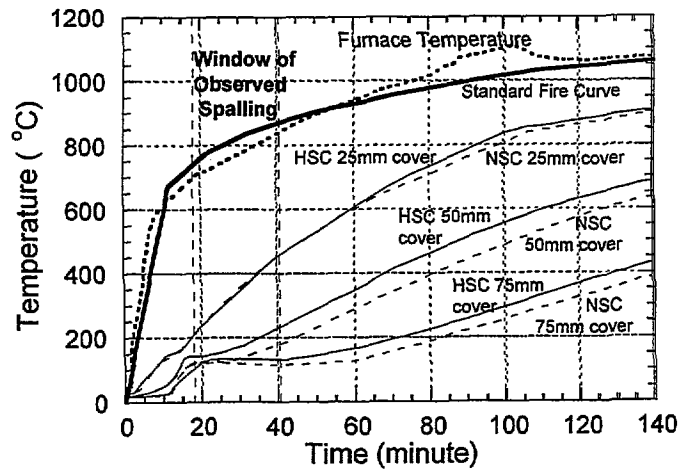


Figure 2.52 Temperature vs. Time At Different Locations in the Specimens (Sanjayan and Stocks, 1991)

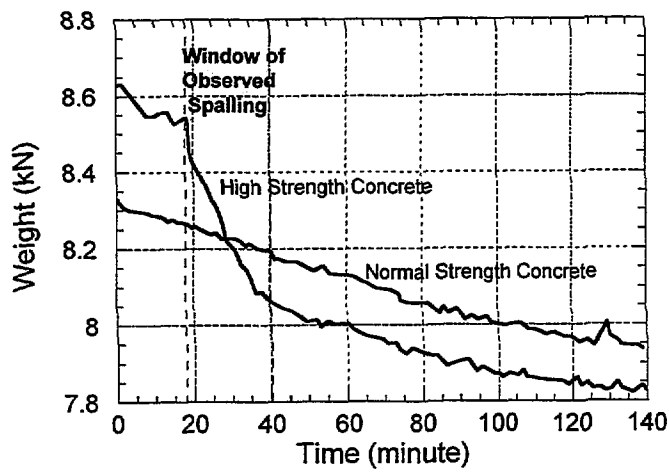


Figure 2.53 Specimen Loss vs. Time for HSC and NSC Specimens (Sanjayan and Stocks, 1991)

2.3.2.3 Beam Tests by Saito, Kumagai, and Morita, 1992 (in Japanese)

Six reinforced concrete beams were used in this study. Five of the specimens were fire tested and one was tested at room temperature as a control specimen. The aim of the study was to assess the residual capacity of the beams after exposure to maximum temperature of 550 °C.

The beams were reinforced longitudinally with four 13-mm reinforcing bars and transversely with 6-mm stirrups. Three different concretes, with specified strengths of 19.6, 39.2, and 58.8 MPa, were used. The fire test specimens were heated and allowed to cool during a five-hour period. The maximum furnace temperature reached 550 °C, in accordance with the heating regime prescribed by JIS A1304 (see Figure 2.54). The beams were loaded at room temperature with two concentrated load until failure, and failure loads were compared to those of the control specimens. The study concluded that there was no significant difference in the residual bending strength due to different concrete compressive strengths.

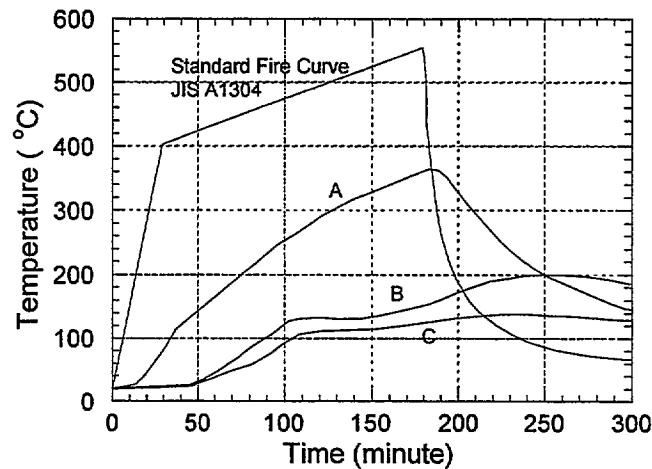


Figure 2.54 Standard Fire Curve and Temperature at Different Points in Beam Specimen (Saito et al., 1992)

2.3.2.4 Report of Column Tests by Diederichs, Jumppanen, and Schneider, 1995

Diederichs et al. (1995) reported general information on fire tests of three short HSC columns (250 x 250 x 1000 mm), tests by the VTT Fire Technology Laboratory (Finland) of ten short HSC columns (150 x 150 x 900 mm), and a fire test on a full scale column (400 x 500 x 5590 mm) by the Institut für Baustoffe, Massivbau und Brandschutz.

The three columns tested by Diederichs et al. were made of three different concrete mixtures (I, II, and III). Mixture I had a specified cube strength of 101 MPa and contained fibers (not clearly specified). Mixture II had a specified cube strength of 105 MPa and contained no fibers. Mixture III had a specified cube strength of 90 MPa and contained fibers. The columns were subjected to 100% of the design load prior to fire testing.

The two columns with fibers experienced minor spalling (mixture I) and no spalling (mixture III) during fire tests. Fire tests on these columns were terminated at 125 minutes after the start of the tests. The mixture II column (without fibers) experienced spalling at about 6 minutes into the fire test. Spalling continued until 30 minutes into the test when it reached the longitudinal reinforcement at the edges of the column. The test was terminated at 45 minutes, which is significantly less than the time of 125 minutes for specimens with fibers.

In the VTT fire tests, the ten HSC specimens were made of three different concrete mixtures, all contained variable fiber contents:

- Group 1: Portland cement PZ 55 F with a concrete cube strength of 85 MPa.
- Group 2: Portland cement PZ 55 F with a concrete cube strength of 105 MPa.
- Group 3: Portland cement PZ 45 F with a concrete cube strength of 45 MPa.

VTT's fire tests were conducted according to the German Standard DIN 4102 (similar to International Standard ISO 834). None of the columns experienced spalling. All columns were reported to have failed due to loss of compressive strength at high temperature. The fire resistance times were 51 minutes for the HSC columns (Groups 1 and 2) and 72 minutes for the NSC columns (Group 3).

In the full scale column test, the specimen was made of concrete with a specified cube compressive strength of 110 MPa and contained fibers. The column was eccentrically loaded with 100% of its design load and exposed to ISO 834 standard fire from all four sides. Shallow spalling occurred at about 10 minutes after starting the test and stopped after 30 minutes. At 181 minutes, the column collapsed due to compressive failure of the concrete near the maximum stressed cross section.

The report by Diederichs et al. indicated that the use of capillary forming fibers help reduce the potential for spalling in HSC columns and suggested that further studies be conducted on the effects of variations in fiber contents.

2.3.2.5 Slab Tests by Shirley, Burg, and Fiorato, 1987

Fire tests were conducted on five reinforced concrete slabs (900 x 900 x 102 mm) following the ASTM E 119 heating regime. Four specimens were fabricated using four high strength concretes (C-9, C-11, G-9, G-14) with nominal compressive strengths from 62 MPa to 97 MPa. The fifth specimen was fabricated using a normal strength concrete (C-5) with a nominal compressive strength of 35 MPa. Two of the high strength concretes (G-9 and G-14) contained silica fume, and two contained fly ash (C-9 and C-11). Properties of concretes used are listed in Table 2.5.

Table 2.5. Summary of Concrete Strengths (Shirley et al., 1987)

Properties	Mix C-5	Mix C-9	Mix C-11	Mix G-9	Mix G-14
Compressive Strength at 56 days, (MPa)	48.2	69.1	86.8	69.4	120.6
Compressive Strength at time of fire test, (MPa)	54.8	70.5	93.8	68.3	116.5
Age at time of fire test, days	113	93	77	123	130

The slabs were instrumented with thermocouples throughout their depths to monitor the temperatures within the concrete during the fire test. Also five thermocouples were used on the top of the slabs to monitor temperatures on the unexposed surface. The specimens were tested after relative humidity at the mid-depth was reduced to between 77 and 84 percent.

Fire tests were conducted at the Construction Technology Laboratories (CTL) using their multipurpose 900 x 900 mm furnace. For each slab, an area of 800 x 800 mm on the underside was exposed to the fire. Each specimen was exposed to 4 hours of the ASTM E-119 heating regime. Fire endurance of the slabs was determined according to the provisions of ASTM E 119-83. This standard identifies fire endurance of a member, or assembly as the time required to reach the first of any of the following three end points (see also chapter 4):

1. The passage or propagation of flame to the unexposed surface of the test assembly;
2. A temperature rise of 181 °C (325 F) at a single point or 139 °C (250 F) as an average on the unexposed surface of the test assembly; and
3. Inability to carry the applied design load or structural collapse.

Table 2.6 lists the fire endurance of the five 102 mm thick specimens, determined according to the

temperature end point (criteria #2). These fire endurance were corrected for internal relative humidity by the procedure outlined in ASTM E 119. The corrections were from 1 to 6 minutes. Figure 2.55 shows the average temperatures on the unexposed surfaces of the slabs and the ASTM E 119 heating regime.

Table 2.6. Summary of Fire Endurance of 102 mm Thick Slabs (Shirley et al., 1987)

	Mix C-5	Mix C-9	Mix C-11	Mix G-9	Mix G-14
Fire Endurance, hr:min	1:28	1:30	1:21	1:37	1:40

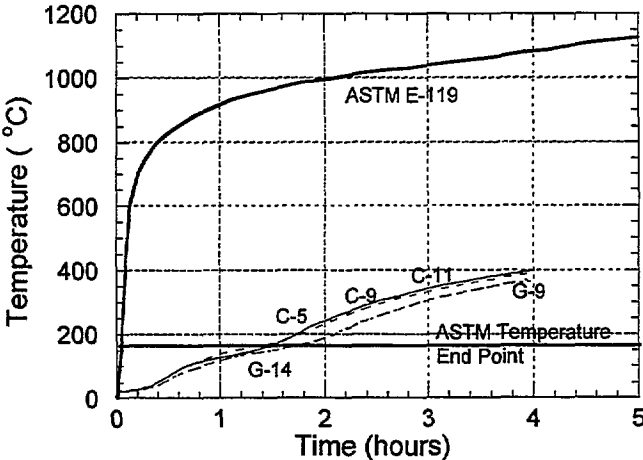


Figure 2.55 ASTM E 119 Heating Regime and Average Temperatures on the Unexposed Surfaces of the Slabs (Shirley et al., 1987)

The study concluded that:

- Fire endurance of nonsilica fume HSC, silica fume HSC, and normal strength concrete were not significantly different, i.e., no measurable difference in performance of high-strength concretes and conventional strength concretes was observed.
- None of the five specimens tested exhibited spalling of the exposed surface nor was any explosive behavior observed.

2.3.3 Other Studies

2.3.3.1 Nassif, Burley, and Rigden, 1995

Nassif et al. (1995) conducted a laboratory investigation into the applicability of the *stiffness damage test* (SDT) to assess fire-damaged concrete structures. The study was performed at Queen Mary and Westfield College, London University.

The specimens were concrete cylindrical cores, 75 x 175 mm, made with 10 mm flint coarse aggregate. The mix proportions by mass were 1 : 1.35 : 3.14 (cement: fine aggregate: coarse aggregate), with a w/c ratio of 0.45. The specimens were exposed to temperatures of 217, 240, 287, 320, 378 and 470 °C, with three replicates at each temperature level. Cooling was carried out in a controlled environment of 20 °C and 65% R.H.

The SDT involves the measurement of the quasi-static uniaxial compressive stress-strain response of concrete under low stress (load-unload) cycles. Tests were carried out after the heated specimens have cooled to room temperature. To minimize damage during testing, the specimens were loaded to a maximum stress of 4.5 MPa at a rate of 0.1 MPa per s, then unloaded at the same rate. The load-unload cycle was repeated four times. To quantify fire damage, the following parameters, calculated for each SDT, were averaged over the number of load-unload cycles:

- Chord loading modulus, E_c (slope of loading response).
- Unloading modulus, E_u (slope of response immediately after unloading).
- Damage Index, DI (area of the hysteresis loops divided by the stress range).
- Plastic strain, PS (permanent strain at the end of the unloading cycles).
- Non-linearity index, NLI (slope of the loading response up to half the maximum load divided by E_c).

The results of the SDT are shown in Figures 2.56 to 2.60. Also shown are the results of ultrasonic pulse velocity test (UPV) (Figure 2.61). As can be seen from these Figures, 320 °C marked the onset of significant modification in the characteristics of the cyclic stress-strain response, with a sudden increase in the damage index (area of hysteresis loops). The UPV test of the fire-exposed concrete showed similar variation with temperature to that of the elastic properties. At temperatures higher than 320 °C, scanning electron microscopy (SEM) photographs showed significant cracks in the cement paste, especially in the interfacial zone (adjacent to aggregate particles).

The results of this study indicate good correlation with other studies, which observed significant property changes, and sometimes spalling, for concrete exposed to temperatures above 300 °C.

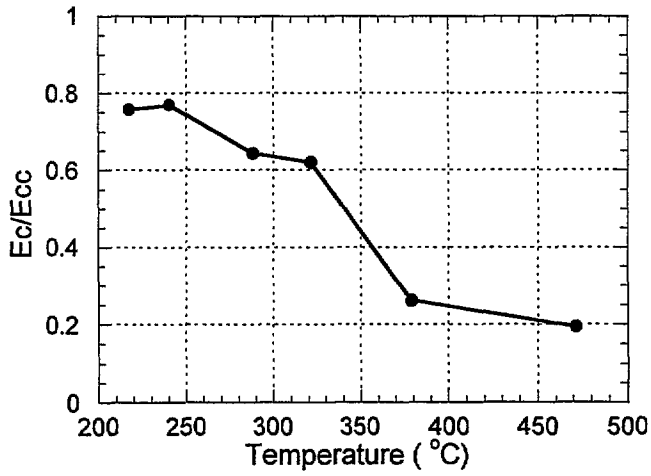


Figure 2.56 Chord Loading Modulus Ratio versus temperature (Ecc is the value of the control specimen at 20 °C, Nassif et al., 1995)

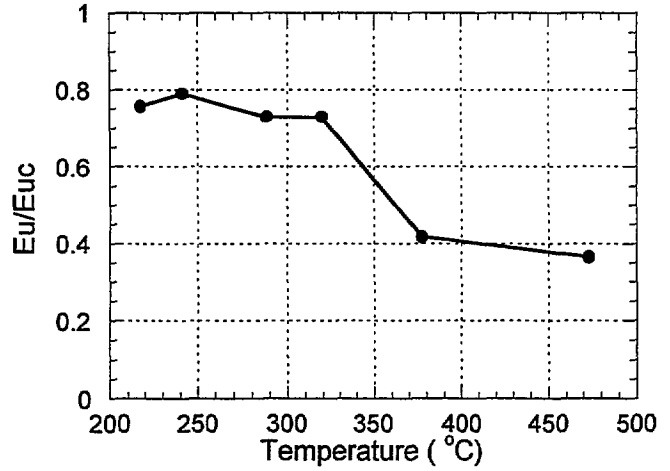


Figure 2.57 Unloading Modulus Ratio versus Temperature (Euc is the value of the control specimen at 20 °C, Nassif et al., 1995)

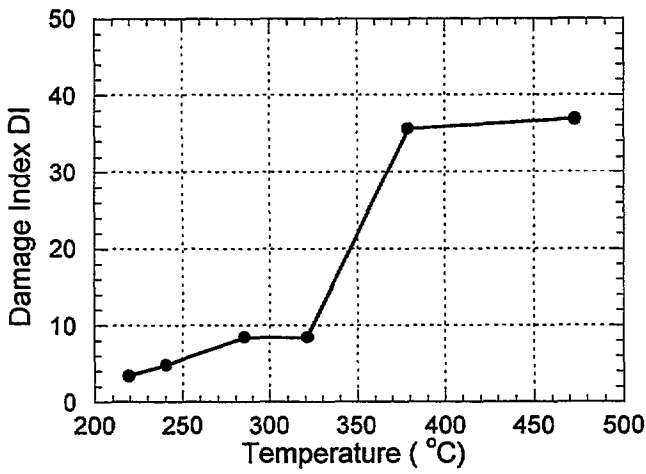


Figure 2.58 Damage Index versus Temperature (Nassif et al., 1995)

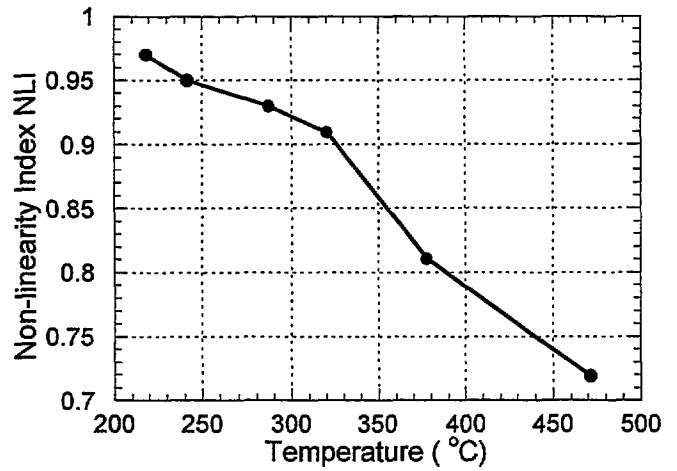
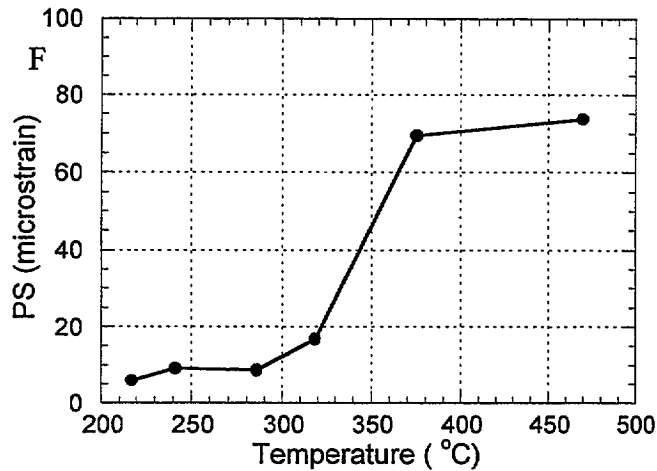


Figure 2.59 Non-linearity Index versus Temperature (Nassif et al., 1995)



2.60 Plastic Strain versus Temperature
(Nassif et al., 1995)

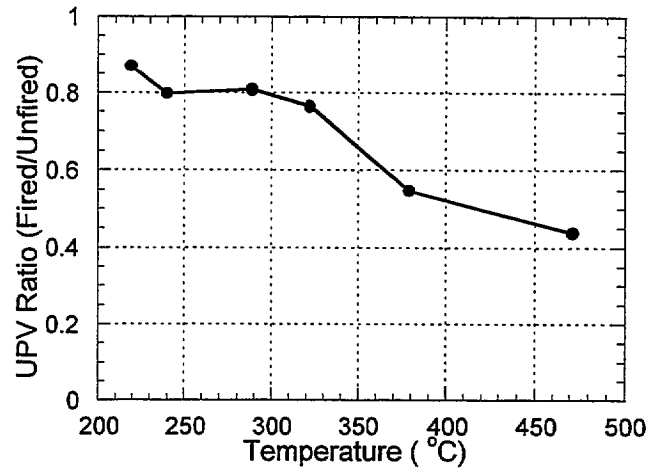


Figure 2.61 Ultrasonic Pulse Velocity Ratio
(fire tested/unfire tested) versus
Temperature (Nassif et al., 1995)

2.3.3.2 Lin, Lin, and Powers-Couche, 1996

Lin et al. (1996) present information obtained from scanning electron microscopy (SEM) and stereo microscopy investigations of fire-damaged concrete to develop an understanding of the behavior of concrete in fire.

The specimens were 150 x 300 mm cylinders, made of portland cement and siliceous aggregate with maximum size of 19 mm. The specimens were demolded 24 hours after casting, steam-cured at 180 °C for 12 hours, and followed by a 14-month curing period at 25 °C and 100 percent R.H.

The specimens were heated to seven temperature levels of 20, 100, 250, 400, 550, 750, and 900 °C by means of an electric furnace. The heating rate was 20 °C/min. The temperature was maintained for 15 min at each temperature level. At the end of the 15-min period, the specimens were removed from the furnace and cooled either in air or in water for 1 week, followed by air drying for 1 day. The specimens were then saw-cut and polished to form thin sections for SEM examinations.

By compiling SEM photographs, a chronological pattern of a failure mechanism could be visualized. For instance, the morphologies of hydrates at room temperature, 250, 400, 550, 750, and 900 °C, and reformation of calcium hydroxides (CH) during cooling all have distinguishable morphological appearances of their own. These SEM investigations showed that no major cracks developed at temperatures below 300 °C, except for fine cracks along the boundaries of CH crystals and unhydrated cement particles. It is likely that concrete exposed to temperatures below 300 °C is dominated only by localized boundary cracking. Cracking around aggregate particle boundaries and intrapaste cracking and isotropy in thin sections were observed between 300 and 500 °C. Above 500 °C, the hydration products decomposed and resulted in major cracks within the cement paste and around the aggregate particles.

2.4 Summary

Ten concrete materials test programs, five element test programs, and two SEM studies dealing with properties of concrete exposed to elevated temperatures were reviewed in this chapter. Most of the materials test programs reviewed used HSC specimens (concrete with specified compressive strength of at least 41 MPa), except for the test program conducted by Abrams (1971). Abrams' test program was reviewed since it is widely referenced and served as the basic information for concrete behavior at high temperature incorporated into many professional committee reports (see chapter 4). Key features of the reviewed materials test programs are summarized in Table 2.7. The darker shaded boxes in this Table indicate the variables studied by a particular reference, and the lighter shaded boxes indicate the test methods used. The element test programs reviewed include 3 beam-test programs, 1 column-test program, and 1 slab-test program. All used HSC for the test elements. Key features of the reviewed element test programs are summarized in Table 2.8. The two SEM studies provided microstructural information to correlate with the changes in concrete mechanical properties with increasing temperature. The specimens used in these two SEM studies were of NSC.

The influences of different variables on the properties and behavior of HSC, such as compressive strength, modulus of elasticity, stress-strain relationships, tensile strength, and spalling failure mechanism, due to short term exposure to high temperature, are summarized in the following sections.

2.4.1 Effect of Temperature on Compressive Strength of HSC

The compressive strength-temperature relationships from the reviewed test programs are shown in Figures 2.62 to 2.67. These relationships are distinguished by the test methods used in obtaining the data (*unstressed*, *unstressed residual strength*, and *stressed tests*) and by the aggregate types (normal or lightweight). Relationships for HSC are shown by solid lines, and relationships for NSC are shown by dashed lines.

In the *unstressed* tests, the specimens are heated in the absence of stress and tested at elevated temperature. For the *unstressed tests*, the strength-temperature relationships are characterized by three stages (Figures 2.62 and 2.63):

- *Initial strength loss stage:* -between room temperature to anywhere between 100 and 200 °C for normal weight concrete.
-between room temperature to 250 °C for lightweight concrete.
- *Stabilizing and regaining stage:* -anywhere between 100 and 200 °C to anywhere between 400 and 450 °C for normal weight concrete.
-between 250 °C to 450 °C for light weight concrete.
- *Permanent strength loss stage:* -beginning anywhere between 400 to 450 °C for normal weight concrete.

-beginning anywhere between 250 to 450 °C for lightweight concrete.

The *unstressed* strength-temperature relationships for HSC appear to follow similar trends as for NSC, except that the loss of strength in temperature range between 25 °C to about 400 °C for HSC is noticeably greater than the loss of strength for NSC. This difference is narrowed in the *permanent strength loss stage*.

In the *unstressed residual strength tests*, the specimens are heated in the absence of stress and tested after cooling to room temperature. For the *unstressed residual strength tests*, the strength-temperature relationships of HSC are characterized by two stages (Figures 2.64 and 2.65):

- *Initial strength gain or minor strength loss stage:* between room temperature to about 200 °C for both normal and lightweight concrete.
- *Permanent strength loss stage:* beginning at about 200 °C for both normal and lightweight concrete.

The *unstressed residual* strength-temperature relationships for HSC and NSC are somewhat similar for the entire range of temperature.

In the *stressed tests*, the specimens are heated in the presence of a service stress and tested for strength at the elevated temperature. Based on a limited number of *stressed tests*, the HSC strength-temperature relationships are characterized by three stages (Figures 2.66 to 2.67):

- *Initial strength loss stage:* between room temperature to about 100 °C for normal weight concrete. Data for lightweight HSC under *stressed tests* are not available.
- *Stabilizing and regaining stage:* between 100 °C to about 400 °C for normal weight concrete.
- *Permanent strength loss stage:* beginning at about 400 °C to 700 °C for normal weight concrete.

Based on the information from the reviewed test programs, the following factors are considered to have an influence on the strength-temperature relationships of HSC:

- Original compressive strength
- Type of aggregate (siliceous or calcareous)
- Test methods (*stressed, unstressed, unstressed residual strength*).

Table 2.7 Summary of Materials Test Programs Reviewed

References	Compressive Strength (MPa)	Test Methods & Conditions			Temp. Range (°C)	Heating Rate (°C/min)	Concrete or Aggregate Type	Specimen Size (mm)	Temp. Range of Explosive Spalling
		Stressed	Unstressed	Unstressed Residual Strength					
Castillo (1990)	28, 62 ¹ 31, 63, 89 ²				25-300	7-8	Conventional Portland Cement	51 x 102 **	320-360 °C
Hertz (1984)	170 ¹ 150 ²				20-650	1	Silica fume concrete+steel fiber	100 x 200 ** 57 x 100 ** 28 x 52 **	350-650 °C
Diederichs (1988)	33-114 ¹				20-850	2, 32	Blast furnace Silica fume Fly ash OPC	100 x 100 x 100 * 80 x 300 **	Cubes heated at 32 °C/min
Hammer (1995)	69-118 ¹				20-600	2	Silica fume LW aggr. Normal aggrt.	100 x 310 **	300 °C
Sullivan & Shansar (1982)	38-65 ¹				20-600	1-1.5	Combinations of cement, silica fume, slag and two types of aggregates	64 x 64 **	Not Observed

References	Variables						Temp. Range of Explosive Spalling		
	Compressive Strength (MPa)	Test Methods & Conditions			Temp. Range (°C)	Heating Rate (°C/min)		Concrete or Aggregate Type	Specimen Size (mm)
		Stressed	Unstressed	Unstressed Residual Strength					
Abrams (1971)	23-45 ¹				23-871		Carbonate Agg. Siliceous Agg. L.W. Agg.	75 x 150**	Not Observed
Morita (1992)	29,39,59 ¹ 29,74 ¹				20-500	1		100 x 200**	Not Observed
Furumura (1995)	23,42,60 ¹ 38,55,79 ²				20-700	1		50 x 100**	300 °C
Felicetti (1996)	72, 95 ¹				20-500	0.2	Silica Fume concrete	100 x 300** 100 x 150** 80 x 275 x 500*	Not Observed
Noumowe (1996)	38, 61				20-600	1	Silica Fume with Calcareous Aggregate	160 x 320** 100 x 100 x 400*	Not Observed

¹ Designed concrete strength

² Measured concrete strength at time of fire testing

* Cube specimens

** Specimens are cylinders, the first dimension is the diameter and the second is the height.

Table 2.8. Summary of Structural Element Test Programs Reviewed

References	Specimens				Fire Test Method	Observations
	Type	Size (mm)	Compressive Strength (MPa)	Concrete Materials		
Hansen et al. (1995)	RC and Prestressed Beams	150x200x2850	50, 75, 95 ¹	-ND aggregate -LW aggregate -LW aggregate w/ fiber	ISO 834 Max. Oven Temp.: 1100 °C	-Severe spalling in higher strength beams/Reduced Spalling in lower strength beams -No spalling in beam with fibers
Sanjayan et al. (1991)	RC T-beams	Length: 2500 Width: 1200 Depth: 450 Web Width: 250 Flange Thickness: 150 and 200	27, 105 ²		ASTM E 119	-Explosive spalling in HSC beam on the thicker flange (200 mm) at furnace temp. of 715 °C. -No spalling in the NSC beam.
Saito et al. (1992)	RC beams	250x400x3600	20, 39, 59 ¹		JIS A 1304	No spalling reported
Diederichs (1995)	RC Columns	250x250x1000 400x500x590	90, 101, 105, 110 ¹	Concrete With and Without fibers	ISO 834	Spalling in columns made of concrete without fibers.
Shirley et al. (1987)	RC Slabs	900x900x102	55-117 ²	OPC, Silica fume, fly ash concretes	ASTM E 119	-No spalling observed -No measurable difference in fire endurance of nonsilica fume HSC, silica fume HSC, and NSC specimens observed.

¹ Designed concrete strength

² Measured concrete strength at time of fire testing

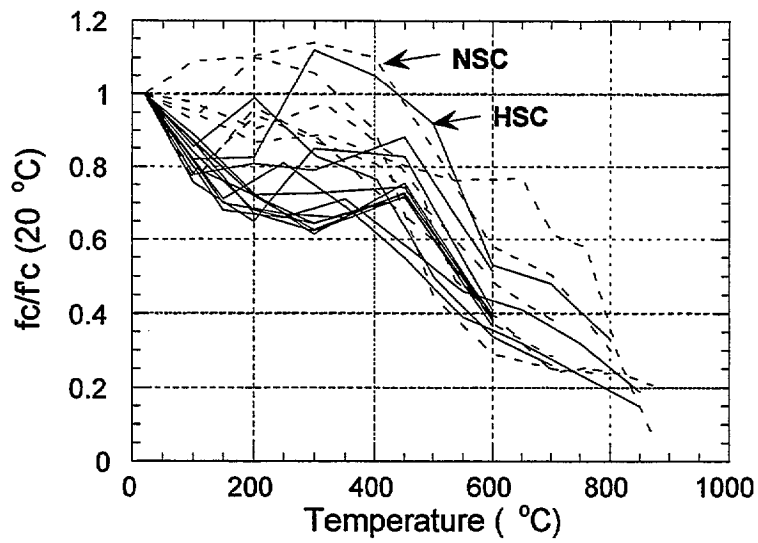


Figure 2.62 Summary of Compressive strength-temperature relationships for normal weight concrete, obtained by **unstressed tests**

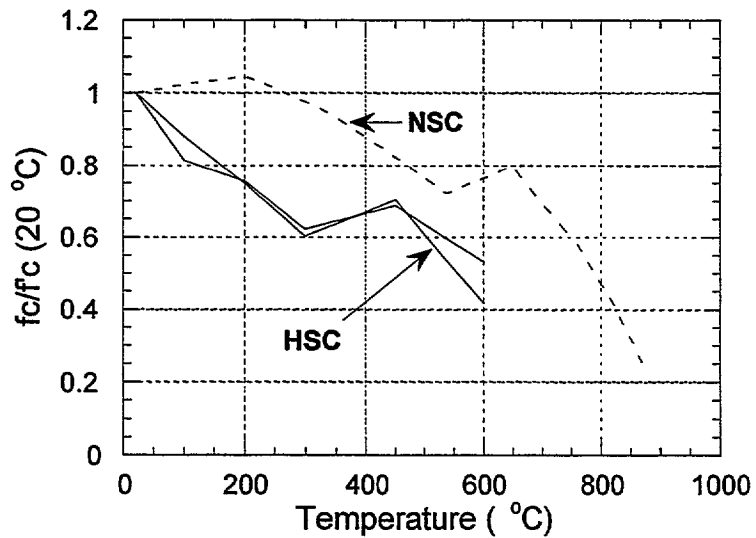


Figure 2.63 Summary of Compressive strength-temperature relationships for lightweight concrete, obtained by **unstressed tests**

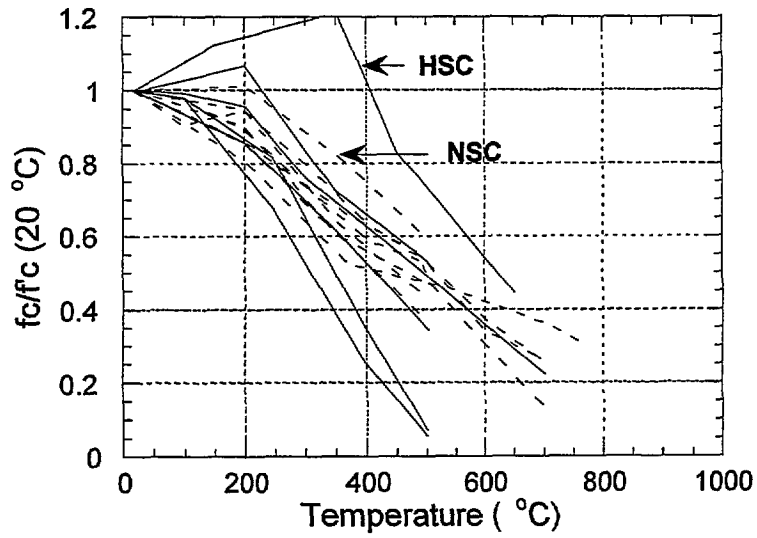


Figure 2.64 Summary of Compressive strength-temperature relationships for normal weight concrete, obtained by **unstressed residual strength tests**

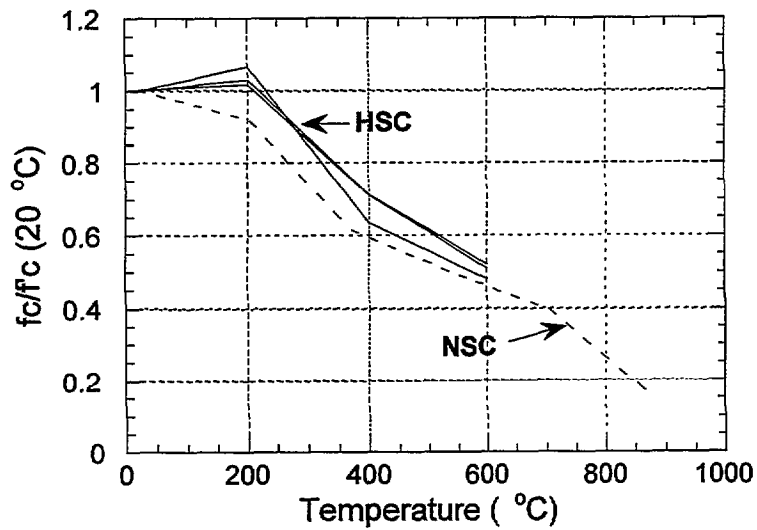


Figure 2.65 Summary of Compressive strength-temperature relationships for lightweight concrete, obtained by **unstressed residual strength tests**

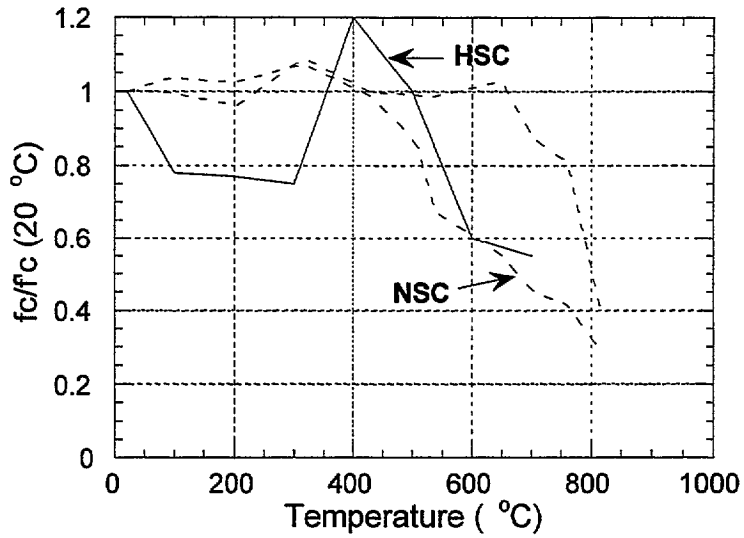


Figure 2.66 Summary of Compressive strength-temperature relationships for normal weight concrete, obtained by **stressed tests**

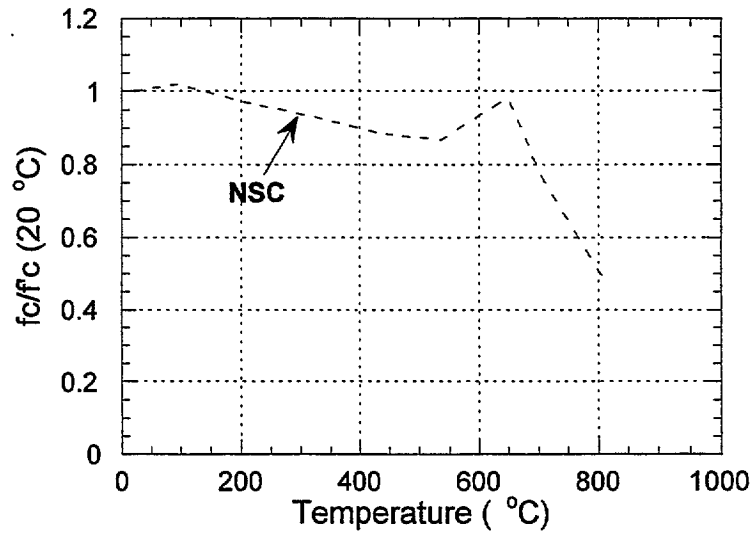


Figure 2.67 Summary of Compressive strength-temperature relationship for lightweight concrete, obtained by **stressed tests**

2.4.2 Effect of Temperature on Modulus of Elasticity of HSC

The elastic modulus-temperature relationships are shown in Figure 2.68 for the *unstressed tests* and in Figure 2.69 for the *unstressed residual strength tests*. There were no data for the modulus-temperature relationship for *stressed tests*.

For the *unstressed tests*, there are no significant differences in the modulus of elasticity-temperature relationships for normal weight HSC (solid, thin lines), NSC (dashed lines), and lightweight HSC (solid, thick lines), as can be seen from Figure 2.68.

For the *unstressed residual strength tests*, the difference in elastic modulus between normal weight HSC and NSC is also insignificant. However, data for lightweight HSC indicates significant differences in the modulus-temperature relationships (Figure 2.69). These lightweight HSC data were obtained from Hertz's 1984 and 1991 experiments which used very high strength concrete (specimens with specified strength of 170 MPa). It is not certain to what extent the very high strength influences this response.

Based on the data from the reviewed test programs, the factors that seem to have an influence on the modulus-temperature relationship is the weight classification of the aggregate (normal vs. lightweight) and the test methods. It is not known to what extent preload (*stressed tests*) would affect this relationship, since no data concerning this relationship were obtained for the *stressed tests*.

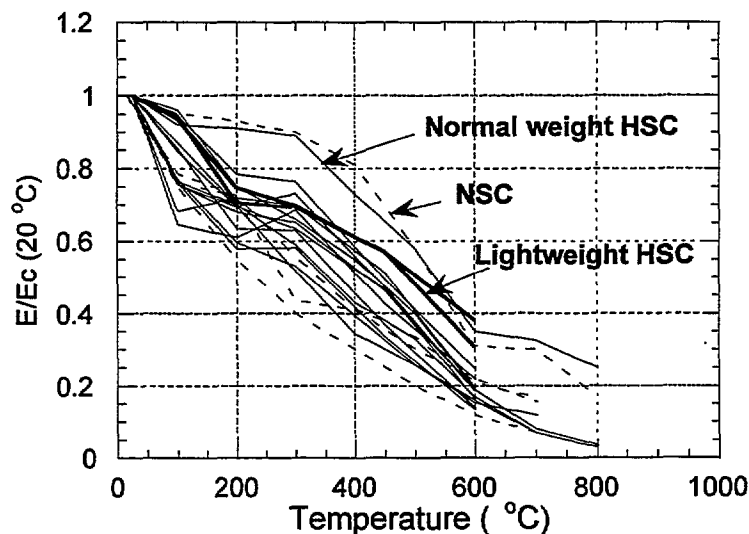


Figure 2.68 Summary of Modulus of elasticity-temperature relationships obtained from **unstressed tests** for normal and lightweight concrete

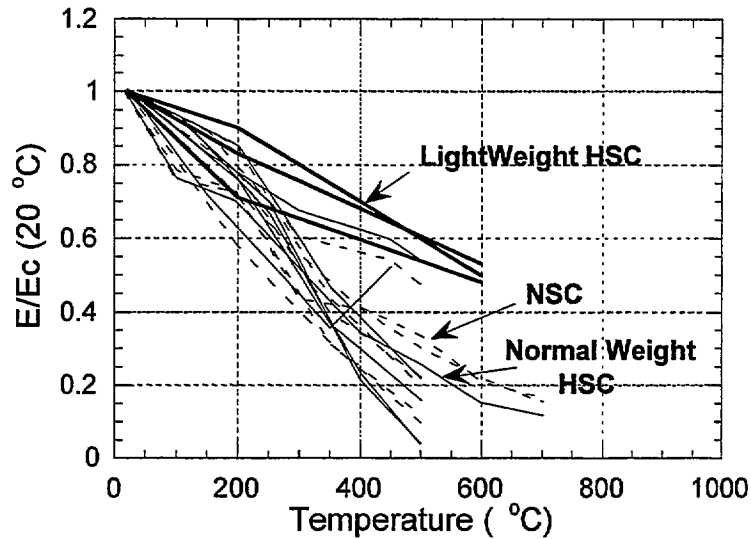


Figure 2.69 Summary of Modulus of elasticity-temperature relationships obtained from **unstressed residual strength** tests for normal and lightweight concrete.

2.4.3 Effect of Temperature on Stress-Strain Relationship of HSC

Stress-strain or load-deformation relationships, for concrete exposed to high temperatures, are not widely reported. These relationships are necessary to develop constitutive models for HSC. Of the ten materials test programs reviewed, only four offered information on stress-strain or load-deformation relationships (*Furumura, 1995; Felicetti, 1996; Diederichs, 1988; Castillo, 1990*). In general, it was observed that higher strength concrete has steeper and more linear stress-strain curves than lower strength concrete, and this difference was maintained up to 800 °C. Typical load-deformation relationships for NSC and HSC specimens are shown in Figure 2.70. HSC specimens also failed in a more brittle manner than the NSC specimens as indicated by the steeper postpeak curves in Figure 2.70.

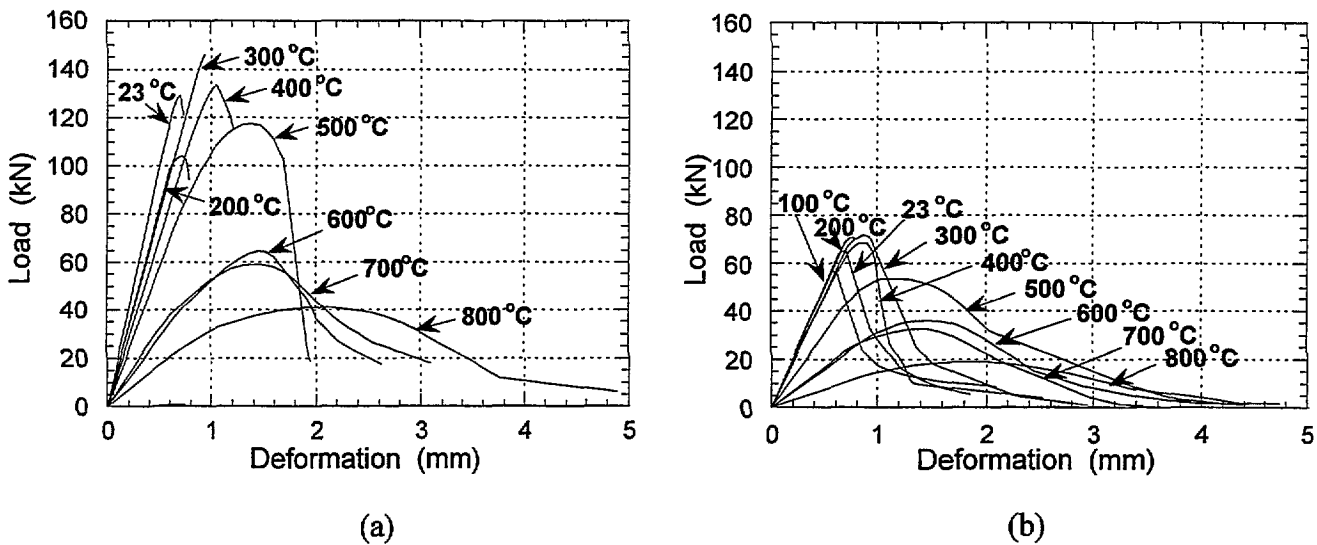


Figure 2.70 Typical load-deformation relationship at different temperature for (a) HSC and (b) NSC (Castillo and Durani, 1990)

2.4.4 Effect of Temperature on HSC Tensile Strength

Only two studies, *Felicetti* (1996) and *Noumowe* (1996), reported data concerning the tensile strength of HSC. From results of *Noumowe*'s study, which included both the direct tension and splitting tension tests, it can be observed that the tensile strengths versus temperature relationships of HSC and NSC follow similar trends (Figure 2.47). Tensile stress-strain relationships are reported by *Felicetti* for HSC of 95 MPa and 72 MPa. No significant difference in the tensile stress-strain relationships of these two concretes was observed (Figures 2.43 and 2.44).

2.4.5 Spalling of HSC at High Temperature

Not all of the experimental programs reviewed observed explosive spalling in fire-exposed HSC. Of the ten materials test programs reviewed, five observed explosive spalling failure (see Table 2.7). Of the five structural element test programs reviewed, three reported explosive spalling (see Table 2.8). Also, within the same test programs, explosive spalling was not always observed in replicate specimens. Despite this inconsistency, it is believed that explosive spalling occurs under the right combination of test conditions and that higher strength concretes, especially those densified with silica fume, are more susceptible to this type of failure.

The lowest temperature at which explosive spalling occurred was reported to be about 300 °C (Hammer, 1995), and the highest temperature was about 650 °C. The following factors were reported to have an influence on occurrence of spalling:

- Original compressive strength
- Moisture content of concrete
- Concrete density
- Heating rate
- Specimen dimensions and shapes

3. MODELING TECHNIQUES FOR THERMAL BEHAVIOR OF CONCRETE

3.1 Introduction

There are three aspects of modeling the performance of concrete structures exposed to fire. One aspect concerns fire development and fire spread. The second aspect concerns the temperature distribution within the structural members being affected. The third aspect of modeling concerns the behavior of concrete materials when subjected to the temperature field. The first and second aspects of modeling indicated above are beyond the scope of this report. Studies concerning the third aspect of modeling, i.e. thermal behavior of concrete, will be reviewed in this report. These include studies by *Bazant and Thonuthai* (1979), *England and Khoylou* (1995), *Ahmed and Hurst* (1995), and *Noumowe et al.* (1996). All focus on the problem of the potential of concrete spalling based on temperature distribution and pore pressure buildup.

3.2 Modeling of Concrete Thermal Behavior

3.2.1 *Bazant and Thonuthai* (1979)

A two dimensional finite element solution was developed by Bazant and Thonuthai (1979) at Northwestern University to predict pore-vapor pressures in heated concrete. The theory is based on thermodynamic properties of water and takes into account the changes in permeability and sorption isotherm with temperature, as well as the changes of pore space due to temperature and pressure. Briefly, the problem of heated concrete is viewed as the problem of coupled moisture transport and heat transfer, in which the *vector of the mass flux of moisture* (convective mass transport of water vapor through a porous medium), \mathbf{J} , and the *heat flux vector* (conductive heat transfer through a porous medium), \mathbf{q} , may be expressed as a linear combination of the gradients of *pore pressure* p and *temperature* T :

$$\mathbf{J} = -(a/g) \text{ grad } p; \quad \text{and} \quad \mathbf{q} = -b \text{ grad } T \quad (3.2.1.1a,b)$$

where:
a = permeability of concrete (m/s)
b = thermal conductivity
g = gravitational acceleration

When concrete is heated, water which is chemically bound in hydrated cement becomes free and migrates into the pores. This must be reflected in the *condition of conservation of mass* as follows:

$$\frac{\partial w}{\partial t} = - \text{div } (\mathbf{J}) + \frac{\partial w_a}{\partial t} \quad (3.2.1.2)$$

where:

w = specific water content of concrete, i.e. the mass of all free water per m^3 of concrete.

w_d = mass of free water that has been released into the pores by dehydration.

The *condition of heat balance* in concrete at temperature T may be written as:

$$\rho C \frac{\partial T}{\partial t} - C_a \frac{\partial w}{\partial t} - C_w \mathbf{J} \cdot \text{grad } T = - \text{div } \mathbf{q} \quad (3.2.1.3)$$

where:

ρ = density of concrete

C = isobaric heat capacity of concrete (per kg of concrete), including chemically combined water but excluding free water.

C_a = latent heat of free water.

C_w = isobaric heat capacity of liquid water.

The *boundary conditions* for the heat and moisture at the surface are as follows:

$$\mathbf{n} \cdot \mathbf{J} = B_w (p_b - p_{en}) \quad (3.2.1.4)$$

$$\mathbf{n} \cdot \mathbf{q} = B_T (T_b - T_{en}) + C_a \mathbf{n} \cdot \mathbf{J} \quad (3.2.1.5)$$

where:

\mathbf{n} = is the unit vector, outward and normal, to the surface,

p_{en} and T_{en} = the partial pressure p and temperature of the adjacent environment,

p_b and T_b = the values of p and T just under the surface of concrete,

B_w, B_T = surface emissivity for moisture and heat, respectively. $B_w \rightarrow 0$ and $B_T \rightarrow 0$ represent the cases of perfectly sealed and perfectly insulated concrete. $B_w \rightarrow \infty$ and $B_T \rightarrow \infty$ represent the case of perfect moisture and heat transmission.

The term $C_a \mathbf{n} \cdot \mathbf{J}$ represents the heat loss due to moisture vaporization at the surface.

By substituting $w = w(T, p)$ along with equations 1a and b into the conditions for *conservation of mass* and *heat balance*, equations 3.2.1.2 and 3.2.1.3, and by substituting equations 3.2.1.1a and b into the *boundary conditions*, equations 3.2.1.4 and 3.2.1.5, the following matrix variational equations may be obtained for triangular (3-noded) finite elements:

$$\mathbf{K}_1(\mathbf{dp}/\mathbf{dt}) + \mathbf{K}_2(\mathbf{dT}/\mathbf{dt}) + \mathbf{K}_3\mathbf{p} + \mathbf{F}_1 = 0 \quad (3.2.1.6)$$

$$\mathbf{K}_4(\mathbf{dT}/\mathbf{dt}) + \mathbf{K}_5(\mathbf{dp}/\mathbf{dt}) + \mathbf{K}_6\mathbf{T} + \mathbf{F}_2 = 0 \quad (3.2.1.7)$$

in which \mathbf{p} and \mathbf{T} are the global column matrices consisting of the nodal values of pore pressure p_i and temperature T_i of the finite elements; \mathbf{K}_i are the global square matrices which are obtained by assembling the elemental matrices (see *Bazant and Thonuthai, 1979* for details); and \mathbf{F}_1 and \mathbf{F}_2 are global force vectors.

3.2.2 Ahmed and Hurst (1995)

The mathematical and computational model proposed by *Ahmed and Hurst (1995)* examines the problem of coupled heat and mass transfer through concrete by considering the dehydration process of heated concrete and the effect this process has on the concrete's pore sizes and mass transport mechanism.

The governing equations, consisting of the equations for *conservation of mass* and for *conservation of energy*, in one dimensional form are as follows:

For *conservation of mass*:

$$\frac{\partial \delta_l}{\partial t} = -\Gamma \quad (3.2.2.1)$$

$$\frac{\partial}{\partial t}(\rho_v \varepsilon_g \varphi) + \frac{\partial}{\partial x}(\rho_v \varepsilon_g V_g \varphi) - \frac{\partial}{\partial x}(\rho_g \varepsilon_g D \frac{\partial \varphi}{\partial x}) = \Gamma \quad (3.2.2.2)$$

$$\frac{\partial}{\partial t}(\rho_g \varepsilon_g) + \frac{\partial}{\partial x}(\rho_g \varepsilon_g V_g) = \Gamma \quad (3.2.2.3)$$

For *conservation of energy*:

$$\rho C_p \frac{\partial T}{\partial t} + \rho_g \varepsilon_g C_{pg} V_g \frac{\partial T}{\partial x} - (\rho_g \varepsilon_g (C_{pv} - C_{pa}) D \frac{\partial \varphi}{\partial x}) \frac{\partial T}{\partial x} = \frac{\partial}{\partial x}(k \frac{\partial T}{\partial x}) - Q\Gamma \quad (3.2.2.4)$$

where:

- $\delta_l =$ mass concentration of liquid water per unit volume of porous medium (kg/m^3),
- $\rho =$ effective density of porous medium (kg/m^3),
- $\rho_v =$ density of water vapor (kg/m^3),
- $\rho_g =$ density of gaseous mixture (kg/m^3),
- $\varepsilon_g =$ volume fraction of gaseous mixture in porous medium (m^3/m^3),

- V_g = velocity of gaseous mixture (m/s),
 ϕ = mole fraction of water vapor of gaseous mixture (kmol/kmol),
 D = modified diffusivity of the gaseous mixture (m^2/s),
 C_p = effective specific heat (kJ/kg K),
 C_{pg} = specific heat of gaseous mixture (kJ/kg K),
 C_{pv} = specific heat of water vapor (kJ/kg K),
 C_{pa} = specific heat of air of the gaseous mixture (kJ/kg K),
 T = absolute temperature (K),
 t = time (s),
 x = space coordinate (m),
 k = effective thermal conductivity (W/m K),
 Γ = mass rate of evaporation per unit volume of porous medium (kg/m^3s).

$Q\Gamma$ is the evaporation/dehydration term in the *conservation of energy* equation and is defined as:

$$Q\Gamma = -\left(Q_l \frac{\partial \delta_{lf}}{\partial t} + Q_{dhev} \frac{\partial \delta_{ld}}{\partial t}\right) \quad (3.2.2.5)$$

where:

- Q_l = latent heat of evaporation (kJ/kg),
 Q_{dhev} = heat of evaporation and dehydration (kJ/kg),
 δ_{lf} = free water content in pores (kg/m^3),
 δ_{ld} = chemically bound water content (kg/m^3).

More numerical details concerning the initial and boundary conditions, and numerical techniques may be found in a related publication (*Abdel-Rahman and Ahmed, 1996*). In general, the model was applied to the problem of a heated concrete slab, and boundary conditions simulating concrete slabs exposed to fire from one side and ambient conditions on the other side were derived. The initial conditions were given by the uniform distribution of temperature, pore pressure, and moisture content in the concrete at time zero. The *conservation of mass* and *conservation of energy* equations, coupled with the boundary and initial conditions, were used to develop a set of three coupled, nonlinear, and second-order partial differential equations by making use of the concepts of continuum mechanics and principles of irreversible thermodynamics. This set of equations were discretized into matrix forms and solved using the finite different scheme (*Ahmed and Hurst, 1995*; and *Abdel-Rahman and Ahmed, 1996*).

The model was used to predict the temperature distribution and internal pore pressure with respect to time of exposure of concrete slabs of different thicknesses that were fire-tested by *Abrams and Gustaferso (1968)*. The slabs were subjected to the ASTM E 119 time-temperature curve (*ASTM E 119, 1988*). The results of the computations are shown in Figures 3.1 to 3.4. Figure 3.1 shows the comparison between the predicted temperatures of concrete on the unexposed surface of the slabs

with measurement by Abrams and Gustafarro. Figure 3.2 shows similar comparison but for temperature distribution across the thickness of the slabs. Figures 3.3 and 3.4 show the predicted pore pressure at different depths in the slabs at different exposure times.

The authors observed good agreements between experimental temperature histories and the predictions made by the model and recommended its use for research and design purposes.

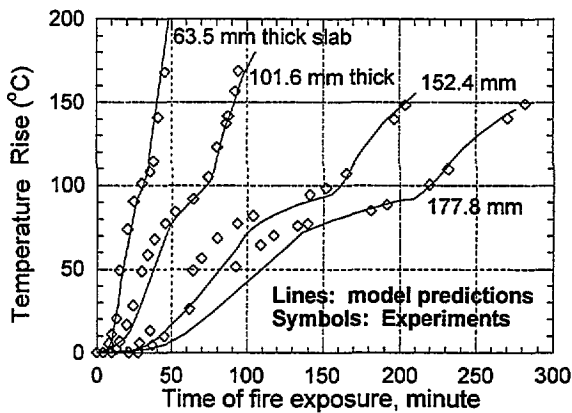


Figure 3.1 Comparison of measured Unexposed Surface Temperatures with Predictions for Different Slabs (Ahmed and Hurst, 1995)

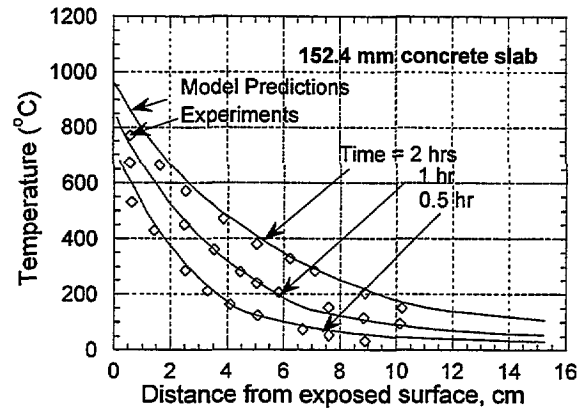


Figure 3.2 Comparison of Predicted Temperature in 152-mm Concrete Slab with Experimental Results (Ahmed and Hurst, 1995)

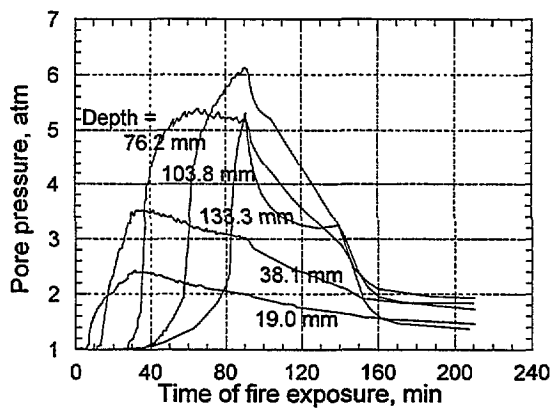


Figure 3.3 Predicted Pore Pressure History at Different Depths in 152-mm Thick Slab (Ahmed and Hurst, 1995)

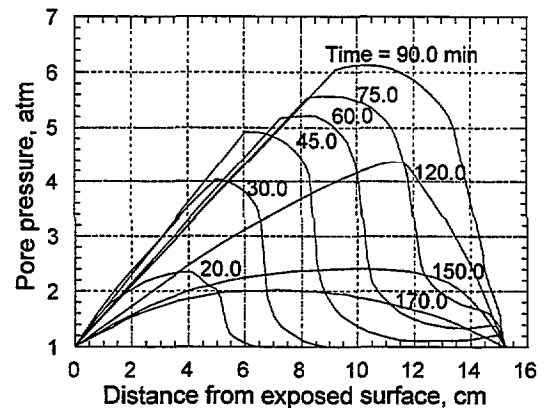


Figure 3.4 Predicted Pore Pressure Distribution at Various Times in 152-mm Thick Slab (Ahmed and Hurst, 1995)

3.2.3 England and Khoylou (1995)

England and Khoylou (1995) presented a numerical model to describe the movement of water and vapor in normal and high performance concretes, as influenced by pore vapor pressures at elevated temperatures.

The volume expansion of water vapor in concrete, which accelerates with increased temperature (above 200 °C) and results in increased pore pressure and potential spalling of concrete, can be described in terms of the rate of change of temperature, dT/dt , and the rate of change of specific volume of water with respect to temperature, dv/dT . The derivation is as follows (England and Khoylou, 1995):

$$\frac{dV}{dt} = \frac{d(mv)}{dt} \quad (3.2.3.1)$$

where dV/dt is the rate of change of pore water volume, and m is the mass of water contained in the pore volume V . The above equation may be rewritten as follows:

$$\frac{dV}{dt} = \frac{m dv}{dt} + \frac{v dm}{dt} \quad (3.2.3.2)$$

or,

$$\frac{dV}{dt} = m \left(\frac{dv}{dT} \right) \left(\frac{dT}{dt} \right) + v \left(\frac{dm}{dt} \right) \quad (3.2.3.3)$$

The last equation may be interpreted in two different ways. One corresponds to the assumption that there is no mass change in the concrete pores, i.e., $dm/dt = 0$. The other corresponds to the assumption that there is no change of pore volume with time, i.e., $dV/dt = 0$.

For the case of *no change of mass in the pores* ($dm/dt=0$), the rate of change of pore volume, dV/dt , is the product of three items: (1) the mass m of liquid water causing saturation at temperature, T , (2) the rate of change of specific volume with respect to temperature, dv/dT , and (3) the rate of change of local temperature with respect to time.

$$\frac{dV}{dt} = m \left(\frac{dv}{dT} \right) \left(\frac{dT}{dt} \right) \quad (3.2.3.4)$$

By modeling the porous structure of concrete as consisting of uniformly distributed cubical pores surrounded by an elastic skeleton of cement paste, as is shown in Figure 3.5, it is possible to acquire an estimate of the pore pressure, time, and temperature which might cause fracture of the cement skeleton (spalling of concrete). The thickness T of the elastic cement skeleton can be determined by equating the maximum tensile stress of the skeleton, σ_t , with the tensile strength of concrete, f_t .

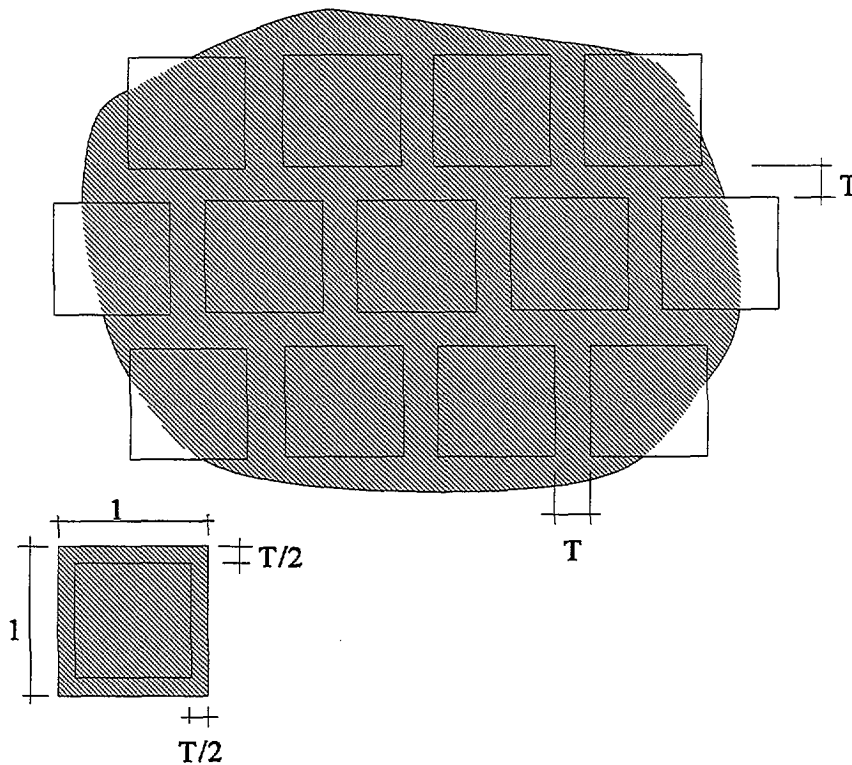


Figure 3.5 Idealization of concrete as porous cubical forms with elastic cement paste skeleton (England and Khoylou, 1995)

For numerical analysis, data such as the w/c ratio, ratio of pore volume to bulk concrete volume (V_p/V_{tot}), ratio of free water volume to pore volume (V_{fw}/V_p), ratio of volume of unfilled pores to bulk volume (V_{uf}/V_{tot}), as well as permeability and concrete strength are necessary. Some of these data can only be obtained from experimental measurements.

For the case of *no change of pore volume with time* ($dV/dt = 0$), the rate of mass flow out of the pores necessary to maintain constant pore volume, due to internal pore pressure P , may be written as:

$$\frac{dm}{dt} = - \frac{m}{v} \left(\frac{dv}{dT} \right) \left(\frac{dT}{dt} \right) \quad (3.2.3.5)$$

To avoid fracture of the paste skeleton (spalling of concrete), the rate of mass expulsion from the saturated zone of heated concrete must exceed the constant pore volume condition above, i.e., the right side of equation 3.2.3.5. The pore pressure P may be estimated from knowledge of the initial percentage pore volume available to water, the tensile strength of the cement paste skeleton and its geometrical modeling.

In the concluding remarks, the authors suggested that HSC is more susceptible to spalling than normal strength concrete since it usually has smaller free pore volume (higher paste density) and thus, at high temperature, the originally unfilled pores become saturated much quicker (due to the small volume of unfilled pores), resulting in excessive pore pressure and spalling of concrete.

3.2.4 Noumowe, Clastres, Debicki, Costaz (1996)

The analytical part of the study by Noumowe et al. (1996) consisted of modeling to calculate thermal stresses and pore pressure in concrete cylinders. Details of the modeling techniques were not offered in the paper. In general, three aspects of modeling were performed:

- Modeling the distribution of the *temperature field* across a section of a concrete cylinder.
- Modeling the *thermal stresses* due to the non-uniform temperature distribution.
- Modeling *water vapor pressure* buildup.

The *temperature field* in a cross section of a cylinder of infinite length is modeled using the following equation, which gives the temperature at a radial position r at time t :

$$T(r,t) = R \left(t - \frac{a^2 - r^2}{4D} \right) \quad (3.2.4.1)$$

The radial temperature difference between the concrete core and the outer surface is expressed by:

$$\Delta T(a) = T(a, t) - T(0,t) = Ra^2/4D \quad (3.2.4.2)$$

where: r = radial position at which the temperature $T(r,t)$ is calculated,
 t = time,
 R = heating rate,
 a = radius of specimen, and
 D = thermal diffusivity.

Given the above *temperature field*, the resulting *thermal stresses* of any point at a radial distance r from the center of the cylinder may be computed as shown below. The terms r , D , and R are the same as in the *temperature field* equation (3.2.4.1). In these equations, α is the coefficient of thermal expansion, ν is Poisson's ratio, and E is Young's modulus of elasticity.

$$\sigma(z) = (a^2 - 2r^2) \frac{\alpha ER}{8D(1-\nu)} \quad (3.2.4.3)$$

$$\sigma(\theta) = (a^2 - 3r^2) \frac{\alpha ER}{16D(1-\nu)} \quad (3.2.4.4)$$

$$\sigma(r) = (a^2 - r^2) \frac{\alpha ER}{16D(1-\nu)} \quad (3.2.4.5)$$

To predict *water vapor pressure*, the authors referred to a finite element program named TEMPOR2 which takes into account variations in permeability, pore volumes, and sorption isotherms as functions of temperature. The types of data used in the calculation include w/c ratio, permeability (m/s), concrete age (days), initial relative humidity (%), thermal conductivity (J/ms°C), and external heating rate (°C/min).

Based on their analytical study, the authors concluded that, "...because of its greater rigidity and its higher coefficient of expansion, HSC is subjected to greater thermal stresses than normal strength concrete. Also because of its low degree of porosity and permeability, HSC is also subjected to higher water vapor pressures than normal strength concrete." Finally, even though there was no report of explosive spalling in their experimental study, the authors suggested that, "...in all likelihood, the explosive spalling in HSC is due to a combination of thermal stresses and water vapor pressure in the pores of concrete." The authors also suggested different techniques for mitigating the risk of explosive spalling, including (1) increasing the thermal diffusivity of concrete by using mineralogically suitable aggregates to minimize the thermal gradients, (2) increasing the open micro porosity of concrete using polypropylene fibers to lower the water vapor pressure, (3) limiting the quantity of fines or ultra fine particles, such as silica fume and fillers, in the concrete, (4) insulating concrete structures to lower the heating rate, thus facilitating the progressive release of water vapor.

3.3 Summary

The limited number of analytical studies dealing with calculating the internal stresses due to pore vapor pressure in fire-exposed concrete is indicative of the complexity of this problem. Bazant and Thonuthai (1979) and Ahmed and Hurst (1995) used similar approaches for modeling moisture transport and internal pore pressure, but different techniques were used for numerical solutions - Bazant and Thonuthai employed the finite element technique while Ahmed and Hurst used the finite difference technique. Some differences between Bazant and Thonuthai (1979) and Ahmed and Hurst (1995) approaches include:

- Bazant and Thonuthai solved for 2 coupled differential equations with temperature and pore pressure as output, while Ahmed and Hurst solved for 3 coupled differential equations with temperature, moisture content and pore pressure as output.
- Bazant and Thonuthai used constant thermal properties, while Ahmed and Hurst used variable thermal properties as functions of temperature, moisture content, and pore pressure.
- Bazant and Thonuthai did not consider heat and mass transfer by diffusion and heat transfer by radiation within the porous medium, while Ahmed and Hurst included these in their model.

While the modeling techniques used in these studies might be useful for modeling the internal stresses and moisture transport of fire exposed HSC, none of these studies offered validation of computed pore pressures with experimental data. Thus experimental validation is needed before these modeling tools can be used for parametric studies of the performance of HSC when exposed to fire.

4. FIRE TEST METHODS AND PROPERTIES OF HEATED CONCRETE ACCORDING TO CODES AND COMMITTEE REPORTS

4.1 Introduction

Experimental programs reviewed in this report were conducted in different countries using different standard fire test methods. To provide a proper perspective for comparison of the test results, three fire test methods (the International Standard ISO 834, ASTM E 119, and Japanese Industrial Standard JIS A 1304) are reviewed in section 4.2.

The material properties of all concretes (not limited to HSC) at elevated temperatures presented in building codes and professional committee reports are reviewed in section 4.3.

4.2 Fire Test Methods

4.2.1 *International Standard ISO 834 (1975)*

The International Standard ISO 834, *Fire Resistance Tests - Elements of Building Construction*, specifies standard heating and pressure conditions, test procedures and criteria for the determination of the fire endurance of elements of building construction of various categories. This test method provides for the determination of the fire resistance of building elements on the basis of the length of time for which the test specimens satisfy the prescribed criteria.

The scope of ISO 834 includes, but is not limited to, the following structural elements:

- Walls and partitions;
- Columns;
- Beams;
- Floors (with or without ceilings);
- Roofs (with or without ceilings).

Elements which fall into none of these categories may be tested by analogy with a similar element.

ISO 834 specifies that the test specimen is subjected to a furnace temperature rise given by the following equation:

$$T - T_o = 345 \log_{10} (8t + 1) \quad (4.2.1.1)$$

where:

- t = time, expressed in minutes,
- T = furnace temperature at time t , expressed in ° C, and
- T_o = initial furnace temperature, expressed in ° C.

Tabulated values obtained from the above relationship are shown in Table 4.1. The curve representing this relationship, known as the *standard time-temperature curve*, is shown in Figure 4.1.

Table 4.1. Time-Temperature Data on ISO 834 Standard Fire Curve

Time, t	Furnace Temperature Rise $T-T_o$	Time, t	Furnace Temperature Rise $T-T_o$
min	°C	min	°C
5	556	90	986
10	659	120	1029
15	718	180	1090
30	821	240	1133
60	925	360	1193

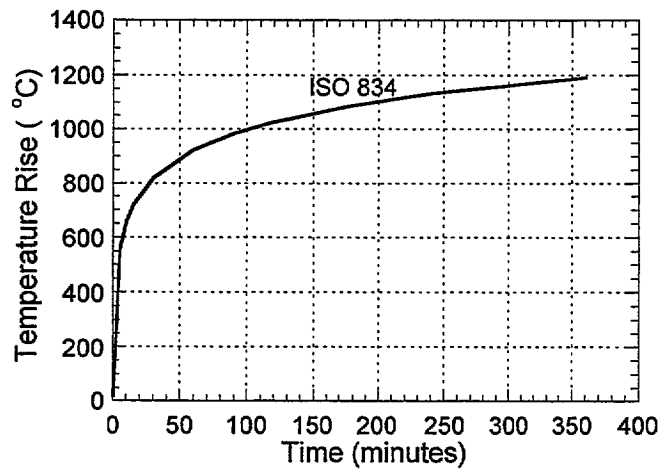


Figure 4.1. Standard Fire Curve for ISO 834

The test specimens are conditioned so that they correspond as closely as possible, in temperature, moisture content and mechanical strength, to the expected state of a similar element in service.

The fire resistance of the test specimens is the time, expressed in minutes, of the duration of heating until failure occurs as defined by one of the following criteria:

- *Load-bearing capacity*: Failure is reached when the test specimen collapses in such a way that it no longer performs the load-bearing function for which it was intended.
- *Insulation*: For test elements, such as walls and floors which have the function of separating two parts of a building, failure occurs when: (1) the temperature on the unexposed face of the specimen increases above the initial temperature by more than 140 °C; (2) the maximum temperature at any point on the unexposed face exceeds the initial temperature by more than 180 °C; and (3) when the surface temperature exceeds 220 °C, irrespective of the initial temperature.
- *Integrity*: For elements such as walls and floors which have the function of separating two parts of a building, failure is reached when: (1) cracks, holes, or other openings, through which flames or hot gases can pass, occur in the test specimen; (2) the 100 mm square by 20 mm thick cotton pads, held at a distance of between 20 and 30 mm from any opening on the unexposed side, is ignited or when sustained flaming, having a duration of at least 10 s, appears on the unexposed face of the test element.

For load-bearing structural elements, the fire resistance is judged by the criterion of load-bearing capacity. For a separating element, the fire resistance is judged by the criteria of insulation and integrity. For a load-bearing and separating element, the fire resistance is determined by all three criteria: load-bearing capacity, insulation, and integrity.

4.2.2 ASTM E 119 (1988)

The ASTM E 119, *Standard Test Methods for Fire Tests of Building Construction and Materials*, specifies the test procedures for evaluating the fire resistance of structural elements for buildings, including bearing and other walls and partitions, columns, girders, beams, slabs, and composite slab and beam assemblies for floors and roofs. The standard is widely used for fire testing in North America.

The test subjects a specimen to a *standard fire exposure*, which is characterized by the standard time-temperature curve shown in Figure 4.2. Some points on the standard time-temperature curve are tabulated in Table 4.2. A more detailed tabulation may be found in Appendix X1 of ASTM E 119. Comparison with the ISO 834 curve shows that these two temperature histories are similar.

The end-point criteria applied to concrete test assemblies are as follows:

- *Heat transmission end point*: As it applies to separating elements such as walls, floors, and roofs. This end point occurs when the specimen's unexposed surface exceeds an average temperature rise of 139° C or when any single point on the unexposed surface exceeds 181° C above its initial temperature.
- *Flame passage end point*: As it applies to assemblies that function as separating elements,

this end point occurs when flames or gases hot enough to ignite combustible material (cotton waste) pass through the test assembly.

- *Structural end point:* As it applies to load-bearing elements, including those that must function as separating elements. This end point occurs when the test assembly can no longer sustain the applied load, or meet other specified conditions of acceptance in ASTM E119, based on the given type of test specimen (for example, temperature limits on steel reinforcement in concrete beams).

Table 4.2. Time-Temperature Data of Points for ASTM E 119 Standard Fire Curve

Time	Standard Fire Temperature
minutes	°C
5	538
10	704
30	843
60	927
120	1010
240	1093
480 and over	1260

Walls must additionally be subjected to a hose stream test for purposes of evaluating specimen stability, durability and resistance to thermal shock. An assembly is considered to have failed the test if an opening develops such that a projection of water from the hose stream passes beyond the unexposed surface at any time during the stream's application

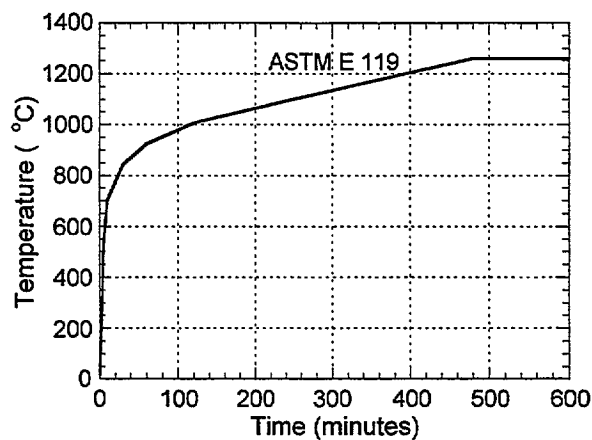


Figure 4.2. ASTM E 119 Standard Fire Curve

4.2.3 Japanese Industrial Standard JIS A 1304 (1994)

The Japanese Industrial Standard JIS A 1304, *Method for Fire Resistance Test for Structural Parts of Buildings*, specifies a test method to measure the fire resistance of building elements such as a wall, column, beam, floor, ceiling, roof, etc. The fire endurance rating system in JIS A 1304 classifies the fire resistance of an element by 5 levels (30-minute heat, 1-hour heat, 2-hour heat, 3-hour heat, and 4-hour heat). One major difference between JIS A 1304 and the ISO 834 and ASTM E 119 is in the heat transmission criterion. The Japanese standard sets the unexposed surface temperature of walls and floors at 260° C. Assuming an ambient temperature of 20° C, this allowable temperature rise is about 100° C greater than that of E119 or ISO 834. This has a significant effect on the fire resistance rating results of assemblies tested to the respective standards. The maximum heat exposure time (duration of the fire test) in JIS A 1304 is limited to 4 hours.

The standard time-temperature curve specified in JIS A 1304 is shown in Figure 4.3. Points on this curve are tabulated in Table 4.3. Wall specimens are heated from one side in a vertical position in accordance with the standard time-temperature curve. Column specimens are heated from four sides in a vertical position. Beams and floors are heated from the under side in a horizontal position. The following criteria are used to determine if the concrete test specimen “passes” the fire test:

- Structural failure due to deformation, destructive spalling or harmful change to fireproofing material does not occur during heating.
- During heating, there are no cracks in walls, floors and roofs which allow flames to penetrate.
- For walls and floors, the temperature on the unexposed side does not exceed 260 °C.
- During heating, all structural materials do not flame remarkably, and after completion of heating any embers do not remain for 10 minutes or more.

Table 4.3. Time-Temperature Values of Points on Standard Fire Curve of JIS A 1304

Time	Heating Temperature						
min.	°C	min.	°C	min.	°C	min.	°C
5	540	50	905	95	985	180	1050
10	705	55	915	100	990	190	1060
15	760	60	925	110	1000	200	1065
20	795	65	935	120	1010	210	1070
25	820	70	945	130	1015	220	1080
30	840	75	955	140	1025	230	1085
35	860	80	965	150	1030	240	1095
40	880	85	975	160	1040		
45	895	90	980	170	1045		

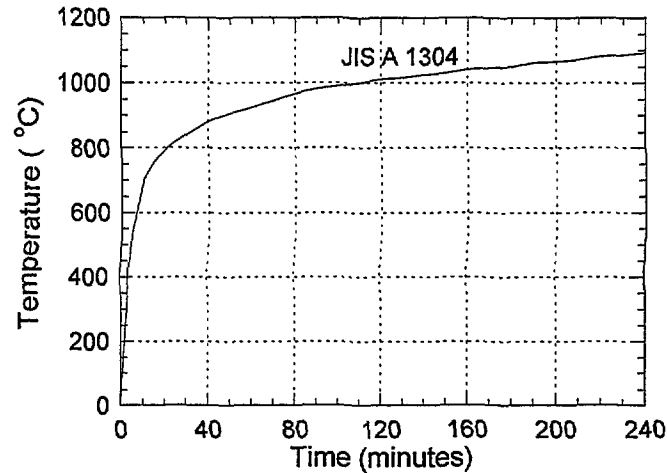


Figure 4.3. JIS A 1304 Standard Time-Temperature Curve

4.3 Properties of Heated Concrete

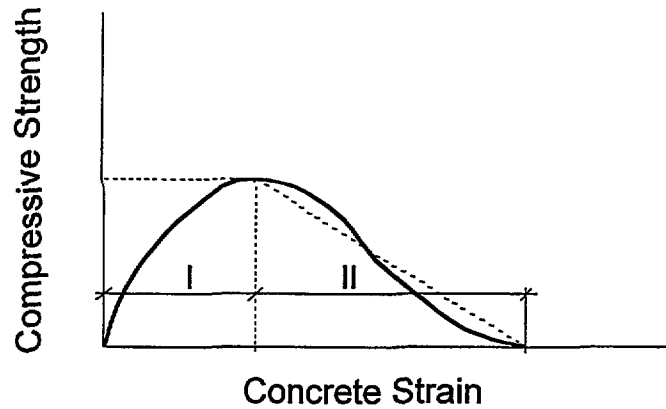
4.3.1 CEN - Comité Européen de Normalisation

The *Eurocode 2 - Design of Concrete Structures - Part 1-2: Structural Fire Design* and *Eurocode 4 - Design of Composite Steel and Concrete Structures - Part 1-2: General Rules for Structural Fire Design* specify rules for strength and deformation properties of uniaxially stressed concrete at elevated temperatures. These rules are as follows:

- The strength and deformation properties of uniaxially stressed concrete at elevated temperatures are characterized by a set of stress-strain relationships which consist of two ranges as presented in Figure 4.4. The first range is up to the ultimate strength and the second range is beyond ultimate strength. For a given concrete temperature θ , the stress-strain relationships for the first range in Figure 4.4 are defined by two parameters:
 - the compressive strength $f_{c,\theta}$
 - the strain $\epsilon_{cu,\theta}$ corresponding to $f_{c,\theta}$
- Tabulated values for these two parameters are given in Table 4.4. Values of $f_{c,\theta}$, for normal weight siliceous and calcareous aggregate concretes (NC) and for lightweight concrete (LW) are obtained by multiplying the corresponding reduction factor $k_{c,\theta}$ by the room-temperature compressive strength $f_{c,20} \text{ } ^\circ\text{C}$. For intermediate values of temperature, linear interpolation

may be used. For lightweight concrete (LW) the values of $\epsilon_{cu,\theta}$, if needed, should be obtained from tests.

- The tensile strength of concrete may be assumed to be zero. If tensile strength is taken into account, it should not exceed 10% of the corresponding compressive strength.



RANGE I:

$$\sigma_{c,\theta} = f_{c,\theta} \left[3 \left(\frac{\epsilon_{c,\theta}}{\epsilon_{cu,\theta}} \right) / \left(2 + \left(\frac{\epsilon_{c,\theta}}{\epsilon_{cu,\theta}} \right)^3 \right) \right]$$

$k_{c,\theta} = f_{c,\theta} / f_{c,20^\circ\text{C}}$ and $\epsilon_{cu,\theta}$ to be chosen according to Table 4.4.

RANGE II:

For numerical purposes a descending branch may be necessary

Figure 4.4. Mathematical model for stress-strain relationships of concrete under compression at elevated temperatures (ENV 1994-1-2).

Table 4.4. Values for the two parameters to describe the ascending branch of the stress-strain relationships of concrete at elevated temperature according to CEN ENV 1994-1-2

Concrete Temperature θ_c ($^{\circ}\text{C}$)	$k_{c,\theta} = f_{c,\theta}/f_{c,20^{\circ}\text{C}}$			$\epsilon_{cu,\theta} \times 10^{-3}$
	NC		LW	NC
	Siliceous	Calcareous		
20	1	1	1	2.5
100	0.95	0.97	1	3.5
200	0.90	0.94	1	4.5
300	0.85	0.91	1	6.0
400	0.75	0.85	0.88	7.5
500	0.60	0.74	0.76	9.5
600	0.45	0.60	0.64	12.5
700	0.30	0.43	0.52	14.0
800	0.15	0.27	0.40	14.5
900	0.08	0.15	0.28	15.0
1000	0.04	0.06	0.16	15.0
1100	0.01	0.02	0.04	15.0
1200	0	0	0	15.0

The reduction factors $k_{c,\theta}$ for normal and lightweight concretes, given in Table 4.4, are plotted for comparison in Figure 4.5. The design strain at ultimate strength, $\epsilon_{cu,\theta}$, at high temperatures is plotted in Figure 4.6.

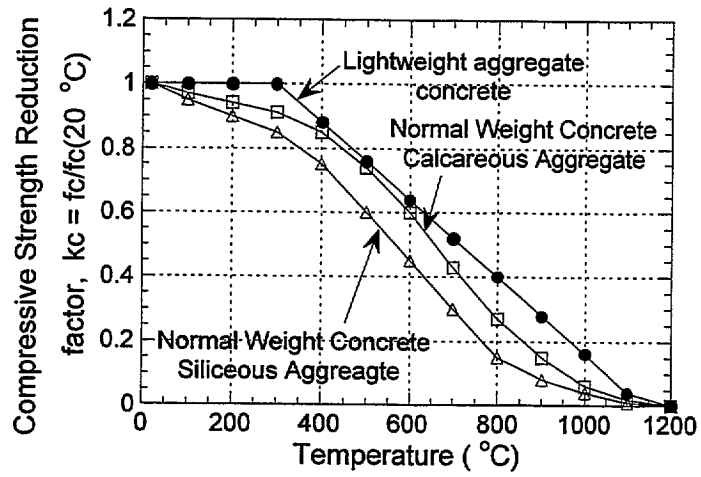


Figure 4.5 Strength Reduction Factor for Concrete with Respect to Temperature (CEN ENV 1994-1-2)

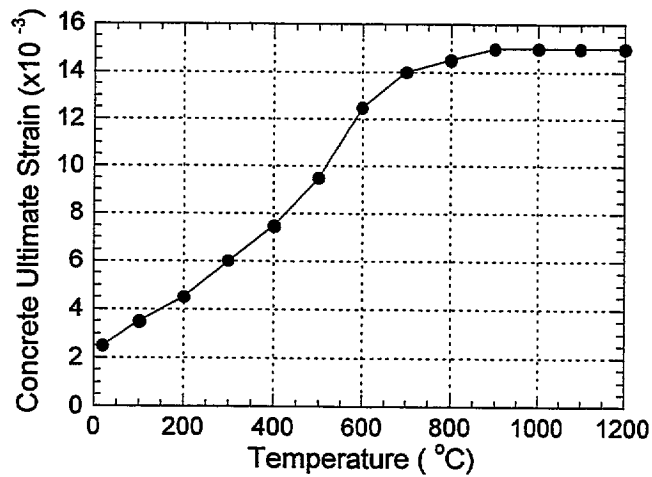


Figure 4.6 Variation of Strain at Ultimate Strength with Respect to Temperature (CEN ENV 1994-1-2)

4.3.2 ACI Committee Report 216R-89

ACI 216R-89, *Guide for Determining the Fire Endurance of Concrete Elements*, illustrates the application of the structural engineering principles and information on properties of building materials (concrete and steel) to determine the fire resistance of reinforced concrete constructions, such as slabs, beams, walls, and concrete columns. The information on properties of concrete at high temperatures, given in chapter 6 of ACI 216R, are summarized here.

Unlike the Eurocodes, where mathematical relationships are prescribed for compressive strength as a function of temperature, the ACI 216 committee report did not propose specific mathematical relationships for compressive strength, modulus of elasticity, and shear modulus with temperature.

With regard to compressive strength, ACI 216R-89 summarizes the results of *stressed*, *unstressed*, and *unstressed residual strength* tests of concrete cylinders conducted by Abrams (1971) (see section 2.3.1.5). ACI 216R-89 cites three of Abrams' observations. These are:

- In the *stressed* tests, stress levels in the range of 0.25 to 0.55 of the room temperature compressive strength had little effect on the strength at high temperatures.
- The *unstressed residual* strengths were, in all cases, lower than the strengths determined by the other two types of tests.
- The original concrete strengths between 28 and 45 MPa had little effect on strength at high temperatures.

The effect of temperatures on the elastic and shear moduli are illustrated by data obtained by Cruz (1966) for normal strength concrete (Figures 4.7 and 4.8). Cruz concluded that aggregate type and concrete strength do not significantly affect the elastic and shear moduli at high temperatures.

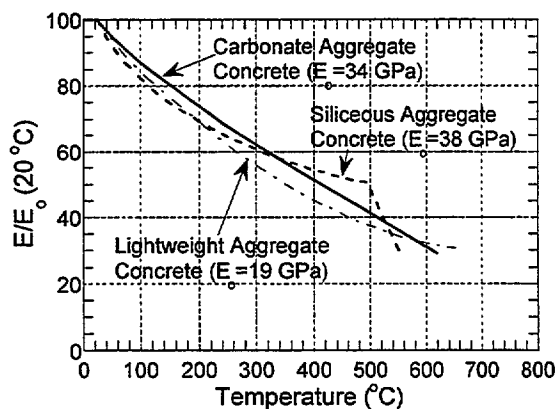


Figure 4.7. Variation of E/E_0 with Temperature (ACI 216R-89)

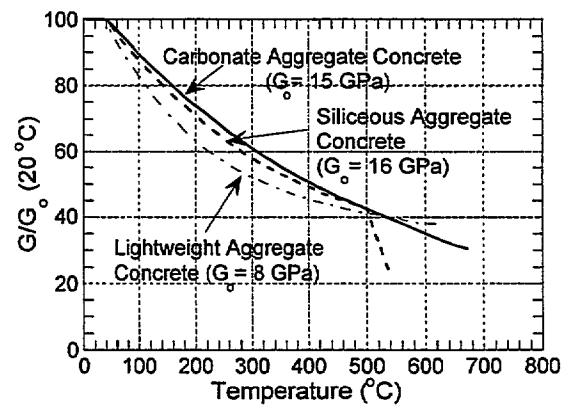


Figure 4.8. Variation of G/G_0 with Temperature (ACI 216R-89)

4.3.3 CEB Bulletin D'Information N° 208 (RILEM - Committee 44-PHT)

RILEM Committee 44-PHT was formed by ISO Technical Committee 92 in 1977 to study existing knowledge on the effects of fire on concrete. A report, *Properties of Materials at High Temperatures - Concrete* (Schneider, 1983 and 1985) which summarized the results of various studies, was published in 1985. This RILEM report was also incorporated into a later publication, *Fire Design of Concrete Structures* (CEB Bulletin D'Information N° 208, 1991). Information from the RILEM report relevant to concrete compressive strength, modulus of elasticity, stress-strain relationships, spalling, and tensile strength are summarized here.

Concerning compressive strength, results of tests conducted by Malhotra (1957), Abrams (1971), Collet (1976), Waubke (1977), and Schneider (1979) were presented, and recommended design curves were proposed (Figures 4.9 and 4.10). The concretes used in these five test programs had a maximum compressive strength of 50 MPa. The following general conclusions were cited:

- Original strength of concrete, type of cement, aggregate size, heating rate, and water/cement ratio have little effect on the relative strength versus temperature characteristics of concrete.
- Aggregate/cement ratio has a significant effect on the strength of concrete exposed to high temperature. The reduction being proportionally smaller for lean mixtures than for rich mixtures.
- Type of aggregate appears to be one of the main factors influencing concrete strength at high temperature. Siliceous aggregate concrete has lower strength (by percentage) at high temperature than calcareous and lightweight aggregate concrete.
- *Stressed* specimens resulted in higher compressive strength at high temperature than *unstressed* specimens.

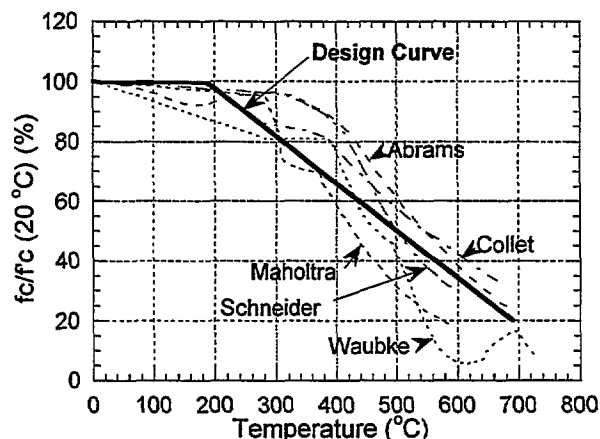


Figure 4.9 Compressive Strength of Siliceous Normal Weight Concrete at High Temperature

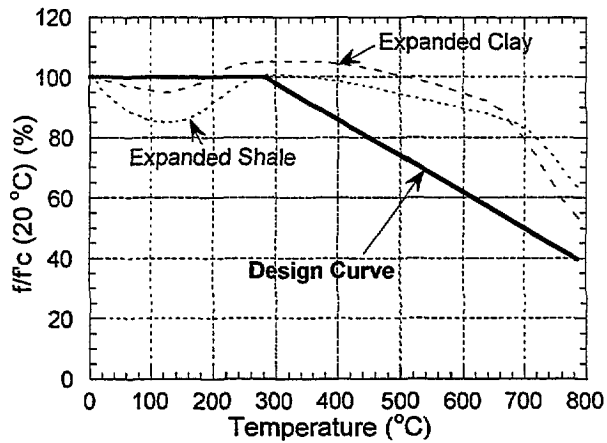


Figure 4.10 Compressive Strength of Lightweight Concrete at High Temperature

For modulus of elasticity, data obtained by Cruz (1966), Maréchal (1970), and Schneider (1975) were summarized, and design curves were recommended as shown in Figure 4.11. The following conclusions were cited:

- Original strength of concrete, water/cement ratio, and type of cement have little effect on the relative modulus of elasticity versus temperature relationship.
- Aggregate type and preload (*stressed tests*) have a strong influence on modulus of elasticity. Lightweight aggregate concrete has smaller reduction in modulus of elasticity with increasing temperature than NSC. Siliceous aggregate concrete has the highest reduction in modulus of elasticity with increasing temperature.

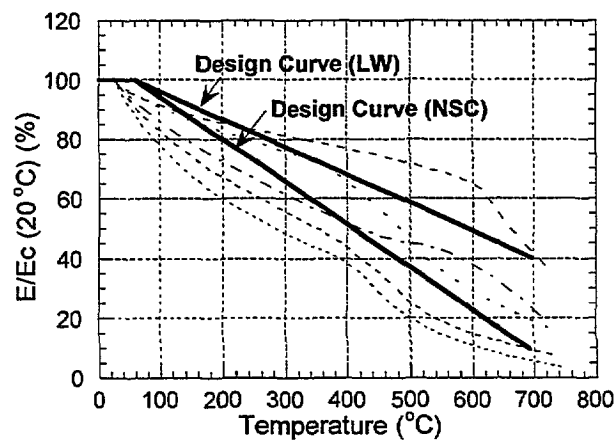


Figure 4.11. Effect of Temperature on Modulus of Elasticity

For tensile strength, tests by Harada (private communication) and Thelandersson (1971) were referenced, and a design curve was recommended as shown in Figure 4.12. The conclusions were:

- Aggregate type and mixture proportions have a significant effect on the tensile strength versus temperature relationships. The decrease in tensile strength of calcareous aggregate concrete is twice as high as that of siliceous aggregate concrete at 500 °C. Concretes with lower cement content have lower reduction in tensile strength than those with higher cement content.
- The rate of heating has minimal effects on tensile strength at high temperature.
- The residual tensile strength is somewhat lower than the tensile strength measured at elevated temperature.

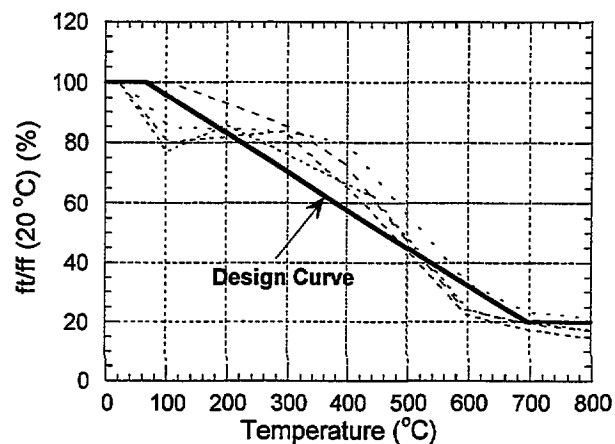


Figure 4.12 Effect of Temperature on Tensile Strength

For concrete stress-strain relationships, tests by Anderberg (1976), Schneider (1975), Weigler (1967) were referenced. The following conclusions were cited:

- Original strength of concrete, water/cement ratio, heating rate, and type of cement have only minor effects on the shape of the σ - ϵ curve.
- The aggregate/cement ratio significantly affects the shapes of the σ - ϵ and ϵ -temperature curves.
- The aggregate type significantly affects the shapes of the σ - ϵ curves and the ϵ -temperature curves. Concretes made with hard aggregate (siliceous, basaltic) generally have a steeper decrease of the initial slope at high temperature than softer aggregate (lightweight aggregates).

For spalling, the RILEM report references the study by Meyer-Ottens (1975), which shows the potential for destructive spalling in concrete structural elements as a function of concrete compressive stress and the element thickness (see Figure 4.13). The following conclusions were cited:

- Moisture content is one of the major factors affecting the likelihood of spalling. An increase in moisture content increases the probability of spalling.
- Heating rate is also one of the major factors affecting spalling. The higher the heating rate, the higher is the probability of spalling. Heating from more than one side also increases the probability of spalling.
- Compressive stresses due to external load or prestressing increase the probability of spalling.
- The probability of spalling decreases with increasing thickness of the concrete element.
- Mixture proportions influence the risk of spalling by changing the pore size distributions. An increase in porosity and a decrease in pore radius increase the risk of spalling.

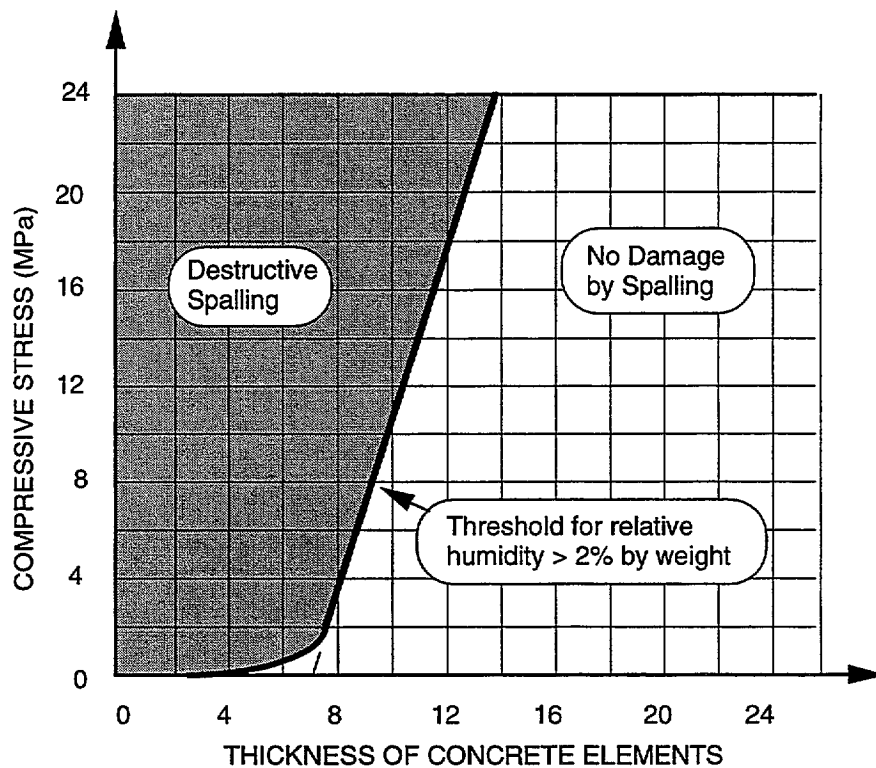


Figure 4.13 Threshold for Spalling of Concrete Elements with Different Thicknesses [Meyer-Ottens (1975)]

4.3.4 CRSI - Reinforced Concrete Fire Resistance

The Concrete Reinforcing Steel Institute (CRSI) has summarized available technical information on fire resistance of reinforced concrete elements to aid in developing rational methods of calculating structural fire endurance. Some information on properties of concrete at high temperature were summarized in the CRSI report *Reinforced Concrete Fire Resistance* (1980). Similar to the reports by ACI Committee 216 and RILEM Committee 44-PHT, information on properties of concrete at high temperature in the CRSI report were also based on tests conducted in the 1960s (Abrams, 1971; and Cruz, 1966). Thus this reference is cited here for completeness but a detailed review will not be given, since the information has already been discussed.

4.4 Applicability of Code Design Recommendations to HSC

An assessment of the applicability of the design curves, prescribed by the Eurocodes (see Figure 4.5) and recommended by RILEM Committee 44-PHT (see Figures 4.9 to 4.11), may be obtained by superposing these design curves onto the results of HSC tests (Figures 2.62 to 2.69). Figures 4.14 and 4.15 show the superpositions of the design compressive strength-temperature curves on *unstressed* test data (Figures 2.62 and 2.63). Figures 4.16 and 4.17 show the superpositions of the same design curves on *unstressed residual strength* test data (Figures 2.64 and 2.65). Similarly, Figures 4.18 and 4.19 show the superpositions of the design curves on *stressed* test data (Figures 2.66 and 2.67). Finally, Figures 4.20 and 4.21 show the superpositions of the design modulus of elasticity-temperature curves on test data obtained by *unstressed* and *unstressed residual strength* tests.

For *unstressed* tests, Figure 4.14 shows that the Eurocode and RILEM's design curves are unconservative in predicting the compressive strength of normal-weight-aggregate HSC in the temperature range between room temperature to about 350 °C. Above 350 °C, the design curves become more applicable to both HSC and NSC, which is consistent with the observation that the difference between HSC and NSC narrowed at this temperature. For lightweight-aggregate concrete, Figure 4.15 shows that, with the limited amount of data available, both the Eurocode and RILEM's design curves are unconservative for HSC and are more suitable for NSC.

For *unstressed residual strength* tests, Figure 4.16 shows that the Eurocode and RILEM's design curves are in better agreement with HSC data than for *unstressed* tests. However, the design curves appear to be slightly unconservative for both HSC and NSC at temperatures above 250 °C. For lightweight-aggregate concrete, the design curves are also unconservative for both HSC and NSC.

Figures 4.18 and 4.19 shows the superposition for *stressed* tests. Given the limited amount of *stressed* test data, it is difficult to make definitive conclusion regarding the applicability of the design curves. In general, the design curves appear to be applicable to NSC made of both normal weight and lightweight aggregate.

For modulus of elasticity, Figure 4.20 shows that the Eurocode design curves are unconservative compared with *unstressed* test data for both normal and lightweight aggregate HSC. For *unstressed residual strength* test, the design curve for lightweight aggregate concrete appears to be in good agreement with data from lightweight aggregate HSC. However, the design curve for normal weight aggregate concrete remains unconservative compared with data of normal weight aggregate HSC (Figure 4.21).

From these superpositions, it may be concluded that the current design compressive strength-temperature curves and modulus of elasticity-temperature curves prescribed by the Eurocode and recommended by RILEM Committee 44-PHT are more suitable for NSC, and thus caution must be used when applying these design curves for HSC.

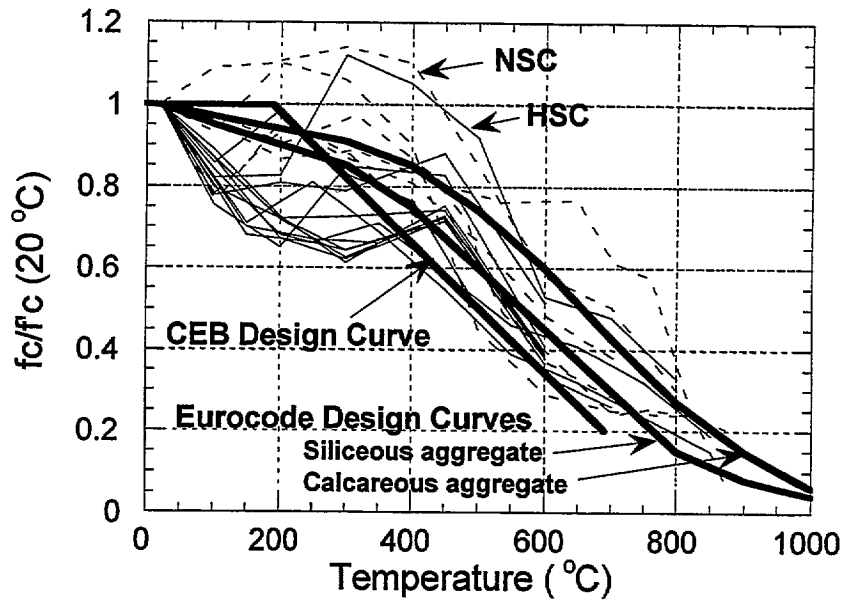


Figure 4.14 Comparison of Design Curves for Compressive Strength and Results of *Unstressed* Tests of Normal Weight Aggregate Concrete

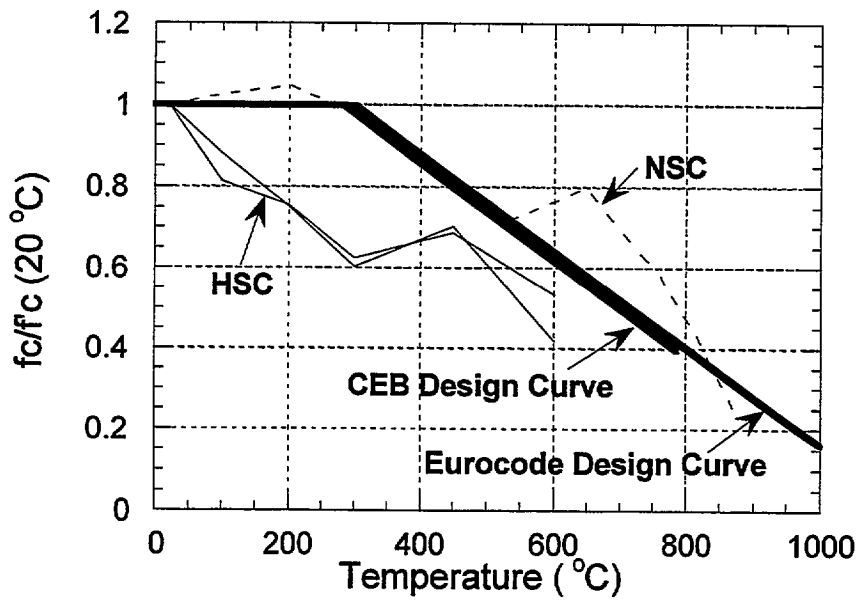


Figure 4.15 Comparison of Design Curves for Compressive Strength and Results of *Unstressed* Tests of Lightweight Aggregate Concrete

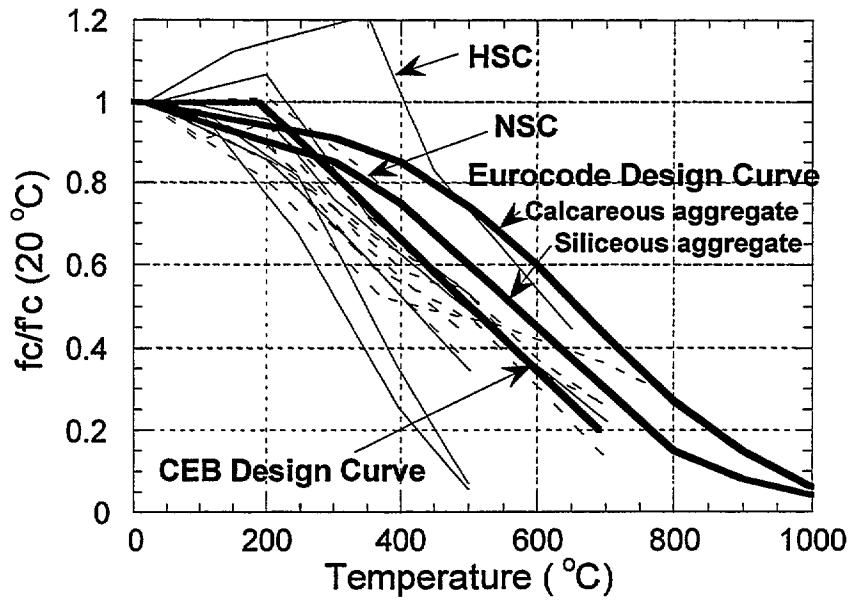


Figure 4.16 Comparison of Design Curves for Compressive Strength and Results of *Unstressed Residual Strength* Tests of Normal Weight Aggregate Concrete

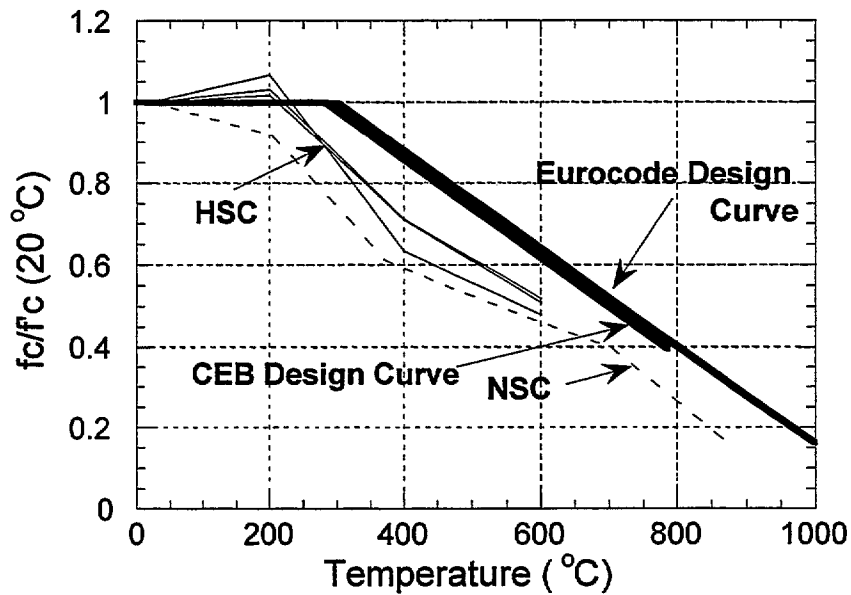


Figure 4.17 Comparison of Design Curves for Compressive Strength and Results of *Unstressed Residual Strength* Tests of Lightweight Aggregate Concrete

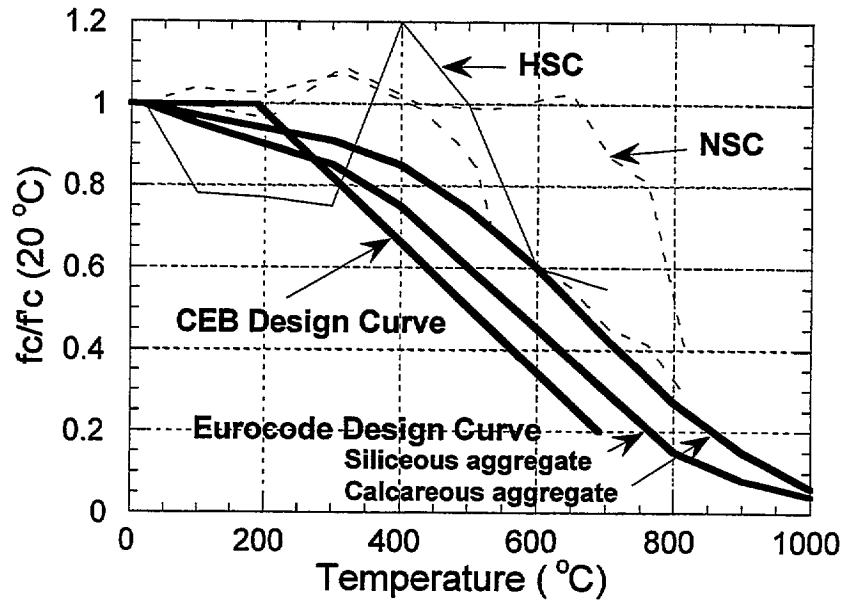


Figure 4.18 Comparison of Design Curves for Compressive Strength and Results of *Stressed Tests* of Normal Weight Aggregate Concrete

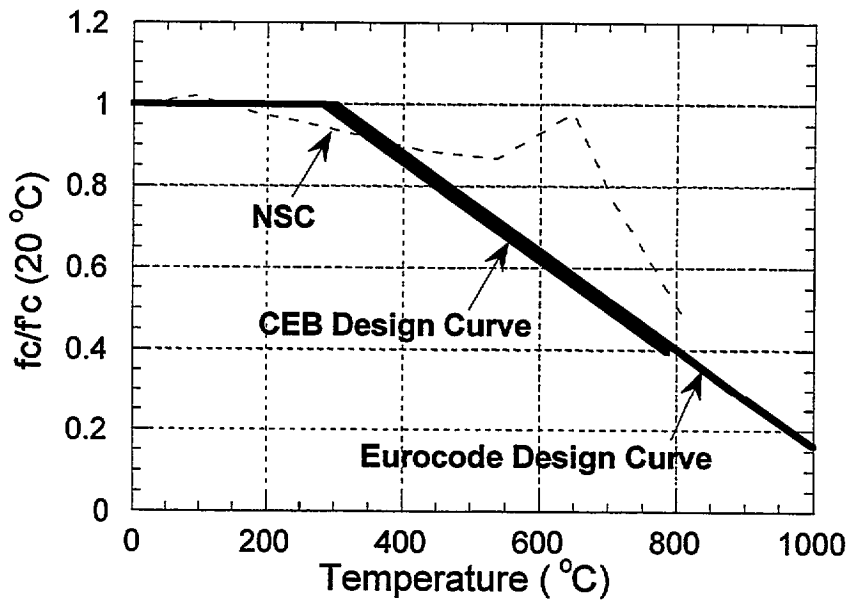


Figure 4.19 Comparison of Design Curves for Compressive Strength and Results of *Stressed Tests* of Lightweight Aggregate Concrete

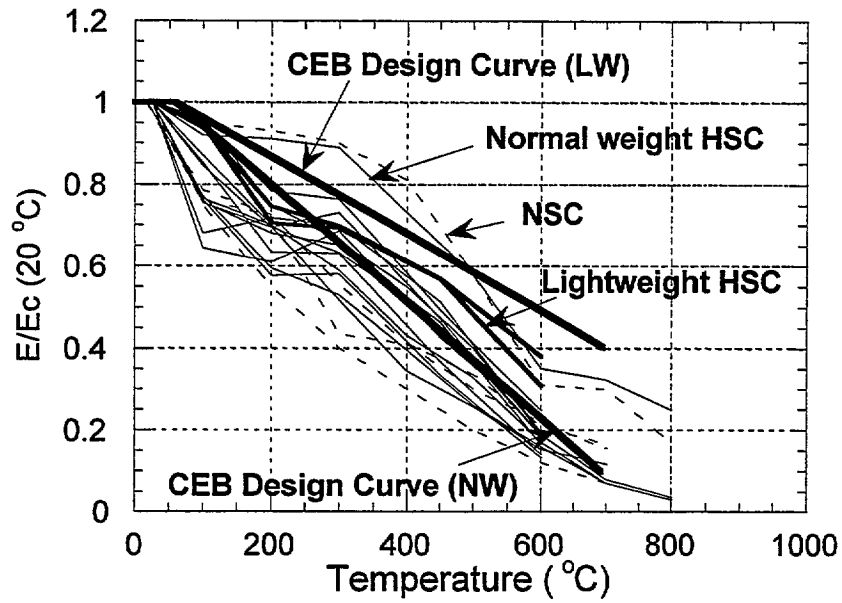


Figure 4.20 Comparison of Design Curves for Modulus of Elasticity and Results of *Unstressed Tests*

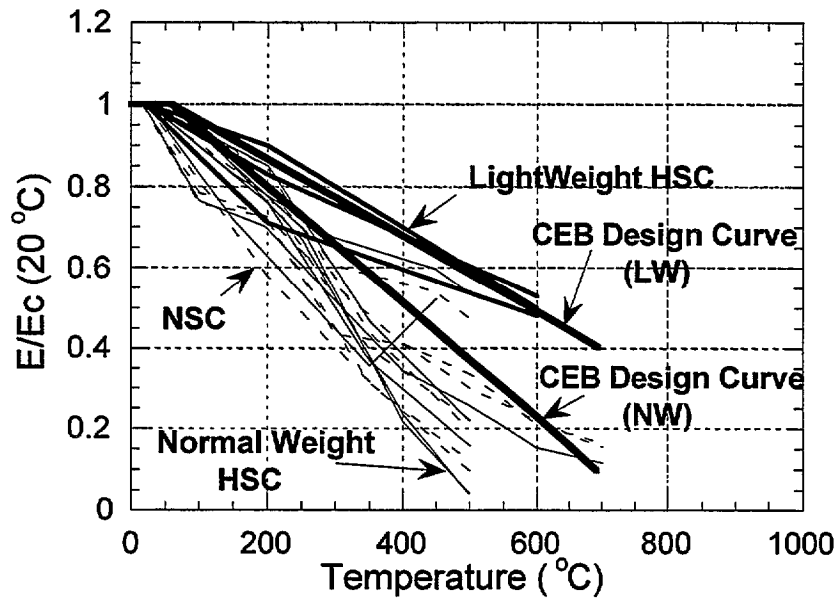


Figure 4.21 Comparison of Design Curves for Modulus of Elasticity with Results of *Unstressed Residual Strength Tests*

4.5 Summary

Three fire test methods, ISO 834, ASTM E 119, and JIS A 1304, were summarized. All three methods prescribe similar criteria for determining fire endurance of concrete structural elements. In terms of temperature history, the standard temperature curves of the three test methods are also similar, as shown in Figure 4.22. The ISO 834 standard fire curve differs from those of ASTM E 119 and JIS A 1304 in that it allows the temperature to rise continuously with exposure time, without a specified upper limit. ASTM E 119 specifies a temperature rise up to 480 minutes, after which the temperature is kept constant at 1260 °C. JIS A 1304 has an exposure time limit of 240 minutes, corresponding to a fire endurance rating of “4 hours heat.”

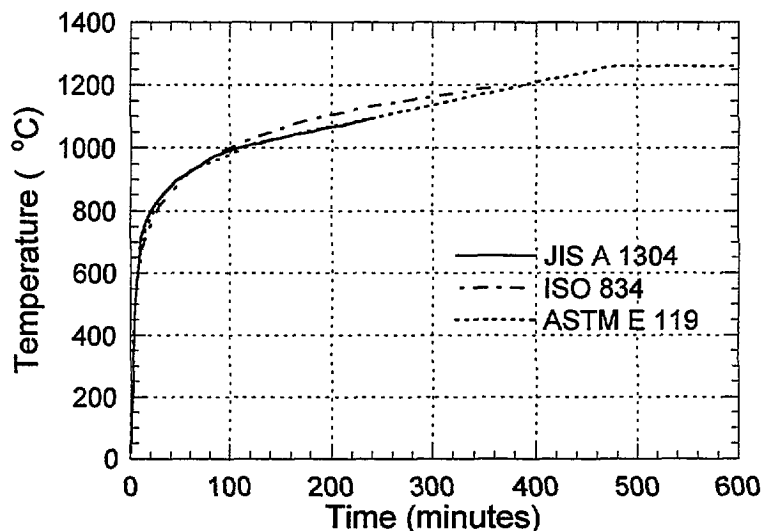


Figure 4.22 Standard Temperature Time Curves

Concerning the properties of concrete at high temperatures, information from the CEN Eurocodes, ACI 216R-89, CEB Bulletin D'Information N° 208, the RILEM 44-PHT, and the CRSI report were reviewed. The CEN Eurocodes (2 and 4) provided the most comprehensive treatment of concrete properties at high temperatures. A mathematical model for the loading branch of the stress-strain curves of concrete is prescribed. A strength reduction factor, $k_{c,6}$, is specified for normal weight and lightweight aggregate concretes. The CEB Bulletin D'Information N° 208, *Fire Design of Concrete Structures*, and the report of RILEM Committee 44-PHT, *Properties of Materials at High Temperatures - Concrete*, provide experimental data for different concrete properties at high temperatures as well as recommended design curves, based on these experimental data. ACI 216R-89, *Guide for Determining the Fire Endurance of Concrete Elements*, and the CRSI report,

Reinforced Concrete Fire Resistance, also described the effect of high temperatures on concrete properties based on experimental data, but without a prescriptive mathematical formulation as that proposed in the CEN Eurocodes.

It should be noted that the experimental data that provided the basis for recommendations and observations made in the above documents were from tests of normal strength concretes. Most of those tests were conducted in the 1960s and 1970s. The maximum room temperature compressive strengths used were about 50 MPa. Thus the applicability of these design recommendations and observations to HSC must be verified prior to using them for fire design of HSC.

5. SUMMARY, DISCUSSION, AND RECOMMENDATIONS

5.1 Summary

The followings summarizes the key findings obtained from this review of experimental studies on the fire performance of high-strength concrete:

- The material properties of HSC vary differently with temperature than those of NSC. The differences are more pronounced in the temperature range of between 25 °C to about 400 °C, where higher strength concretes have higher rates of strength loss than lower strength concretes. These differences become less significant at temperatures above 400 °C. Compressive strengths of HSC at 800 °C decrease to about 30% of the original room temperature strengths.
- For *unstressed* and *stressed tests* of HSC, the variations of compressive strength with temperature are characterized by 3 stages: (1) an initial stage of strength loss (25 °C to approximately 100 °C), followed by (2) a stage of stabilized strength and recovery (100 °C to approximately 400 °C), and (3) a stage above 400 °C characterized by a monotonic decrease in strength with increase in temperature.
- For *unstressed residual strength tests* of HSC, the compressive strength versus temperature relationships are characterized by 2 stages: (1) an initial stage of minor strength gain or loss (25 °C to 200 °C), followed by (2) a stage above 200 °C in which the strength decreases with increasing temperature.
- The strength recovery stage of higher strength concretes occurs at higher temperatures than lower strength concretes.
- Compressive strengths of HSC obtained from the *stressed tests* are higher than those obtained from the *unstressed* and *unstressed residual strength tests* in the temperature range of (25 °C to 400 °C). The application of preload reduces strength loss in this range of temperature. Varying the preload levels from 25 to 55% of the original compressive strength, however, does not cause significant difference in compressive strengths of HSC at elevated temperatures.
- HSC mixtures with silica fume have higher strength loss with increasing temperatures than HSC mixtures without silica fume.
- The difference between the compressive strength versus temperature relationships of normal weight and lightweight aggregate concrete appears to be insignificant, based on the limited amount of existing test data.

- The tensile strength versus temperature relationships decrease similarly and almost linearly with temperature for HSC and NSC. HSC retains approximately 50% of its original tensile strength at 500 °C. NSC retains an average of 45% of its original tensile strength at this same temperature.
- Explosive spalling failure occurs more in HSC than in NSC specimens. This failure mode was observed in all three types of test (*stressed*, *unstressed*, and *unstressed residual strength*). However, explosive spalling was not observed in all the reviewed test programs. Of the ten materials test programs reviewed, five reported explosive spalling. Of the five element test programs reviewed, three reported spalling. Also, within the same test program, explosive spalling did not occur to every specimen tested under identical conditions. The reported temperature range when explosive spalling occurs is between 300 °C to 650 °C.
- Concrete with dense pastes due to the addition of silica fume are more susceptible to explosive spalling. Likewise, HSC made with lightweight aggregate appears to be more prone to explosive spalling than HSC made of normal weight aggregate concretes. HSC specimens heated at higher heating rates, and larger specimens are more prone to spalling than specimens heated at lower rates and of smaller size.
- The failure of HSC is more brittle than NSC at temperature up to 300 °C. With further increase in temperature, specimens exhibit a more gradual failure mode.
- A temperature of 300 °C marks the beginning of higher rate of decrease in modulus of elasticity for all concretes. Lightweight aggregate concretes retain higher proportions of the original modulus of elasticity at high temperature than normal weight aggregate concretes. The difference is more pronounced for *unstressed residual strength tests* than for *unstressed tests*.
- There are a limited number of numerical techniques for modeling the development of internal stresses caused by heat-induced water vapor pressure in the concrete pores. The accuracy of these modeling techniques is highly dependent upon using the correct concrete properties, such as diffusivity, permeability, porosity, etc. While the numerical basis of the modeling techniques are promising, none of the analytical studies reviewed in this report provided validation of the numerical predictions using HSC test data.
- Fire design recommendations for fire-exposed concretes are applicable to NSC, but not HSC.

5.2 Discussion and Recommendations

Important trends concerning the performance of HSC at elevated temperature are revealed from this review of previous studies. From these trends, three important conclusions can be drawn:

- HSC is more susceptible to explosive spalling failure when exposed to high temperature (above 300 °C) than NSC.
- HSC has a higher rate of compressive strength loss in the temperature range between 100 °C to 400 °C compared with NSC.
- Existing code provisions, such as the CEN Eurocode and the CEB's design curves, for properties of fire-exposed concretes are not applicable to HSC.

Given the increased usage of HSC in structural applications, the behavioral differences observed for HSC and the inapplicability of existing code provisions for fire-exposed HSC must be recognized and addressed so as to reduce the likelihood of structural collapse in the event of fire. The amount of test data on fire-exposed HSC is insufficient relative to the number of variables (concrete strength, aggregate types, test conditions, specimen size, concrete density, concrete permeability, concrete porosity, heating rate, etc...). Of particular interest are data from the *stressed tests*, which simulate the condition of structural elements when exposed to a fire. Such data are scarce, as can be seen from Figures 2.66 and 2.67. Data are also scarce for fire-exposed HSC made of lightweight aggregate concretes and tested under all three types of tests (see Figures 2.63, 2.65, 2.67). Furthermore, to effectively address the behavioral differences observed in HSC, especially explosive spalling, the effects of a number of variables such as those listed above must be quantified. Also, the variation of the stress-strain relationships of HSC with temperatures must be established experimentally. Such relationships are not widely reported in the existing literature but are essential for the development of constitutive models of HSC to predict structural performance during a fire.

Based on the observed behavioral differences for HSC and the research needs discussed above, the following three high-priority research areas are identified:

- *Experimental studies:*

Experimental studies should be designed to obtain a more complete body of data on the fundamental behavior of HSC at high temperature and, more importantly, to develop data necessary for the development and validation of numerical models which can predict moisture transport and the sudden spalling of HSC when subjected to fire. The experimental study should consist of both *materials testing* (tests of fire-exposed HSC specimens) and *element testing* (tests of fire-exposed HSC beams, columns, slabs, walls). The following test variables should be considered for the *materials test* program:

- test methods (with emphasis on the *stressed tests*)
- aggregate type (siliceous, calcareous, lightweight)
- water/cement ratio
- addition of silica fume
- moisture content and maturity at time of test
- heating rate

The measurements should include compressive strength, tensile strength, modulus of elasticity, compressive stress-strain relationships as function of temperatures. These data should provide definable behavioral trends for the properties of fire-exposed HSC. Also, to investigate the explosive spalling failure mechanism of HSC, measurements of internal temperature, changes in permeability, porosity, and mass loss should be obtained.

The *structural element test* program should include columns with preload, beams, and slabs. Measurements of internal temperature should be obtained in addition of the furnace temperature.

- *Analytical study:*

The experimental data obtained from the materials studies will be used to develop a material model to predict structural performance of HSC elements exposed to high temperature. The basis for the model may be adopted from the pore pressure models by *Bazant* or *Ahmed*, but including the measured properties (permeability, moisture content, thermal conductivity, etc.) characteristic of HSC. Data obtained from *element tests* may be used for model validation.

- *Development of Code Provisions:*

The experimental and analytical data will be synthesized and tabulated into a form, such as practical constitutive models similar to that of CEN Eurocode, that is suitable for design purposes. Such constitutive models and/or design criteria will be presented to code writing organizations for implementation to provide guidance for fire design of HSC members.

6. REFERENCES

1. American Concrete Institute, "Temperature and Concrete", *Publication SP 25*, Detroit, Michigan, 1971.
2. Abrams, M.S., "Compressive Strength of Concrete at Temperatures to 1600F", *American Concrete Institute (ACI) SP 25*, Temperature and Concrete, Detroit, Michigan, 1971.
3. Abrams, M.S., and Gustaferrro, A.H., "Fire Endurance of Concrete Slabs as Influenced by Thickness, Aggregate Type, and Moisture," *Journal, PCA Research and Development Laboratories*, V.10, No. 2, May 1968, pp. 9-24.
4. American Concrete Institute, "State-of-the-Art Report on High-Strength Concrete", *ACI 363R-92*.
5. American Concrete Institute, "Guide for Determining the Fire Endurance of Concrete Elements", *ACI 216R-89*.
6. American Society for Testing and Materials, "Standard Test Methods for Fire Tests of Building Construction and Materials", *ASTM E 119-88*.
7. Ahmed, G.N., and Hurst, J.P., "Modeling the Thermal Behavior of Concrete Slabs Subjected to the ASTM E119 Standard Fire Condition," *Journal of Fire Protection Engineering*, 7(4), 1995, pp. 125-132
8. Abdel-Rahman, A.K., and Ahmed, G.N., "Computational Heat and Mass Transport in Concrete Walls Exposed to Fire," *Numerical Heat Transfer*, Part A, 29:373-395, 1996
9. Bazant Z.P., and Thonuthai W., "Pore pressure in heated concrete walls: Theoretical prediction", *Magazine of Concrete Research*, Vol. 31, No 107, pp 67-76.
10. Binner, C.R., Wilkie, C.B., and Miller, P., "Heat Testing of High Density Concrete," *Supplement, Declassified Report HKF-1*, U.S. Atomic Energy Commission, June, 1949.
11. Concrete Reinforcing Steel Institute, "Reinforced Concrete Fire Resistance", *CRSI*, 1980.
12. Comites Euro-International Du Beton, "Fire Design of Concrete Structures - in accordance with CEB/FIP Model Code 90 (Final Draft)", *CEB Bulletin D'Information No. 208*, July 1991, Lausanne, Switzerland.

13. Comité Européen de Normalisation (CEN), "prENV 1992-1-2: Eurocode 2: Design of Concrete Structures. Part 1 -2: Structural Fire Design," *CEN/TC 250/SC 2*, 1993.
14. Comité Européen de Normalisation (CEN), "Eurocode 4: Design of Composite Steel and Concrete Structures. Part 1 -2: General Rules - Structural Fire Design," *CEN ENV 1994*.
15. Castillo, C., and Durrani, A. J., "Effect of transient high temperature on high-strength concrete," *ACI Materials Journal* (American Concrete Institute) v 87 n 1, Jan-Feb 1990 p 47-53.
16. Carette, Georges G., and Malhotra, V. Mohan, "Performance of Dolostone and Limestone Concretes at Sustained High Temperatures," *Temperature Effects on Concrete*, American Society for Testing and Materials (ASTM)'s Special Technical Publication 858, Philadelphia, PA, USA p 38-67.
17. Chung, H. W., "Ultrasonic Testing of Concrete After Exposure to High Temperatures", *NDT International*, v. 18, n. 5, October 1985, p. 275-278, Univ of Hong Kong, Department of Civil Engineering, Hong Kong.
18. Chow, W.K., and Chan, Y.Y., "Computer Simulation of the Thermal Fire Resistance of Building Materials and Structural Elements", *Journal of Construction & Building Materials*, Vol. 10, Number 2, pp. 131, 1996, ISSN: 0950-0618 CODEN: CBUMEZ.
19. Concrete Society, "Assessment and Repair of Fire-damaged concrete Structures", *Technical Report 33*, The Concrete Society, London, 1990.
20. Chabot, M., and Lie, T.T., "Experimental Studies on the Fire Resistance of Hollow Steel Columns Filled with Bar-Reinforced Concrete," National Research Council Canada (NRC-CNRC), Institute for Research in Construction, Report No. 628, April 1992.
21. Din Deutsches Institut Fur Normung E.V. (German Institute for Standardization), *DIN 4102*, "Behavior of Building Materials and Components in Fire," German Standard, May, 1981.
22. Diederichs, U., and Schneider, U., "Bond Strength at High Temperatures," *Magazine of Concrete Research*, v. 33, n. 115, June 1981, p. 75-84.
23. Diederichs, U., Jumppanen, U.M., Penttala, V., "Material Properties of High Strength Concrete at Elevated Temperatures", *LABSE 13th Congress*, Helsinki, June 1988.
24. Diederichs, U., Jumppanen, U.M., Penttala, V., "Behavior of High Strength Concrete at High Temperatures", *Report #92*, Helsinki University of Technology, Department of Structural Engineering, 1989.

25. Diederichs, U., Jumppanen, U-M., Schneider, U., "High Temperature Properties and Spalling Behavior of High Strength Concrete," *Proceedings of the Fourth Weimar Workshop on High Performance Concrete: Material Properties and Design*, held at Hochschule für Architektur und Bauwesen (HAB), Weimar, Germany, October 4th and 5th, 1995, pp. 219 - 236.
26. Davis, H.S., "Effects of High Temperature Exposure on Concrete", *Materials Research and Standards*, V.7, No.10, October 1967, pp. 452-459.
27. England, G.L., and Khoylou, N. "Modeling of Moisture Behavior in Normal and High Performance Concretes at Elevated Temperatures," *Proceedings of the Fourth Weimar Workshop on High Performance Concrete: Material Properties and Design*, held at Hochschule für Architektur und Bauwesen (HAB), Weimar, Germany, October 4th and 5th, 1995, pp. 53 - 68.
28. "High Strength Concrete State of the Art," *FIP-CEB Working Group on HSC*, Draft 5B, April, 1990.
29. Fire Protection Planning Report, "Assessing the Condition and Repair Alternatives of Fire-Exposed Concrete and Masonry Members," *Building Construction Information from the Concrete and Masonry Industries*, August 1994.
30. Furumura, F., Abe, T., Shinohara, Y., "Mechanical Properties of High Strength Concrete at High Temperatures," *Proceedings of the Fourth Weimar Workshop on High Performance Concrete: Material Properties and Design*, held at Hochschule für Architektur und Bauwesen (HAB), Weimar, Germany, October 4th and 5th, 1995, pp. 237 - 254.
31. Felicetti, R., Gambarova, P.G., Rosati, G.P., Corsi, F., Giannuzzi, G., "Residual Mechanical Properties of High-Strength Concretes Subjected to High-Temperature Cycles," *Proceedings, 4th International Symposium on Utilization of High-Strength/High-Performance Concrete*, Paris, France, 1996, pp.579-588.
32. Gustafarro, A.H., and Selvaggio, S.L., "Fire Endurance of Simply Supported Prestressed Concrete Slabs," *Journal, Prestressed Concrete Institute*, V.12, No. 1, February 1967, pp. 37-52.
33. Hertz K., "Danish Investigations on Silica Fume Concretes at Elevated Temperatures," *Proceedings, ACI 1991 Spring Convention*, Boston, MA, March 17-21.
34. Hertz K., "Heat Induced Explosion of Dense Concretes," *Report No. 166*, Institute of Building Design, Technical University of Denmark, 1984.

35. Hammer, T.A., "HIGH-STRENGTH CONCRETE PHASE 3, Compressive Strength and E-modulus at Elevated Temperatures," SP6 Fire Resistance, *Report 6.1*, SINTEF Structures and Concrete, STF70 A95023, February, 1995.
36. Hammer, T.A., "HIGH-STRENGTH CONCRETE PHASE 3, Spalling Reduction through Material Design," SP6 Fire Resistance, *Report 6.2*, SINTEF Structures and Concrete, STF70 A95024, February, 1995.
37. Hammer, T.A., Justnes, H., Smepllass, S., "A Concrete Technological Approach to Spalling during Fire," Paper presented at a Nordic mini-seminar, Trondheim, 1989. SINTEF Report STF65 A89036.
38. Hansen, P.A., and Jensen, J.J., "HIGH-STRENGTH CONCRETE PHASE 3, Fire Resistance and Spalling Behavior of LWA Beams," SP6 - Fire Resistance, *Report 6.3*, SINTEF NBL - Norwegian Fire Research Laboratory, STF25 A95004, March 1995.
39. Opheim, E., "HIGH-STRENGTH CONCRETE PHASE 3, Residual Strength of Fire Exposed Structural Elements," SP6 Fire Resistance, *Report 6.4*, SINTEF Structures and Concrete, STF70 A95025, February, 1995.
40. Ikeda K., Kumagai T., Nakamura K., and Saito H., "Fire Resistance Test on Unbonded Tubular Steel Concrete Column", March 1988.
41. Inha T., "Effect of High Strength Concrete on Structural Fire Design According to Finnish Tests," American Concrete Institute Spring Convention, Boston, MA, March 1991.
42. Inha, T., Korander, O., Penttala, V., and Soderland, K., "High-Strength Concrete in Finland", *FIP '90 XI Congress*, Hamburg, Germany.
43. "ISO 834 - Fire Resistance Tests - Elements of Building Construction," *International Organization for Standardization (ISO)*, 1975.
44. Janhunen P., "High Strength Concrete - Application and Standardization in Finland", *Concrete Precasting Plant and Technology*, Vol. 2, pp 74-80.
45. Jumppanen U-M, "Effect of Strength on Fire Behavior of Concrete", *Nordic Concrete Research*, No. 8, pp 116-127.
46. Jahren, P.A., "Fire Resistance of High Strength/Dense Concrete with Particular Reference to the Use of Condensed Silica Fume - A Review", *Proceedings*, Trondheim (Norway) 1989 Conference, pp 1013-1049.

47. Jumppanen, U-M, Diederichs U., Hinrichsmeyer K., "Material Properties of F-Concrete at High Temperature," Valtion Teknillinen Tutkimuskeskus, *Research Reports*, Technical Research Center of Finland, Espoo, November 1986.
48. "Method for Fire Resistance Test for Structural Parts of Buildings- JIS A 1304," *Japanese Industrial Standard (JIS)*, Japanese Standards Association, Japan, 1994.
49. Kodur V.K.R., and Lie T.T., "Structural Fire Protection Through Concrete Filling for - Hollow Steel Columns," *Proceedings*, International Conference on Fire Research and Engineering, September 1995, Orlando, Florida.
50. Khoury, G.A., Grainger, B.N., and Sullivan, P.J.E., "Strain of Concrete During First Heating to 600 °C under Load", *Magazine of Concrete Research*, Vol. 37, pp 195-215.
51. Khoury, G.A., Grainger B.N. and Sullivan G.P.E., "Transient Thermal Strain of Concrete: Literature Review, Conditions within Specimen and Behavior of Individual Constituents," *Magazine of Concrete Research*, Vol. 37, No. 132, pp 131-144.
52. Kasami, H., Okuno, T., and Yamane, S., "Properties of concrete exposed to sustained elevated temperature," *Transactions of the Third International Conference on Structural Mechanics in Reactor Technology*, London, September 1-5, 1975. Amsterdam, North-Holland Publishing Co., 1975, Vol. 3. pp. 1-10. Part H 1/5.
53. Krampf, L., and Haksever, A., "Possibilities of Assessing the Temperatures Reached by Concrete Building Elements During a Fire", *Evaluation and Repair of Fire Damage to Concrete*, T.Z. Harmathy, editor, ACI SP 92, American Concrete Institute, Detroit, MI, 1986, P.127.
54. Kumagai, H., Saito, H., and Morita, T., "Residual Mechanical Properties of High Strength Concrete Members Exposed to High Temperature - Part 3. Test on Reinforced Concrete Columns," *Summaries of Technical Papers of Annual Meeting*, Architectural Institute of Japan, Niigata, August, 1992 (in Japanese).
55. Lankard, D.R., Birkimer, D.L., Fondfriest, F.F., and Snyder, M.J., "Effects of Moisture Content on the Structural Properties of Portland Cement Concrete Exposed to Temperatures up to 500 F," *Temperature and Concrete*, ACI SP-25, American Concrete Institute, Detroit, 1971, pp. 59-102.
56. Lie, T.T., and Chabot, M., "Experimental Studies on the Fire Resistance of Hollow Steel Columns Filled with Plain Concrete," National Research Council Canada (NRC-CNRC), Institute for Research in Construction, Report No. 611, January 1992.

57. Lie, T.T., and Woollerton, J.L., "Fire Resistance of Reinforced Concrete Columns - Test Result," *Internal Report No. 569*, Institute for Research in Construction, National Research Council of Canada, Ottawa, Canada, 1988.
58. Lin, W-M, Lin, T.D., Powers-Couche, L.J., "Microstructure of Fire-Damaged Concrete," *Technical Paper 93-M22*, ACI Materials Journal, V. 93, No. 3, May-June 1996.
59. Malhotra V.M., Wilson H.S., and Painter K.E., "Performance of Gravelstone Concrete Incorporating Silica Fume at Elevated Temperatures," *Proceedings*, 1989 Trondheim (Norway) Conference, pp. 1051-1076.
60. Malhotra,H.L., "The Effect of Temperature on the Compressive Strength of Concrete," *Magazine of Concrete Research* (London), V.8, No. 22, 1956, pp.85-94.
61. Malhotra, H.L., "The Effect of Temperature on the Compressive Strength of Concrete," *Magazine of Concrete Research* (London), V.8, No.22, 1956, pp. 85-94.
62. Murota T., and Hirosawa, M., "Development of Advanced Reinforced Concrete Buildings Using High-Strength Concrete and Reinforcement," *NIST SP 776*, Proceedings of the 21st US-Japan Joint Meeting on Wind and Seismic Effects.
63. Maruta, M., Yamazaki, M., and Miyashita, T., "Study on shear behavior of reinforced concrete beams subjected to long-term heating," *Nuclear Engineering and Design*, v. 156, n. 1-2, Jun. 1, 1995, p 29-37.
64. Mohamedbhai, G. T. G., "Residual Strength of Concrete Subjected to Elevated Temperatures," *Concrete* (London), v. 17, n. 12, December 1983, p. 22-23, 25-27.
65. Morita, T., Saito, H., and Kumagai, H., "Residual Mechanical Properties of High Strength Concrete Members Exposed to High Temperature - Part 1. Test on Material Properties," *Summaries of Technical Papers of Annual Meeting*, Architectural Institute of Japan, Niigata, August, 1992 (in Japanese).
66. Menzel, C.A., "Tests of the Fire Resistance and Thermal Properties of Solid Concrete Slabs and Their Significance," *Proceedings*, American Society for Testing and Materials (ASTM), v.43, 1943, pp. 1099-1153.
67. Naik, Tarun R. (Ed.), "Temperature Effects on Concrete," *American Society for Testing and Materials (ASTM)'s Special Technical Publication 858*, Published by ASTM, Philadelphia, PA, USA 184p.

68. Nasser, K. W., and Marzouk, H. M., "Properties of Concrete Containing Fly Ash at Normal and High Temperatures," *Proceedings*, 2nd Australian Conference on Engineering Materials, Sydney, Aust, Jul 6-8, 1981.
69. Nasser, K.W. and Marzouk, H.M., "*Properties of Mass Concrete Containing Fly Ash at High Temperatures*," *ACI Journal*, v. 76, n. 4, April 1979.
70. Nassif, A.Y., Burley, E., and Rigden, S., "A New Quantitative Method of Assessing Fire Damage to Concrete Structures," *Magazine of Concrete Research*, 1995, 47, No. 172, September, pp. 271-278.
71. Neville, A.M., "Properties of Concrete," Halsted Press, John Wiley & Sons Inc., New York, 1973.
72. Noumowe, A.N., Clastres, P., Debicki, G., and Costaz, J.-L., "Thermal Stresses and Water Vapor Pressure of High Performance Concrete at High Temperature," *Proceedings*, 4th International Symposium on Utilization of High-Strength/High-Performance Concrete, Paris, France, 1996.
73. Pettersson O., "Rational Structural Fire Engineering Design, Based on Simulated Real Fire Exposure," Department of Fire Safety Engineering, Lund Institute of Technology, Lund University, Sweden.
74. Piasta, J., Sawicz, Z., Rudzinski, L., "Changes in the Structure of Hardened Cement Paste due to High Temperature", *Materiaux et Constructions*, Materials and Structures v. 17, n. 100, Jul-Aug 1984, p 291-296.
75. PCA, "High Strength Concrete-Costs More in the Truck, Costs Less in the Structure," *Concrete Technology Today*, No. 4, December 1980, p. 3.
76. Riley, M. A., "Assessing fire-damaged concrete", *Concrete International: Design and Construction*, v. 13, n. 6, Jun 1991, p. 60-63.
77. Rio, A., Biagini, S., "Influence of High Temperatures on Mechanical Characteristics of Polymer-Impregnated Concrete," *Polymers in Concrete*, 3rd International Congress on Polymers in Concrete, Koriyama, Japan, May 13-15, 1981, v. 2, Published by the Organizing Committee of the 3rd International Congress on Polymer in Concrete, p. 888-903.
78. Schneider U., "Concrete at High Temperatures - A General Review", *Fire Safety Journal*, The Netherlands, 1988, pp 55-68.

79. Schneider, U., and Franssen J-M, "A Concrete Model Considering the Load History Applied to Centrally Loaded Columns Under Fire Attack," *Proceedings of the Fourth International Symposium, Fire Safety Science*, pp 1101-1112.
80. Shirley, S.T., Burg, R.G., and Fiorato, A.E., "Fire Endurance of High-Strength Concrete Slabs," *Task Force Report, Chicago Committee on High-Rise Buildings*, Report No. 11, October 1987.
81. Sanjayan, G., and Stocks, L., "Spalling of High Strength Concrete in Fire," *ACI Spring Convention*, March 1991, Boston, MA.
82. Sanjayan, G., and Stocks, L., "Spalling of High Strength Silica Fume Concrete in Fire," *ACI Materials Journal*, Vol. 90, No. 2, March-April 1993.
83. Sullivan, P.J.E., Khoury, G.A., and Grainger, B.N., "Apparatus for Measuring the Transient Thermal Strain Behavior of Unsealed Concrete under Constant Load for Temperatures up to 700 °C," *Magazine of Concrete Research*, Cement and Concrete Association, Vol. 37, No. 125, pp 229-236, 1983.
84. Sullivan, P. J. E., and Sharshar, R., "Performance of concrete at elevated temperatures (as measured by the reduction in compressive strength," *Fire Technology*, v. 28, n. 3, August 1992, p. 240-250.
85. Schneider, U., and Diederichs, U., "Bond Behavior and Bond Strength of Reinforced Concrete at High Temperatures", *Betonwerk und Fertigteil-Technik*, v. 46, n. 6, June 1980, p. 351-359.
86. Schneider, U., "Behavior of Concrete at High Temperatures", *RILEM - Committee 44 - PHT*, February 1983.
87. Schneider, U., "Behavior of Concrete at High Temperatures," *HEFT 337*, Deutscher Ausschuss Für Stahlbeton, Vertrieb Durch Verlag Von Wilhelm Ernst & Sohn, Berlin - München, Berlin 1982.
88. Schneider, U., "Properties of Materials at High Temperatures - Concrete", *RILEM - Committee 44 - PHT*, Department of Civil Engineering, University of Kassel, Kassel, June, 1985.
89. Smith, L.M., "The assessment of fire damage to concrete structures", PhD Thesis, Paisley College of Technology, 1983

90. Saito, H., Kumagai, H., and Morita, T., "Residual Mechanical Properties of High Strength Concrete Members Exposed to High Temperature - Part 2. Test on Reinforced Concrete Beams," *Summaries of Technical Papers of Annual Meeting*, Architectural Institute of Japan, Niigata, August, 1992 (in Japanese).
91. Saemann, J.G., and Washa, G.W., "Variation of Mortar and Concrete Properties and Temperature," *ACI Journal*, Proceedings V.54, No.5, November 1957, pp.385-397.
92. Thienel, K.-Ch., Rostasy, F.S., "Strength of concrete subjected to high temperature and biaxial stress: Experiments and modeling," *Materials and Structures/Materiaux et Constructions*, v. 28, n. 184, December 1995. p 575-581

